Taming Highly Reactive Species for Use in Organic Synthesis

By

Eric Skrotzki

Thesis submitted to the University of Ottawa in partial fulfillment of the requirements for the M. Sc. Degree in Chemistry and Biomolecular Sciences

Department of Chemistry and Biomolecular Sciences

Faculty of Science

University of Ottawa

Candidate	Supervisor
Eric A. Skrotzki	Stephen G. Newman

Abstract:

Chemical processes and reactions are never perfect; there are always some problems in scope, scalability, applicability or safety. Sometimes, if these limitations pose a seemingly insurmountable barrier to the chemistry's overall usefulness, decades can go by without a single new development even in fields that were initially very promising or popular in their infancy. By looking back on these forgotten topics through the lens of modern technology, new cutting-edge materials and methods can be applied to solve the problems that posed too great a challenge in previous decades. In this thesis, two such examples of reactions initially discovered and developed around the late 1960's and remained largely untouched ever since will be explored.

Chapter 1 will describe the use of ozone as an oxidant to transform amines into the corresponding alkyl nitro species. Ozone is a very powerful oxidant but tends to overreact with most organic substrates, which significantly reduces its potential as a commonplace synthetic tool. These limitations in applicability stem from an inherent lack of control over the reaction, which is the issue that we sought out to address. By applying modern principles of flow chemistry, the functional group tolerance of this oxidation reaction has been drastically increased from its initial state of simple small hydrocarbons.

Chapter 2 will follow a similar narrative involving the use of 'super-bases' to activate benzylic C-H bonds and generate a variety of benzyllithium species. Organolithiums

have also had historic issues with tolerance in transition metal-catalyzed cross coupling reactions. With a surge of new publications addressing this issue by using principles of flow chemistry, there remains a lack of easy methods to generate organolithium nucleophiles as coupling partners. Generation of benzyllithiums from toluene derivatives has historically been limited to require solvent quantities of substrate, along with unreasonably long reaction times at cryogenic temperatures. By utilizing modern tools and synthetic strategies, an easy and streamlined path from toluene derivatives to organolithiums for direct use in cross coupling has been developed.

Acknowledgements:

First and foremost, I would like to thank Prof Stephen Newman for accepting me into his lab and teaching me through the last 2 and a half years. Your means of guiding and teaching your students is truly unmatched by any other professor I have encountered. If I had the chance to do it all over, I wouldn't hesitate before asking you again as my first and only choice.

To my co-workers and colleagues, I would like to thank you for your support and friendship. Whether just bouncing chemistry ideas off each other, or long drawn out lunch breaks, you have always been a valuable and appreciated part of my every day. Eric (Isbrandt), Omid, Garrett, Amrah, Adam, Piers and August, my experience here wouldn't have been the same without you. To members who have left our group, I also wanted to thank you for lessons and knowledge you shared with me before moving on: Ryan and Yanlong, I wish you the best of success in your future endeavors.

I feel a special mention should be given to Saeed Kashani, not just a PhD student, but a good friend who was taken from us too soon. We all miss you Saeed, rest in peace.

To all the undergrads that have come and gone from our group while I was here, I wish you the best of success in your future pursuits, school or otherwise. Jonathan, Katie, Rama, Casey, Max, Jean-Danick, and Karen: you're all awesome! Keep it up and you'll all be stars.

Finally, and most importantly, I would like to thank my family, who knew I would be here long before I did and kept pushing and encouraging me to be the best I could be. To my parents in particular, I would not have been able to reach this far without your constant love and support. As you always say, this degree is really yours.

Thank you. For everything.

Table of Contents:

List of Tables:

List of Figures:

List of Schemes:

List of Abbreviations:

9-BBN	9-borabicyclo(3.3.1)nonane
Ac	acetyl
aq.	aqueous
Ar	aryl
BA	Brönsted acid
BDE	bond dissociation energy
Bn	benzyl
BOC	tert-butyloxycarbonyl
BPR	back pressure regulator
Bu	butyl
calcd	calculated
cat.	catalytic or catalyst
Cp	cyclopentadienyl
CPME	cyclopentyl methyl ether
Cy	cyclohexyl
Cyp	cyclopentyl
d	doublet
DABCO	1,4-diazabicyclo[2.2. 2]octane
dba	dibenzylideneacetone
DFT	density functional theory
DMAP	4-dimethylaminopyridine
DMF	dimethylformamide
DMSO	dimethylsulfoxide
dppp	1,3-bis(diphenylphosphino)propane
E or E^+	electrophile

e.e.	enantiomeric excess
e.r.	enantiomeric ratio
EDG	electron-donating group
EI	electron impact
equiv	equivalent
ESI	electrospray ionization
Et	ethyl
EWG	electron-withdrawing group
FID	flame ionization detector
g	gram(s)
GC	gas chromatography
h	hour(s)
HPLC	high performance liquid chromatography
HRMS	high resolution mass spectrometry
HTE	high throughput experimentation
Hz	hertz
i	iso
IR	infrared
J	coupling constant
KO^{t}Bu	potassium tert-butoxide
L	neutral ligand
LA	Lewis acid
LED	light emitting diode
LDA	lithium di-isopropylamine
KHMDS	potasssium bis(trimethylsilyl)amide
M	generic metal, or molecular ion, or molar
m	meta or multiplet

m/z	mass over charge
m-CPBA	meta-chloroperbenzoic acid
Me	methyl
MeCN	Acetonitrile
mg	milligram(s)
min	minute(s)
mL	milliliter(s)
mol	mole(s)
mp	melting point
MS	mass spectrometry
NHC	N-heterocyclic carbene
NMR	nuclear magnetic resonance
Nu	nucleophile
o	ortho
p	para
Pent	pentyl
PFA	perfluoroalkoxy
Ph	phenyl
ppm	parts per million
q	quartet
quin	quintet
R	generic chemical group
r. t.	room temperature
S_NAr	nucleophilic aromatic substitution
t	triplet
T. or temp.	temperature
TMEDA	*N,N,N′,N′*-tetramethylethylenediamine

TMCDA	*N,N,N′,N′*-tetramethylcyclohexane-1,2-diamine
TBS	tert-butyldimethylsilyl
^{t}Bu or *t*-Bu	tert-butyl
THF	tetrahydrofuran
TLC	thin layer chromatography
TMS	trimethylsilyl
Ts	tosyl
UV	ultraviolet
V	volts
X	generic halogen/heteroatom

Statement of Contributions:

In Chapter 1, the initial hit for the amine oxidation project were discovered by Dr. Jaya K. Vandavasi. All further optimization, development of methodology, and scope expansion of amine oxidation was performed by me. In addition, the 7-hydroxy-3,7-dimethyloctyl acetate (**3a**) example was discovered and optimized by Dr. Jaya K. Vandavasi, with all further exploration into the reported C-H oxidation being done by me.

The project described in Chapter 2 was performed in collaboration with my fellow Masters student, Garrett P. R. Freure. All experiments and research regarding deprotonation or generation of organolithium species were performed by me, while all experiments and research concerning their subsequent use in cross coupling was performed by Garrett. Frequent discussion of our respective topics occurred, ensuring we were both up to date on each other's latest results. In addition, advice and suggestions on experiment design were mutually shared in times of need. Due to the nature of my contribution being the preparation of intermediates, not final products, quantification and optimization was performed using crude GC and crude NMR data. This data was used by Garrett to perform the desired deprotonation followed by the desired coupling. As such, no isolated deprotonation products are presented, rather the final coupled products are described herein.

Chapter 1: Ozone-Mediated Amine Oxidation

1.1: Introduction

This chapter focuses on the development of a technique for transforming amines into nitroalkanes using a flow-based packed bed reactor system and ozone as a stoichiometric oxidant. Discussion about ozone and its reactivity, (Section 1.1.1) nitroalkanes and their uses (Section 1.1.2 and Section 1.1.3), and common methods of amine oxidation (Section 1.1.4) provide the key background necessary to contextualize this research.

1.1.1: Utility of Ozone

1.1.1.1: Discovery and History

Ozone was first discovered in 1840 by Christian Friedrich Schönbein, who noted a pungent odor while performing an experiment with water and electricity.[1] He recognized this odor as similar to what follows a bolt of lightning during a thunderstorm. This chemical presented quite the analytical challenge at the time, and it was almost 30 years before its chemical structure or formula was determined. With a very high oxidation potential of 2.07 V, ozone is an incredibly reactive substance. This is especially true with organic materials and has resulted in its quite successful use as a sanitizing agent. This was first started during World War 1, when ozone was tested for use as a

[1] Schonbein, C. F. Research on the Nature of the Odour in Certain Chemical Reactions, 1840.

disinfectant during surgery on wounded soldiers.[2] Its extreme reactivity resulted in it being rejected in favour of antiseptic wipes, which were much less prone to causing damage to human tissue. However, since then, ozone has enjoyed great popularity in water decontamination industry where it is hailed as the go-to method alongside UV irradiation for bacterial elimination and a flocculent for trace metal removal.

1.1.1.2: Use in Chemical Synthesis

The most significant application of ozone in synthetic organic chemistry is the ozonolysis reaction. This was also first performed by Schönbein in 1847 when he mixed ozone with ethylene and noticed the smell of both vanished. In addition, he noted that reaction of ozone with organic materials did not yield fully oxidized CO_2, but a mixture of oxidation states such as carboxylic acids.[3]

This reaction involves the cycloaddition of ozone to an alkene to form a malozonide intermediate. Highly unstable, this quickly undergoes a retro cycloaddition to form the 'Criegee intermediate' which bears the name of the Rudolph Criegee, who elucidated this mechanism.[4] This intermediate undergoes another cycloaddition to form the final trioxolane intermediate. From this point, a reductive workup such as dimethyl sulfide can yield ketones or aldehydes, while an oxidative workup can yield carboxylic acids.

---

[2] Stoker, G. *The Lancet* **1916**, *188* (4860), 712.
[3] Schonbein, C. F. *Ber. Verh. Nat. Ges. Basel* **1847**, *7*, 7.
[4] Criegee, R. *Angew. Chem. Int. Ed. Engl.* **1975**, *14*, 745–752.

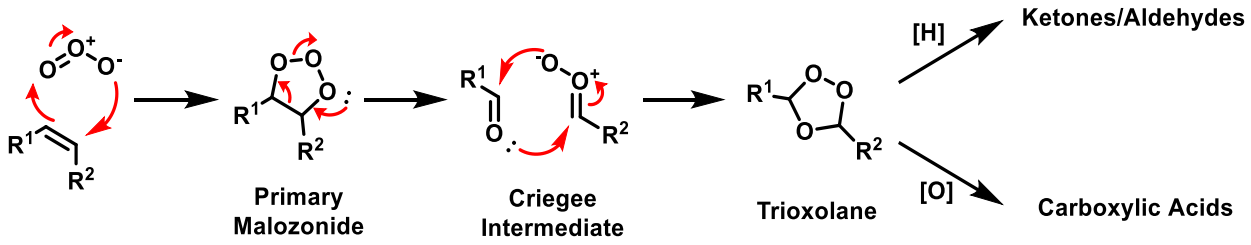

Scheme 1: Ozonolysis Mechanism with workup pathways

This reaction played a key role in early analytical chemistry for the purpose of determining location and number of double bonds in long carbon chains.[5]

1.1.2: Nitro Groups in Organic Synthesis

1.1.2.1:Alkyl Nitro Groups

Much less popular than its aromatic cousin, the alkyl nitro group contains an extreme amount of synthetic utility packed into a very small package. Due to the strong electron withdrawing nature, α-carbon bearing this functionality has a very strong partial positive charge associated with it. This makes it much more willing to undergo acidic, reductive and electrophilic paths, which form the core of reactivity associated with alkyl nitro groups. There is also the zwitterionic localization of negative charge on the oxygen atoms of the nitro group which give the whole assembly significant ambiphilic and amphoteric character (these moieties can be used in various paths as weak nucleophiles or weak bases).

[5] Rubin, M. B. *Helv. Chim. Acta* **2003**, *86*, 930–940.

1.1.3: Chemistry of the Nitro Group

1.1.3.1: Common Synthesis Routes to Nitro Compounds

A large variety of methods exist to access nitro compounds and virtually any functional group can be converted to a nitro group in a handful of steps.

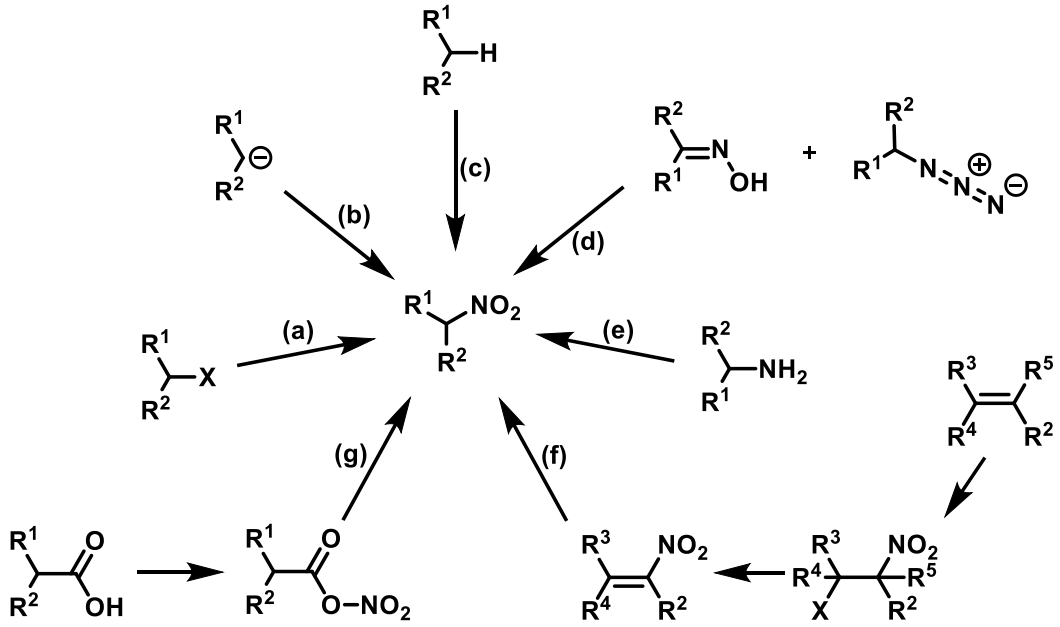

Scheme 2: Accessibility of alkyl nitro compounds

As seen in **Scheme 2**, alkyl nitro products can be accessed through either nucleophilic (path a) or electrophilic (path b) methods. By using nucleophilic sources of the nitro group, such as $AgNO_2$, halides can be displaced.[6] Other metal nitrite species can also be used, such as sodium nitrite, due to significantly lower costs. Alternatively, electrophilic nitrating agents such as fluorotrinitromethane[7] or alky nitrates[8] can provide a convenient source of nitronium ions to react with carbon-centered nucleophiles. C-H

[6] Meyer, V.; Stüber, O. *Berichte Dtsch. Chem. Ges.* **1872**, *5*, 203–205.
[7] Sitzmann, M. E.; Kaplan, L. A.; Angres, I. *J. Org. Chem.* **1977**, *42*, 563–564.
[8] Feuer, H.; Hall, A. M.; Golden, S.; Reitz, R. L. *J. Org. Chem.* **1968**, *33*, 3622–3624.

bonds can also be directly nitrated by using concentrated nitric acid (**Scheme 2** path c), but classically this has led to very poor selectivity and functional group tolerance as extreme temperatures are required.[9] This issue was resolved by Ishii, who developed a catalytic use of *N*-hydroxythalamide to enable direct nitration of alkanes under much milder conditions.[10] Oxidation of nitrogen-containing molecules can also provide a more direct path to nitro products. Particularly oximes, sometimes referred to as isonitroso groups, have been oxidized using a variety of methods, from regular nitric acid[11] to sophisticated transition metal complexes (**Scheme 2** path d).[12] Azides can also be oxidized in much the same way. Oxidation of amines in particular (**Scheme 2** path e) will be discussed in greater detail in section **1.1.4:** . Direct conversion of activated alkenes (α-β unsaturated ketones) into nitro compounds is possible in a single step by using nitrite salts, similarly to the previously mentioned displacement pathways.[13] But conversion of inactivated alkenes requires a preliminary nitrohalogenation, followed by elimination and oxidation reactions to yield the saturated nitroalkane (**Scheme 2** path f).[14] Alternatively, any of these subsequent steps could be changed if they are unnecessary for

[6] Meyer, V.; Stüber, O. *Berichte Dtsch. Chem. Ges.* **1872**, *5*, 203–205.
[7] Sitzmann, M. E.; Kaplan, L. A.; Angres, I. *J. Org. Chem.* **1977**, *42*, 563–564.
[8] Feuer, H.; Hall, A. M.; Golden, S.; Reitz, R. L. *J. Org. Chem.* **1968**, *33*, 3622–3624.
[9] Bachman, G. B.; Addison, L. M.; Hewett, J. V.; Kohn, L.; Millikan, A. *J. Org. Chem.* **1952**, *17*, 906–913.
[10] Isozaki, S.; Nishiwaki, Y.; Sakaguchi, S.; Ishii, Y. *Chem. Commun.* **2001**, *15*, 1352–1353.
[11] Usherwood, E. H.; Whiteley, M. A. *J. Chem. Soc. Trans.* **1923**, *123*, 1069–1089.
[12] Ballistreri, F.; Barbuzzi, E.; Tomaselli, G.; Toscano, R. *Synlett* **2000**, *1996*, 11, 1093–1094.
[13] Öhrlein, R.; Schwab, W.; Ehrler, R.; Jäger, V. *Synthesis* **1986**, 7, 535–538.
[14] Seebach, D.; Colvin, E. W.; Lehr, F.; Weller, T. *Chimia* **1979**, *33*, 1–18.

the desired synthetic transformation. Finally, carboxylic acids can also be converted into nitro groups through initial functionalization with nitric acid to form an acyl nitrate species. At elevated temperatures these species were found to undergo a decarboxylative nitration to yield nitroalkanes (**Scheme 2** path g).[15]

1.1.3.2: Alkyl Nitro molecules as Useful Intermediates

Alkyl nitro compounds are rarely the end point in a synthetic plan. Rather, their synthetic use stems from their ability to be a versatile intermediate that can be accessed from virtually any functional group, as seen above. From this point, oxidative, reductive, elimination and C-C bond forming processes are available at a variety of positions. This combination of wide accessibility of starting materials and diverse range of possible products is what inspired Dieter Seebach to – somewhat provocatively – dub them: "Ideal Intermediates in Organic Synthesis".[14]

Modifications at the Alpha Position

Two key reactions stand centre stage when it comes to synthetic modification at the α position of nitroalkanes: The Nef reaction, and the Henry Reaction.

The Nef Reaction

Discovered in 1894 by John Ulric Nef,[16] the Nef reaction provides a means to directly transform alkyl nitro species into carbonyls. This is accomplished through formation of a nitronate salt by treatment of nitroalkanes with a strong base. For synthetic

[15] Bachman, G.; Biermann, T. *J. Org. Chem.* **1970**, *35*, 4229–4231.
[16] Nef, J. U. *Justus Liebigs Ann. Chem.* **1894**, *280*, 263–291.

purposes, these nitronate salts can be formed *in situ* or directly used as starting materials. A plausible mechanism of the Nef reaction is illustrated in **Scheme 3**, highlighting some of the features that allow alkyl nitro molecules to be converted into useful products.

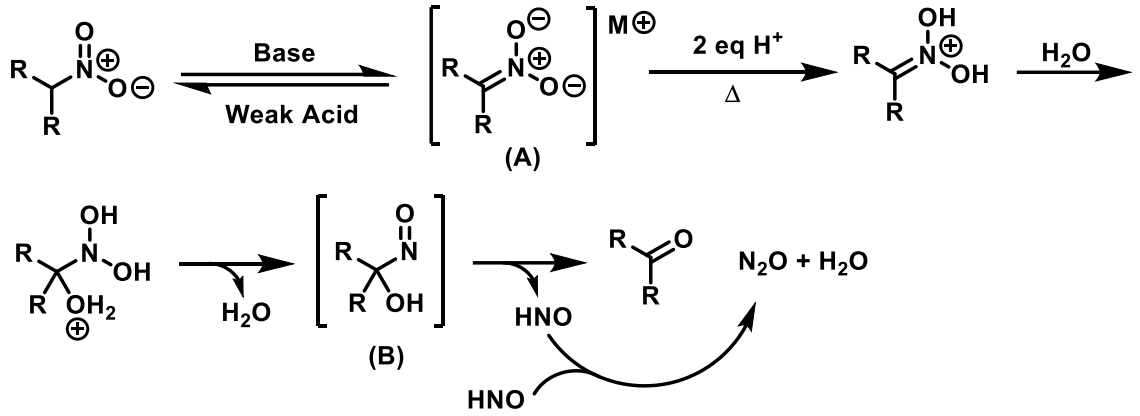

Scheme 3: Generally accepted reactive pathway for the Nef reaction

Contradictory to what might be expected at first glance, these nitronate salts **(Scheme 3** Intermediate **A**) are not trivial to turn back into their nitroalkane starting point once formed. Very dilute solutions of weak acids such as hydroxylamine hydrochloride, acetic acid, or carbonic acid are required to return to the nitroalkane in good yields at low temperatures. Otherwise, strong acids and higher temperatures yield exclusively the nitronic acid and favour the Nef reaction. The chemoselectivity between these forward and reverse paths seems to he heavily based on the stabilization of the nitronate intermediate. Resonance is normally viewed as a promoting effect in reaction kinetics, usually involving stabilization of an intermediate. However, in this case, resonance has a negative effect on the forward reaction, and instead promotes reformation of the alkyl nitro species even when strong acids are employed. This is due to increased stabilization

of the starting material making forward reaction unfavourable. This swap in selectivity can be seen in **Scheme 4** with such molecules as phenylnitromethane.[17]

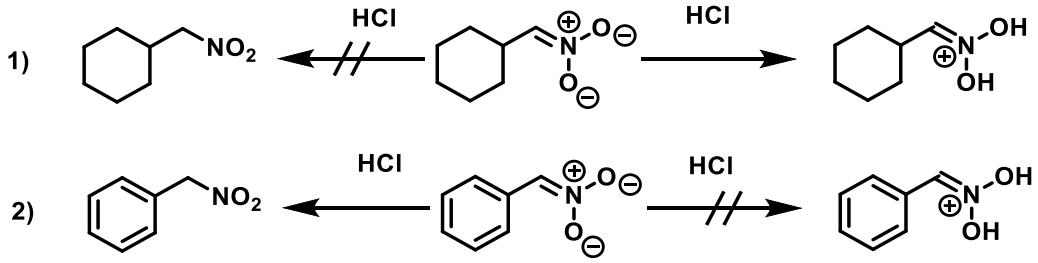

Scheme 4: Path selectivity dependence on resonance

After protonation of the nitronate salt forms the nitronic acid, it becomes very prone to isomerization, catalyzed by addition, proton transfer and elimination of water at the α position. This leaves an α hydroxy nitroso compound signaled by the appearance of a green/blue colour (**Scheme 3** Intermediate **B**).[18] While these nitroso intermediates have never been isolated directly as mechanistic proof, they are very prone to dimerization under the right conditions. Thus, a very closely related dimer of 1-chloro-1-nitrosoethane was isolated by Steinkopf and Juergens[19] to provide some generally accepted proof of the mechanistic pathway. In any case, the nitroso intermediate *in situ* can then rapidly undergo expulsion of nitroxyl to form the desired carbonyl. Two of these nitroxyl molecules can combine to form an equivalent of nitrous oxide and an equivalent of water.

[17] Kornblum, N.; Graham, G. E. *J. Am. Chem. Soc.* **1951**, *73*, 4041–4043.
[18] Bamberger, Eug.; Rüst, E. *Berichte Dtsch. Chem. Ges.* **1902**, *35*, 45–53.
[19] Steinkopf, W.; Jürgens, B. *J. Für Prakt. Chem.* **1911**, *84*, 686–713.

There have been many modifications to the Nef reaction, using its general reactive groundwork to arrive at slightly different products. For instance, if dry HCl is used instead of aqueous, the mechanism is modified to yield α-chloro nitroso compounds as seen in **Scheme 5** (or oximes if a tautomerization is possible). Alternatively, strong acids have also been used to yield carboxylic acids as final products.[20] While these modifications technically exclude these reactive paths from being true Nef reactions, they are similar enough to be included in a general overview.

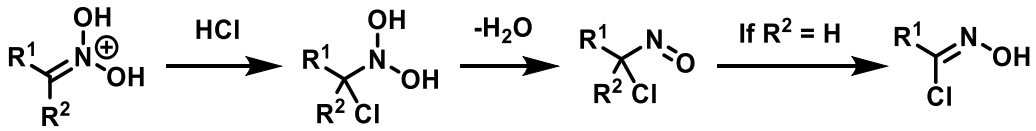

Scheme 5: Alternate path of Nef reactivity

Henry Reaction

The second reaction that forms a cornerstone of alkylnitro utility is the Henry reaction. This carbon-carbon bond forming reaction is sometimes referred to as the "nitro-aldol" reaction, due to its similarity to the classic aldol addition. A plausible mechanism is presented in **Scheme 6**. Similar to the Nef reaction, the Henry reaction begins with the deprotonation of the nitroalkane, at the α position. However, unlike the Nef reaction, no acid is added at this point and instead, the addition of a ketone or aldehyde promotes the attack in the same fashion as an enolate, which is where the comparison between this reaction and the aldol reaction is drawn.

[20] Hass, H. B.; Riley, E. F. *Chem. Rev.* **1943**, *32*, 373–430.

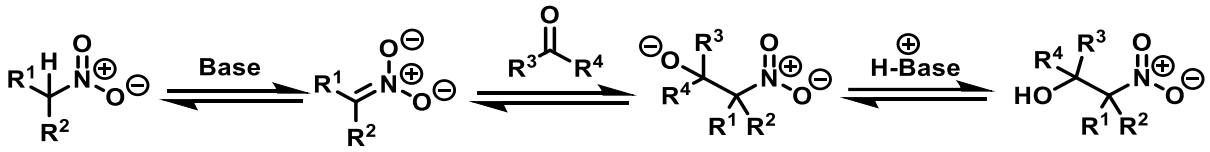

Scheme 6: General mechanism of the Henry reaction

After protonation, the initial reaction yields β-nitro alcohols. However, the true synthetic utility of the Henry reaction only begins with these products, as they require only trivial transformations to access a wide array of potential targets as can be seen in **Scheme 7.**[21] For example, dehydration (**Scheme 7** path **a**) of these β-nitro alcohols will yield nitroalkenes, which can be further reduced to yield a nitroalkane furnished with the groups on the ketone or aldehyde. If aldehydes were used then oxidative pathways will yield α-nitro ketones, which then opens all the doors typically available with carbonyl chemistry. On the other hand, reductive pathways (**Scheme 7** path **b**) will strip the nitro group down to β-amino alcohols, an interesting pair of functionalities ready to undergo more bond forming processes. Alternatively, other transformations using the nitro group could be employed to build further functionality into the molecule.

[21] Ono, N. *The Nitro Group in Organic Synthesis*; Feuer, H., Series Ed.; Wiley Series in Organic Nitro Chemistry; John Wiley & Sons, Inc.: New York, USA, 2001.

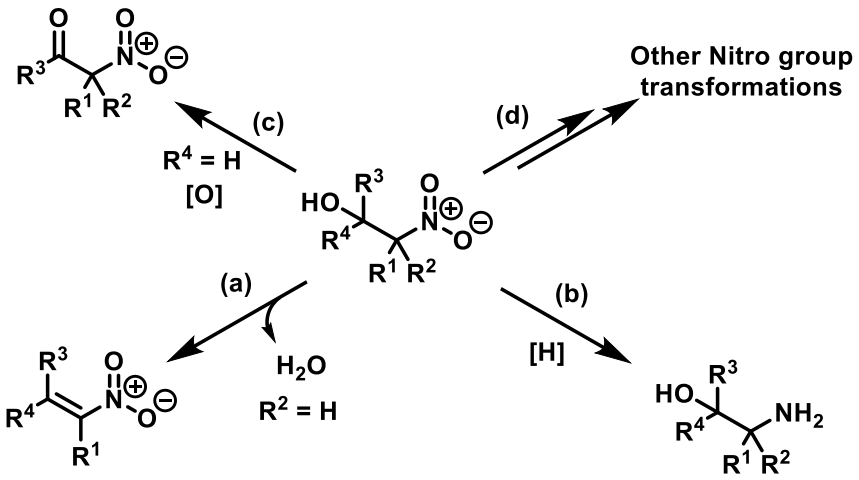

Scheme 7: Possible paths after the Henry reaction

One important use of the Henry reaction is in the generation of two chiral centres. However, each individual step of the reaction scheme is reversible, presenting a significant problem of epimerization and loss of stereochemical information when performing the reaction without additives. That is why most developed uses of the Henry reaction involve some sort of modification to help induce stereochemical selectivity and drive material conversion to products. The first instance of an enantioselective Henry

reaction seen in **Scheme 8**) appeared in 1992 by Shibasaki using heterobimetallic catalysis and rare earth metals to achieve good yields and moderate enantiomeric excess.[22,23]

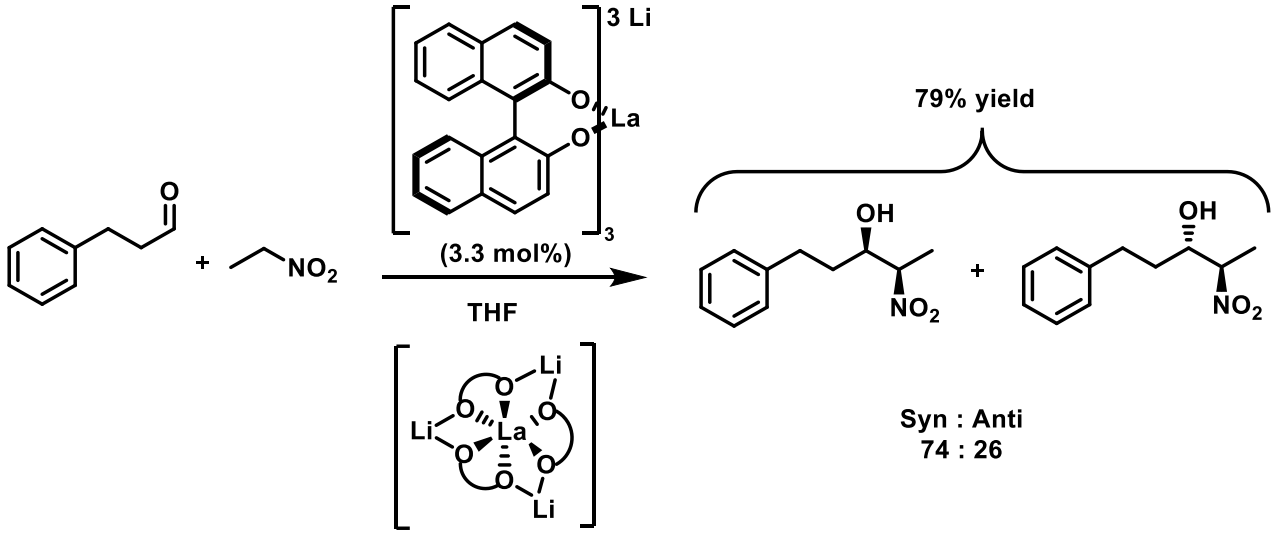

Scheme 8: Shabisaki's discovery of asymmetric Henry reactions

These catalysts, as with most reactions with chiral ligands, work by biasing the favoured conformation at the transition state, effectively creating diastereomers based on the molecule's interactions with the ligand/complex. In this case, the authors found a modest selectivity for the *syn* isomer. They proposed that this is due to rotation of the Newman projection favouring the *syn* isomer as it causes the least steric tension between the substituents and the extremely bulky [La(binol)$_3$Li$_3$] catalyst, as can be seen in **Scheme 9**.[24]

[22] Shibasaki, M.; Sasai, H.; Arai, T. *Angew. Chem. Int. Ed. Engl.* **1997**, *36*, 1236–1256.
[23] Sasai, H.; Suzuki, T.; Arai, S.; Arai, T.; Shibasaki, M. *J. Am. Chem. Soc.* **1992**, *114*, 4418–4420.
[24] Dong, L.; Chen, F.-E. *RSC Adv.* **2020**, *10*, 2313–2326.

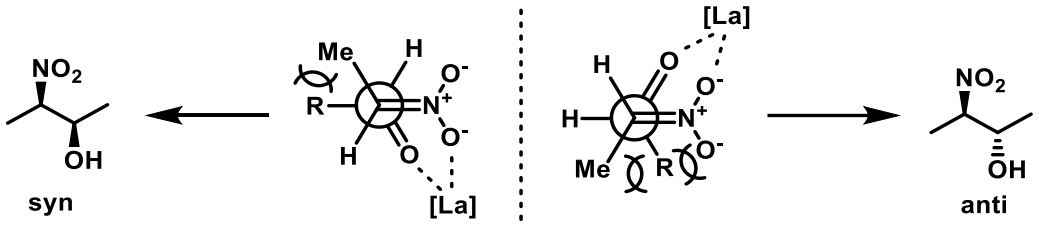

Scheme 9: Most stable transition states for *syn* and *anti* configurations.

In the following thirty years since this approach was developed, many different variations and ideas have spawned using similar methodology including traditional transition metal catalysts with chiral ligands such as palladium[25] and copper.[26] Organocatalysts featuring such moieties as thioureas,[27] guanidine derivatives,[28] and even chiral phosphine catalysts[29] have been employed as well with similar effectiveness.

Modifications of Nitro Group

The Henry and Nef reactions (and their variations) offer a powerful set of tools to perform transformations using nitro groups as a central key. If these α and β transformations are all that is needed, the nitro moiety can be easily and cleanly cleaved using a combination of AIBN and tributyltin hydride once it has served its purpose (**Scheme 10** path a).[30] Alternatively, direct manipulation of the nitro group itself can lead

[25] Handa, S.; Nagawa, K.; Sohtome, Y.; Matsunaga, S.; Shibasaki, M. A. *Angew. Chem. Int. Ed.* **2008**, *47*, 3230–3233.
[26] Christensen, C.; Juhl, K.; Jorgensen, K. A. Catalytic *Chem. Commun.* **2001**, *21*, 2222–2223.
[27] Marcelli, T.; van der Haas, R. N. S.; van Maarseveen, J. H.; Hiemstra, H. *Angew. Chem. Int. Ed.* **2006**, *45*, 929–931.
[28] Sohtome, Y.; Hashimoto, Y.; Nagasawa, K. *Eur. J. Org. Chem.* **2006**, *2006*, 2894–2897.
[29] Ooi, T.; Uraguchi, D.; Sakaki, S. *J. Am. Chem. Soc.* **2007**, *129*, 12392–12393.
[30] Ono, N.; Miyake, H.; Tamura, R.; Kaji, A. *Tetrahedron Lett.* **1981**, *22*, 1705–1708.

to a variety of nitrogen containing functional groups. These products can, in theory, all be used to facilitate subsequent transformations and synthetic steps.

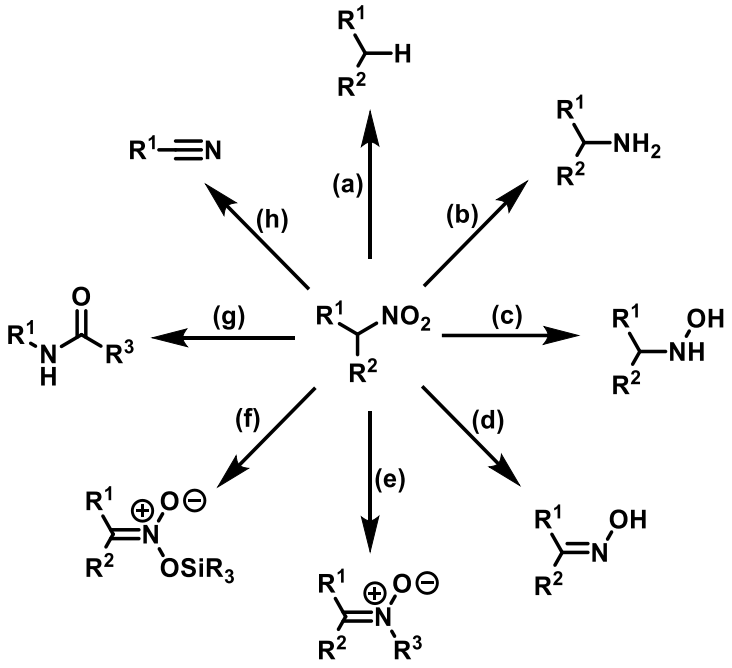

Scheme 10: Synthetic transformations of the nitro group

Being such a highly oxidized functional group, there are a great number of reductive pathways that nitro groups can take to access analogous nitrogen containing moieties. Some of these paths can include hydrogenation with a variety of catalytic metals such as Pd/C, Ra-Ni, or PtO_2 to access amines (**Scheme 10** path b). Other methods can include iron catalysis in refluxing AcOH, or simple reduction with $LiAlH_4$. If less reduced intermediates want to be targeted, gentler reducing paths can be chosen to stop the reaction before the fully reduced amine is obtained. Some examples include reaction with zinc dust in ammonium chloride to yield the doubly reduced hydroxylamine **(Scheme 10** path c).[31] Nitro groups can also be converted to their nitronate salt form, then reduced to

hydroxylamines by using diborane reagents.[32] These reductive paths can occur with retention of any stereochemistry that the nitro group had. Oximes are also a feasible target for nitro starting materials and can be accessed through a series of metal salts such as stannous[33] or chromium (II) chloride (**Scheme 10** path d).[34] Additionally, hydrogenation reactions as described above can be employed if tight control of hydrogen equivalence can be achieved.[35] Nitrones can be accessed through direct attack of strong nucleophiles such as carbanions or Grignard reagents (**Scheme 10** path e). However, this synthetic pathway appears to be highly dependent on the exact identity of nitro and carbanion. With many nitrones being base sensitive, there exists a significant barrier to their generation, while preventing degradation.[36]

A less common nitro group derivative, silyl nitronates are extremely useful for synthesis of heterocycles. Unlike other precursors that have been used to perform this transformation, silyl nitronates are stable enough to retain a configuration, making them ideal precursors to chiral heterocycles such as isoxazolines via [1,3] dipolar cycloadditions.[37,38] They are quite easily synthesized from nitro groups via an interrupted

---

[31] Lee, T.; Keana, J. *J. Org. Chem.* **1976**, *41*, 3237.
[32] Feuer, H.; Bartlett, R. S.; Vincent, B. F.; Anderson, R. S. *J. Org. Chem.* **1965**, *30*, 2880–2882.
[33] Bartra, M.; Romea, P.; Urpí, F.; Vilarrasa, J. *Tetrahedron* **1990**, *46*, 587–594.
[34] Hanson, J. R.; Premuzic, E. *Tetrahedron* **1967**, *23*, 4105–4110.
[35] Grundmann, C. *Angew. Chem.* **1950**, *62*, 558–560.
[36] Hassner, A.; Fitchmun, D. R. *Tetrahedron Lett.* **1966**, *7*, 1991–1995.
[37] Jiang, M.; Feng, L.; Feng, J.; Jiao, P. *Org. Lett.* **2017**, *19*, 2210–2213.
[38] Dong, L.; Geng, C.; Jiao, P. *J. Org. Chem.* **2015**, *80*, 10992–11002.

Henry reaction (see above), quenched with an electrophilic source of silicon, such as trimethylchlorosilane (**Scheme 10** path f).[39] Nef-like reactions, as stated previously, can be altered to arrive at a wide range of products. One example of this is the use of umpolung (polarity reversal) reactivity and a halogenation mixture of *N*-iodosuccinimide and 1,2-dibromotetrachloroethane to yield a two step, one pot method to access functionalized amides (**Scheme 10** path g).[40,41] Finally, nitro to nitrile transformations (**Scheme 10** path h) can be facilitated by using a mixture of isocyanides and isocyanates along with a base.[42]

Therefore, it has been shown that with the right planning in a total synthesis, nitro groups can provide extremely useful shortcuts to transform almost any common functional group into any other in only a handful of steps.

1.1.4: Oxidation of Amines

1.1.4.1: General Methods for Amine Oxidation

Oxidation of aromatic amines (e.g. anilines) is relatively easy, and able to be achieved by mild oxidants such as *m*-CPBA[43] and hydrogen peroxide.[44] However, there are a limited number of ways to perform alkyl amine oxidations to nitro groups, most

[39] Colvin, E. W.; Seebach, D. *J. Chem. Soc. Chem. Commun.* **1978**, 16, 689.
[40] Shen, B.; Makley, D. M.; Johnston, J. N. *Nature* **2010**, *465*, 1027–1032.
[41] Schwieter, K. E.; Johnston, J. N. *Chem. Commun.* **2016**, *52*, 152–155.
[42] Kaim, L. E.; Gacon, A. *Tetrahedron Lett.* **1997**, *38*, 3391–3394.
[43] Liu, J.; Li, J.; Ren, J.; Zeng, B.-B. *Tetrahedron Lett.* **2014**, *55*, 1581–1584.
[44] Voutyritsa, E.; Theodorou, A.; Kokotou, M. G.; Kokotos, C. G. *Green Chem.* **2017**, *19*, 1291–1298.

involving very harsh reagents and undesirable conditions. One of these such undesirable reagents is Caro's acid (H_2SO_5), an extremely strong peroxide which is known to be prone to spontaneous explosions.[45] In addition to being extremely hazardous, it normally yields product as a mixture of oxidation states, making it both unsafe and unreliable as a reagent.[46,47] Alternatively, Rozen and co-workers developed an oxygen transfer reagent generated from fluorine gas, MeCN, and water. This forms a hypoflourous acid–MeCN complex, which is reported to be decently stable and safe to work with by its developers.[48,49] However, use of this reagent does require the presence and operation of a source of F_2 gas. The safety hazards associated this cannot be understated, as F_2 gas is extremely toxic,[50] and presents a significant explosion hazard if at all mishandled due to its extreme reactivity.[51]

Other oxidants can be used to avoid the above safety risks; however they come with their own, less severe, concerns. *m*-CPBA or other related organic peroxides are often the preferred choice to perform this type of oxidation and the reaction conditions have been well optimized.[52,53] However, *m*-CPBA in particular is notorious for having an

---

[45] Safety. *Chem. Eng. News* **1955**, *33*, 3336.
[46] Bamberger, E.; Seligman, R. *Berichte Dtsch. Chem. Ges.* **1903**, *36*, 685–700.
[47] Bamberger, E.; Seligman, R. *Berichte Dtsch. Chem. Ges.* **1903**, *36*, 701–710.
[48] Rozen, S.; Kol, M. *J. Org. Chem.* **1992**, *57*, 7342–7344.
[49] Rozen, S.; Bar-Haim, A.; Mishani, E. *J. Org. Chem.* **1994**, *59*, 1208–1209.
[50] Keplinger, M. L.; Suissa, L. W. *Am. Ind. Hyg. Assoc. J.* **1968**, *29*, 10–18.
[51] Fluorine; MSDS No. 001061 [Online]; Airgas: Radnor, PA, April 25, 2003. https://www.airgas.com/msds/001061.pdf accessed 07/7/21).
[52] Gilbert, K. E.; Borden, W. E. *J. Org. Chem.* **1979**, *44*, 659.
[53] Robinson, C. H.; Milewich, L.; Hofer, P. *J. Org. Chem.* **1966**, *31*, 524–528.

extremely poor atom economy. The transformation of amines to nitro groups requires three sequential oxidations, meaning a minimum of three equivalents of oxidant is required. *m*-CPBA has a molecular weight of 172.57 g/mol and over the course of these three oxidations only adds two oxygen atoms to the product. If the oxidation of butylamine to nitrobutane is used as an example, it can be seen in **Scheme 11** that the reaction only has an atom economy of 17%.

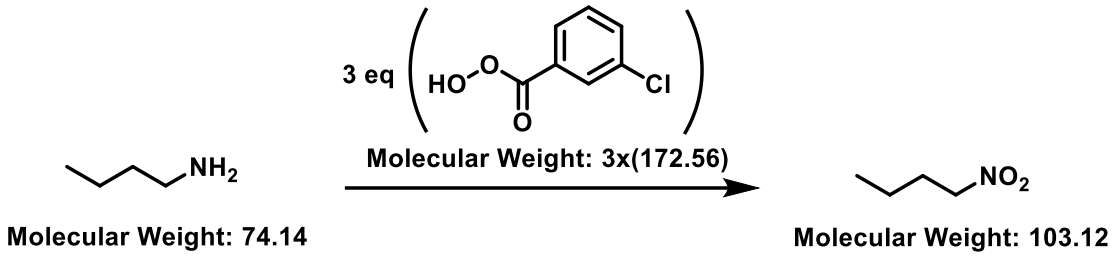

$$AE = \frac{\text{MW of Products}}{\text{MW of Reactants}}(100\%) = \frac{103}{74 + 3(172)}(100\%) = 17\%$$

Scheme 11: Atom economy of *m*-CPBA mediated amine oxidation

An alternative to *m*-CPBA with a better atom economy is dimethyldioxirane, but this comes with its own set of issues as well. Dimethyldioxirane is prepared from acetone and oxone and can either be synthesized ahead of time and stored, or made *in situ* (see **Scheme 12**). If generated ahead of time, typically a solution of around 0.1 M concentration in acetone is obtained. This must be stored at -20 °C over drying agents and used within a week to avoid degredation.[54] Co-solvent quantities of this solution must be used to perform amine oxidations to minimize side product formation.

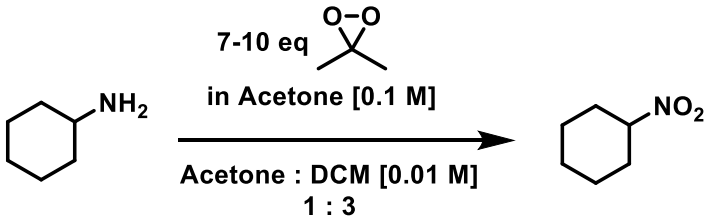

Scheme 12: Oxidation of cyclohexylamine with dimethyldioxirane

If generated in situ, a large excess of oxone (e.g. 20 equiv) is generally employed to try and maximize product formation.[55] While these seem stringent restrictions, this method is not without its benefits, and extremely mild reaction conditions make it an attractive option for oxidation of a great number of substrates in good to excellent yields.[56] However, the amount of waste generated must be a considered when evaluating the 'greenness' of this approach, as extremely dilute solutions to generate the reagent and perform the reaction are often employed.

The third mild strategy involves the use of more traditional peroxides such as hydrogen or *tert*-butyl hydrogen peroxide. However, these oxidants usually require the presence of an additive to facilitate this transformation. Some examples of these additives can include catalysts such as zirconium (IV) *tert*-butoxide,[57] chromium silicalite-2,[58] and phosphotungstic acid.[59] Furthermore, extremely high concentrations (>70%) of these

[54] Crandall, J. K.; Batal, D. J.; Sebesta, D. P.; Lin, F. *J. Org. Chem.* **1991**, *56*, 1153–1166.
[55] Crandall, J. K.; Reix, T. *J. Org. Chem.* **1992**, *57*, 6759–6764.
[56] Murray, R. W.; Jeyaraman, R.; Mohan, L. *Tetrahedron Lett.* **1986**, *27*, 2335–2336.
[57] Krohn, K.; Kupke, J. *Chem. Eur. J.* **1998**, 679–682.
[58] Jayachandran, B.; Sasidharan, M.; Sudalai, A.; Ravindranathan, T. *J. Chem. Soc. Chem. Commun.* **1995**, *15*, 1523.
[59] Rassat, A.; Rey, P. *Tetrahedron* **1974**, *30*, 3315–3325.

peroxides are usually employed, which starts to reintroduce the above health and safety hazards such as explosion risk and toxicity if inhaled.

1.1.4.2: Amine Ozonation

The first step in discovering amine ozonation to form nitro groups was made by Horner in 1958, whereupon he found that ozone could electrophilically attack tertiary amines to form amine oxides.[60] This initial discovery was further explored by Bailey, who found that primary amines proceed through an identical first intermediate as the tertiary amines, but are able to undergo further oxidations to yield triply oxidized nitroalkanes.[61] However, these oxidations are plagued by a slew of side reactive pathways which give rise to significant amount of product degradation if not properly controlled. Some plausible intermediates in the transformation of amines to nitroalkanes proposed by Bailey and co-workers is presented in **Scheme 13**.[61,62]

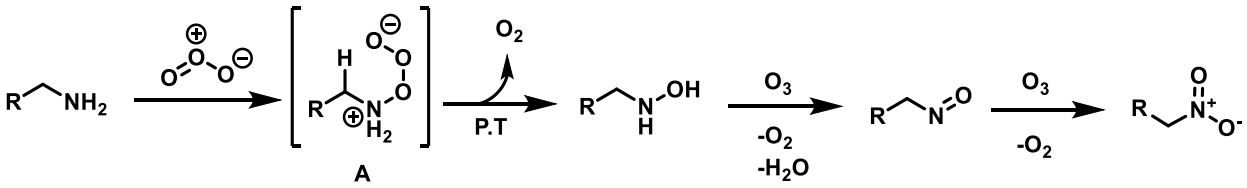

Scheme 13: Proposed reaction path

[60] Horner, L.; Schaefer, H.; Ludwig, W. *Chem. Ber.* **1958**, *91*, 75–81.
[61] Bailey, P. S.; Keller, J. E.; Mitchard, D. A.; White, H. M. Ozonation of Amines. In *Oxidation of Organic Compounds*; Mayo, F. R., Ed.; Advances in Chemistry; American Chemical Society: Washington, D.C., 1968; Vol. 77, pp 58–64.
[62] Bailey, P. S.; Michard, D. A.; Kashhab, A.-I. Y. *J. Org. Chem.* **1968**, *33*, 2675–2680.

Intermediate A eliminates O_2 (most likely in the singlet electronic state, which would also have oxidative implications) to form a hydroxylamine which, upon a second addition of ozone and subsequent elimination of O_2, can lose water to form a nitroso group. A third and final addition of ozone (and elimination of oxygen) yields the final nitro product.

Intermediate A has also been implicated as a major source of decomposition, resulting in multiple paths of side chain oxidation and product degradation. These paths, the resulting products, and mechanistic proposals for how they came about from a variety of starting materials have been thoroughly investigated by Bailey and coworkers over the course of a series of publications regarding ozonation of amines.[61–66] A general overview of the relevant information obtained by Bailey will be presented herein.

Reaction (**1**) in **Scheme 14** shows deprotonation to form an imine, which can then be attacked by the same ozone equivalent to form an α,α-amino alcohol. Bailey proposed that either further reaction with ozone can be convert this to an amide, or dehydration can lead to an allylic amine, which can then be quickly cleaved via ozonolysis. Alternatively, reaction (**2**) shows that intermediate **A** can undergo homolysis to form a radical pair.

---

[63] Bailey, P. S.; Keller, J. E. *J. Org. Chem.* **1968**, *33*, 2680–2684.
[64] Bailey, P. S.; Keller, J. E.; Carter, T. P. *J. Org. Chem.* **1970**, *35*, 2777–2782.
[65] Bailey, P. S.; Keller, J. E. *J. Org. Chem.* **1970**, *35*, 2782–2785.
[66] Bailey, P. S.; Carter, T. P.; Southwick, L. M. *J. Org. Chem.* **1972**, *37*, 2997–3004.

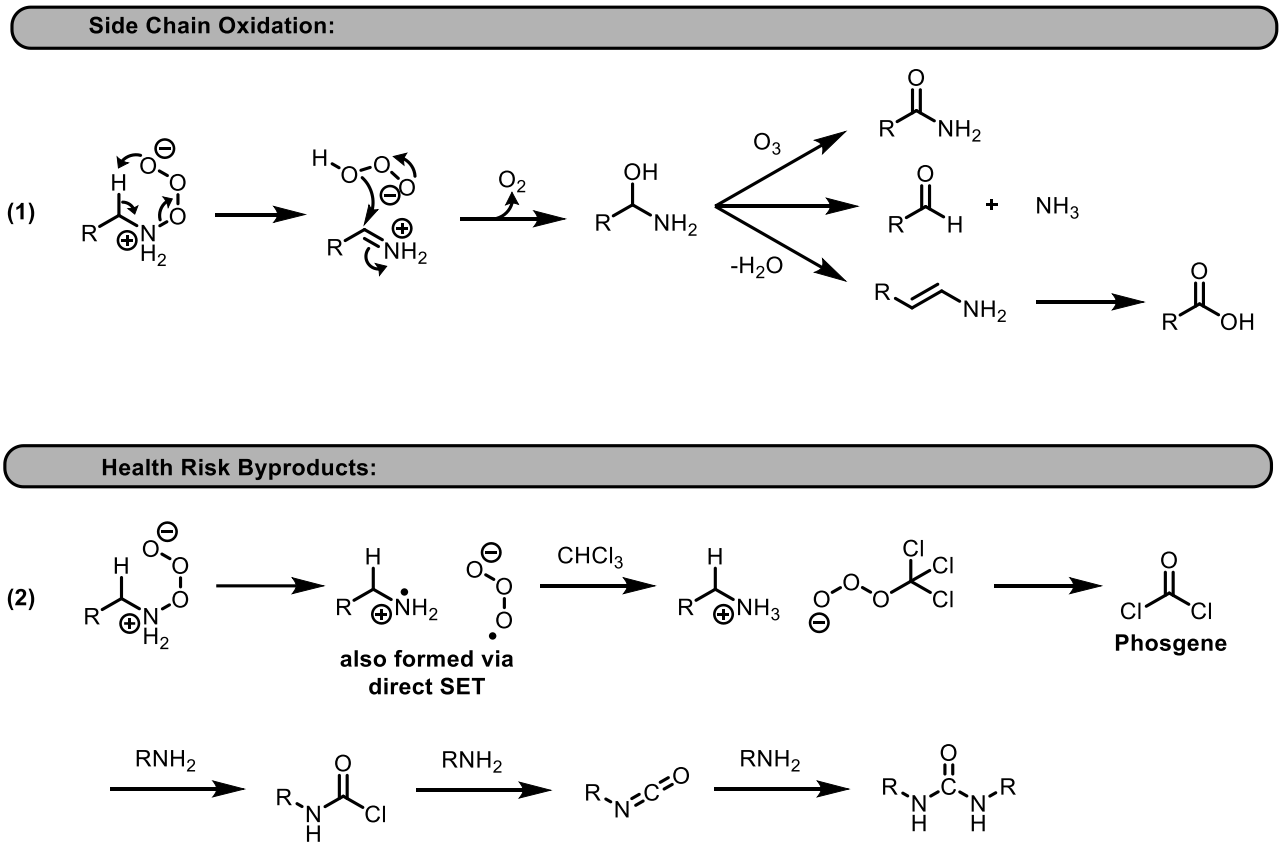

Scheme 14: Side chain oxidations

It should be noted that these radicals can pose a significant health risk if this reaction is performed in solvents such as chloroform (as was commonly done in the early days of its research). Abstraction of the lone hydrogen on chloroform by the nitrogen radical cation, followed by radical addition of the ozone can result in significant formation of phosgene in the reaction solution (reaction **2** in **Scheme 14**). Bailey rationalized this hypothesis through observation of amine chloride salts. Furthermore, this phosgene can react with more equivalents of starting amine to form isocyanates. While significantly less toxic than phosgene, isocyanates are far from harmless, and still present a significant health hazard.[67] The isocyanate product can also consume *another* 2

equivalents of amine starting material to form a final urea, or undergo dimerization reactions, as they are known to do.[68] With all these side paths available to this reaction, control proves to be a requirement of paramount importance to ensure acceptable selectivity and yield.

Mazur revisited this chemistry almost a decade later by applying a new methodology he had developed which allowed removing the most problematic part of the reaction: the solvent. By first adsorbing starting materials onto a silica gel matrix, ozonation could be performed in absence of organic solvent (**Scheme 15**). This allowed Mazur to study the reaction quite closely, discovering many interesting characteristics and requirements.[69]

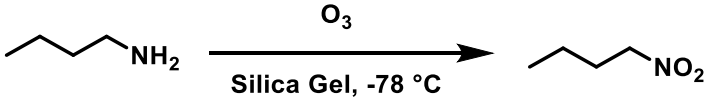

Scheme 15: Ozone mediated amine oxidation on silica gel

His first finding was that lower concentrations of amine on the silica gel led to higher yields of nitroalkane, and an improved mass balance. This was rationalized that after the physical surface of the silica gel grains were coated with monolayer of amine,[70] any additional amine would be able to undergo intermolecular reactions with the

[68] Parodi, F. Isocyanate-Derived Polymers. In *Comprehensive Polymer Science and Supplements*; Elsevier, 1989; pp 387–412.
[69] Keinan, E.; Mazur, Y. *J. Org. Chem.* **1977**, *42*, 844–847.
[70] Rosen, M. J.; Eden, C. *J. Phys. Chem.* **1970**, *74*, 2303–2309.

oxidation intermediates and lead to unproductive side paths. For this reason, Mazur's batch methods never exceeded a concentration of 0.2% w/w of amine on the silica gel. For reference, that means that each gram of silica gel would only be able to tolerate ~20 mg of amine. Secondly, he found that the temperature of the reaction correlated strongly with yield, as is usually expected. However, in this case, lower temperatures led to higher product conversion. This is due to the lower temperatures on the reaction increasing the solubility of ozone as it is passed over the silica gel, increasing reaction rate. Interestingly, he also identified an acute sensitivity to moisture which could lower yields by as much as 50% with only 5% water present in the silica gel. Thus, rigorously oven and vacuum dried silica gel was used for all his experiments. Finally, he identified that product degradation started as soon as any product was formed and, consequently, reaction time would have to be tightly controlled to achieve the maximum yield before degradation started outcompeting product formation.

1.2: Project Goals

Just as Mazur improved on the work of Bailey, so too did we seek to improve on the work of Mazur. With no one having touched this area of research in so long, it seemed clear that it faced some fundamental problems that inhibited its use and development. We identified these problems as: a severely lacking substrate scope; containing only very simple aliphatic amines, and significant barriers to scaling the reaction; involving very extended reaction times and substantial waste of silica gel. We sought to develop and

provide solutions to these problems by adapting Mazur's batch method to a continuous flow approach using a packed column containing starting material impregnated silica gel.

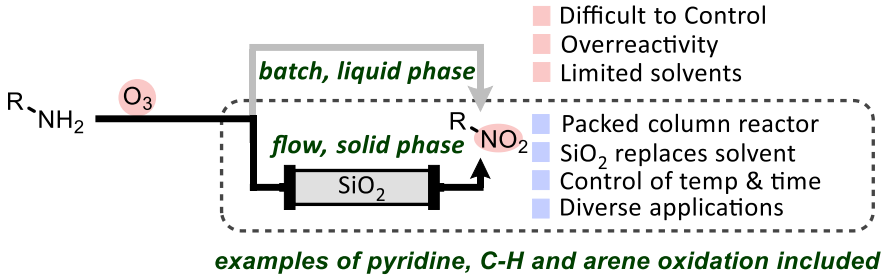

Scheme 16: Overview of proposed solution

Our hypothesis was based upon the lack of control that was observed in Mazur's method, specifically regarding ozonation time. By simply exposing silica gel to a flow of ozone in oxygen and looking for a qualitative change to indicate saturation, there is no precise control over how long that may take or how many equivalents of ozone are getting the chance to react. Given the aggressive nature of ozone, dialing in a specific contact time at a specific temperature is important but challenging in a batch system. In the batch system, silica gel and adsorbed substrate are chilled to cryogenic temperatures, saturated with O_3, and allow to age for an appropriate amount of time before stopping the O_3 stream and warming to room temperature. We proposed that a packed column reactor would allow more precision. Controlling temperature, saturating the system with O_3, and terminating the reaction by flushing with O_2 may be achieved more efficiently due to the compact size of the system and the improved contact between the gas and solid

phases in the column relative to a flask. Furthermore, these problems of heat and mass transfer are only exacerbated in batch when the reaction is attempted at scale, as the silica gel required (100x the weight of the starting material) will get exponentially worse at dispersing ozone and temperatures evenly throughout the reaction matrix. The reaction times required to achieve sufficient cooling, ozone saturation, and warming also quickly becomes synthetically impractical (44 mmol [500g silica gel] reaction time requirements: 2h for suspension, 2h for cooling, 2h for ozonation, 3h for warming).

1.3: Results and Discussion

Our group had spent some time previously trying to gain a base of knowledge regarding potential reactivity of ozone, and how much control could be attained using flow chemistry. This was started by Dr. Jaya K. Vandavasi, who reproduced the studies of Mazur and conducted a rigorous comparison of how 'batch' versions of this chemistry compared to our 'flow' version. It should be noted that at the time of optimization, Dr Vandavasi's investigation was concerning oxidations of C-H bonds to form tertiary alcohols, which will be briefly discussed in section **1.3.3**: . Regardless, it was found that the adaptation to a flow system yielded comparable results to those of the batch process and, upon starting my graduate studies, I began investigating whether the flow system could be applied to amine oxidation.

1.3.1: Optimization of Ozone-Mediated Amine Oxidation

To overcome the limitations of challenging ozone-mediated oxidations, a reactor featuring ease of cooling to cryogenic temperatures, facile loading and harvest of silica gel, and in line connection to the ozone/oxygen source. This was ultimately realized by utilizing the Vapourtec 'cooled column' reactor that could be connected to an ozone generator (and by consequence, to the oxygen source), as can be seen in **Figure 1**.

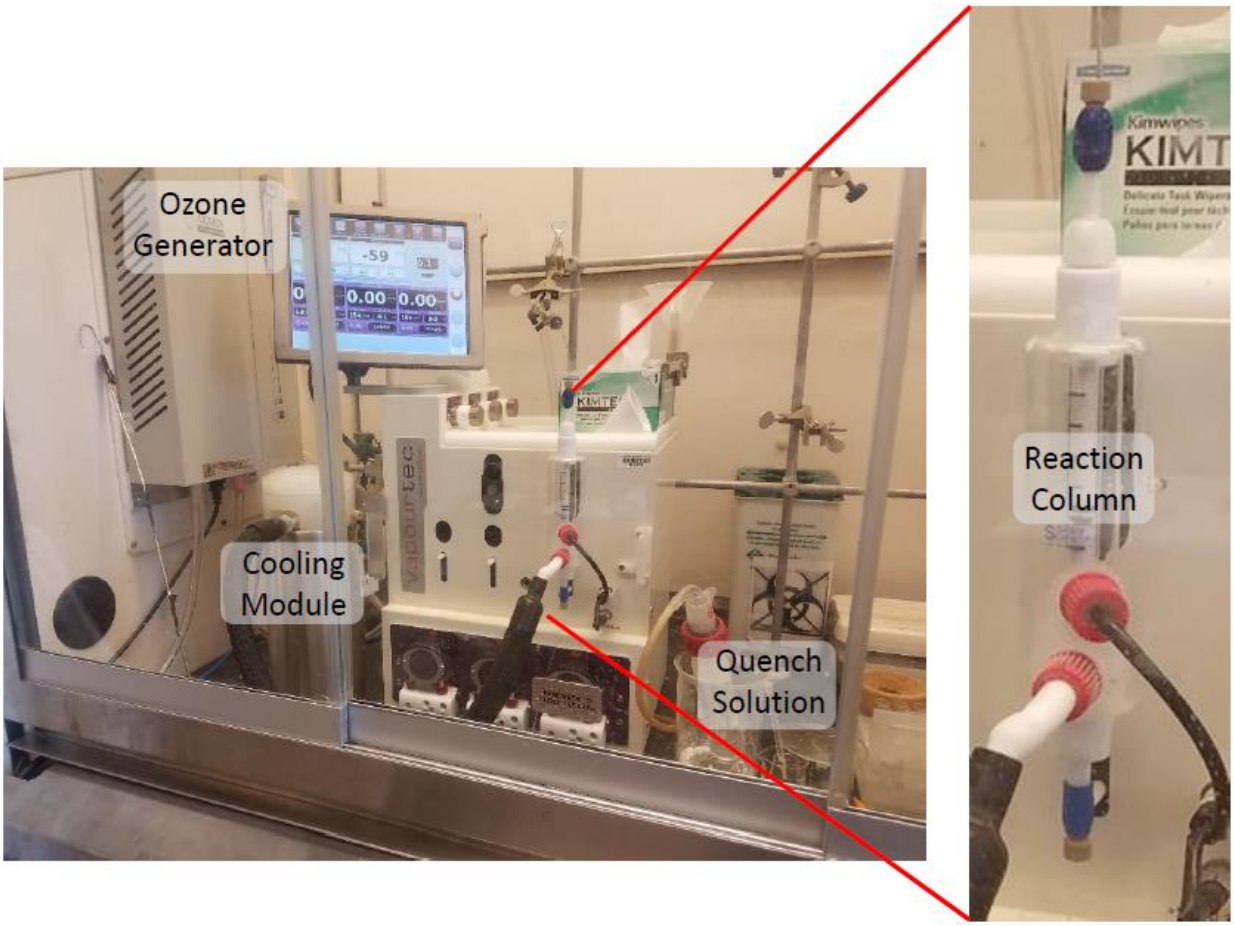

Figure 1: Photograph of the complete reactor setup

The ozone generator has an inlet tube (going into the generator) and an outlet tube (exiting the generator). The inlet tube is connected to an O_2 tank, and acts as the source of oxygen for the generator to convert to ozone. The outlet tube, containing a percentage of

ozone in a stream of oxygen, is connected directly to the top (inlet) of our reaction column. This gas flows along the length of the reaction, before exiting at the bottom (outlet) of the reaction column.

The labeled quench solution in **Figure 1** contains an aqueous solution of sodium metabisulfite, and all oxygen/ ozone flow from the reaction column outlet is bubbled through this solution before it is allowed to exit into the atmosphere. This is to prevent excess and repeated ozone exposure to the interior of the fumehood, and should be replaced regularly for the safety of the operator.

The cooling module labeled in **Figure 1** is filled with dry ice before the reaction can proceed and connected to a tank of N_2 gas. This gas functions as a carrier for the cooling power of the dry ice and when the thermometer reports the reaction is warming, this cold N_2 is automatically allowed to flow into the glass jacked surrounding the reaction column, where the thermometer reads the cooling, and automatically shuts off this flow when desired temperature has been reached again. We observed that this system keeps the reaction at the set temperature usually ± 1 °C.

With this design, we are able to accurately control exact temperature of the reaction vessel using an automated thermometer that will automatically maintain this set temperature for the course of the entire reaction. Additionally, by using an in-line ozone generator, ozone production can be switched off at a desired time while maintaining O_2

flow to purge ozone off the silica gel in a matter of seconds (indicated by colour change). It is our belief that these mechanisms of greater control have a significant effect on our ability to perform this reaction effectively and with greater functional group tolerance.

Using this reactor, the oxidation of dodecylamine was studied (**Table 1**). Initial results suggested rapid conversion of the amine to the nitroalkane at temperatures of -20 °C for reaction times of 1-15 mins (see **Table 1** Entries 1-4). Notably, this is significantly faster than previous studies on ozone-mediated tertiary C-H hydroxylation, which necessitates an hour or more long reaction time at -20 °C.

Table 1: Optimization Data for Time and Temperature[a]

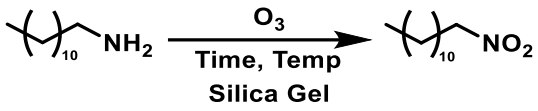

Entry	Temperature (°C)	Time	Product (%)	Starting Material (%)
1	-20	1 min	32	33
2	-20	5 min	50	n/a
3	-20	10 min	60	n/a
4	-20	15 min	52	n/a
5	-40	10 sec	10	47
6	-40	5 min	23	40
7	-40	15 min	50	25
8	-40	30 min	42	n/a
9	-60	1 min	12	64
10	-60	5 min	51	33
11	**-60**	**15 min**	**70**	**29**
12	-60	30 min	50	13
13	-70	20 min	29	n/a

[a] Reactions were run on a 0.1 mmol scale. Yields were obtained via crude ^{1}H NMR using 1,3,5-trimethoxybenzene as an internal standard.

It was already discovered by Mazur that yields for this oxidation increase as temperature decreases.[69] This is explained by an increase in solubility of ozone into the silica gel matrix with decreasing temperatures, enabling faster reactivity. Therefore, ozonation times were screened at decreasing temperatures; first -40 °C (**Table 1** entries 5-8), followed by -60 °C (**Table 1** entries 9-12); until an optimal balance between reaction selectivity and rate was achieved. This balance was found at -60 °C with a reaction time

of 15 mins (see **Table 1** entry 11). As can be seen in each group of temperatures, the yield of product rises until a certain time point, whereupon the product begins to degrade with continued ozone exposure. When performing ozonation reactions on silica in batch there is a significant lack in control over ozonation temperature and time. In batch, dry ice baths must be consistently monitored and maintained to ensure even temperatures. This potential for temperature fluctuation most likely would have a small effect at most so long as the temperature is kept in the general desired range. However, a much greater problem in Mazur's method is the lack of control over the amount of time ozone spends in contact with the reaction matrix, which we have just demonstrated to be an important factor in controlling yield. By blowing ozone and looking for a qualitative colour change, there is no quantitative method to ensure accuracy and consistency between reactions. In addition, there is no mechanism to remove the ozone at a specified time once the desired reaction length is reached besides sparging the headspace.

While performing these optimizations, a small issue was noted along the lines of reproducibility. When a batch of silica was impregnated with starting material and used immediately, reaction yields were consistent and reproducible. However, when more than a few hours were allowed to pass between suspension and use, yields began to vary and drop. This was attributed to the silica gel being allowed to absorb water from the air, which has been shown in literature to be detrimental to this oxidation.[69] Therefore, silica gel of various dryness was tested (**Table 2**). When silica gel was used directly from the

bottle on the bench, low yields were observed (**Table 2** entry 1). Two methods of drying this silica gel were tested: a regular oven at 140 °C, and a vacuum oven at 250 °C, both for 16 h overnight. Fortunately, both showed drastic increases in yield and simply drying silica gel in an oven proved to be just as effective as the vacuum oven. After that, two reactions of amine-impregnated silica were prepared and left to sit overnight and for 48 hours (**Table 2** entries 4 and 5). These reactions both displayed decreased yields from freshly dried silica gel, with the 48 h trial showing no improvement from undried sources.

Table 2: Importance of Silica Gel Dryness in the Oxidation of Dodecylamine with Ozone[a]

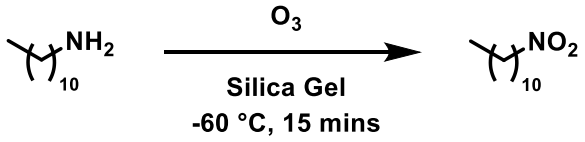

Entry	Silica Drying Methods	Yield (%)[b]
1	none	35
2	**Regular oven dried (140 °C)**	**66**
3	Vacuum oven dried (250 °C)	65
4	16 h old oven dried	57
5	48 h old oven dried	36

[a] Reactions were run on a 0.1 mmol with 1 g of silica gel scale at -60 °C for 15 mins using cooled column reactor.
[b] Yields were obtained via crude ^{1}H NMR using 1,3,5-trimethoxybenzene as an internal standard.

Therefore, unless otherwise specified, all future reactions reported were performed using silica gel that had been dried in a 140 °C oven at least overnight and used within 5 hours of suspension. After optimal reaction time and temperature had been found, the next factor to be optimized was reaction concentration. In our case, this

concerns the concentration of starting amine adsorbed onto the silica gel, since we have no conventional solvent. Herein, we found we were unable to improve on the limitations that Mazur found (see Section **1.1.4.2:**), and were likewise limited to 0.1 mmol of amine per gram of silica gel, where yields would start decreasing if that loading was exceeded (**Table 3** entry 1-3). We hypothesized that perhaps the greater amount of material would simply require a longer ozonation time to convert it, but that proved to be false, as no significant improvement was seen when the reaction time was doubled (**Table 3** entry 7 and 8).

Table 3: Attempted Scale Optimization

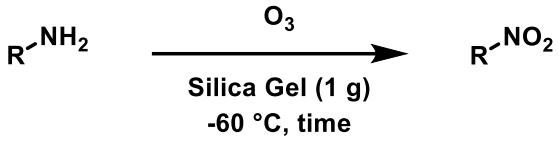

Entry	Amine	Reaction Time (min)	Reaction Scale (mmol)[a]	Yield (%)
1	Dodecylamine	15	0.1	70 [b]
2			0.2	65 [b]
3			0.3	22 [b]
4	Adamtanamine	15	0.1	78 [b]
5			0.3	25 [b]
6	3-Aminopropylbenzene	15	0.1	92 [c]
7		15	0.2	40 [c]
8		30	0.2	45 [b]

[a] mmol of substrate per gram of silica gel. 1 g of silica used for all reactions with no change in O_3 concentration of flow rate.

[b] Crude ^1H NMR yield using 1,3,5-trimethoxybenzene as an internal standard.

[c] Isolated yield.

While we face the same limitations of concentration for each individual reaction, we sought to develop a work around by applying more principles of continuous flow chemistry (**Table 4**). Instead of preparing 1 g batches of amine-impregnated silica gel in a 'dry loading' fashion, a single portion of silica gel can be loaded with amine dissolved in solvent repeatedly (for further detail, see section 3.1.1.4:). For this to work, a sufficiently polar solvent system must be employed to ensure even dispersion of the amine along the length of the column. If a non-polar solvent system is used to load the amine, it will stick to the silica gel right at the column entrance and will result in a failed reaction. This was observed after an experiment where the amine was loaded in a solution of pentane and, after the reaction and warming, a slight yellow band of product was seen clustered at the entrance of the column. After elution of the products, the reaction was found to have only trace yield (**Table 4**, entry 2).

Table 4: Optimization of 'Automation' Process Using Dodecylamine[a]

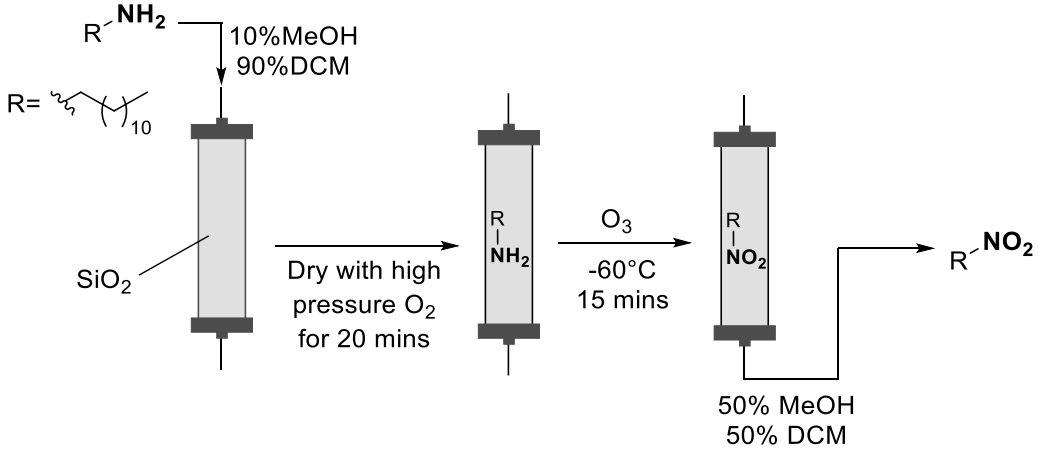

Entry	Deviation from standard conditions	%Yield[b]
1a	None	60
1b	None – first reproduction	59
1c	None – second reproduction	62
2	Amine loaded in pentane	0
3	Column dried using heat only	55
4	Column dried using high pressure only	57
5	Column not fully dried after loading	20

[a] Reactions performed on 0.1mmol scale.
[b] ^{1}H NMR yield using 1,3,5-trimethoxybenzene as an internal standard

After the amine is successfully loaded onto the column, the solvent needed to load the amine must then be removed to restore gas flow. We found that this was best achieved through using a high-pressure stream of oxygen to force the solvent out of the reaction vessel. We also found this drying could be aided by heating the reaction vessel to promote solvent removal (**Table 4** entry 3 and 4). Using both a high-pressure flow of oxygen and heating the reaction vessel resulted in rapid drying of the silica gel and restoration of gas flow.

After proper gas flow is restored, the reaction can proceed as normal with cooling and subsequent ozonation for the desired length of time. After the reaction is complete and the vessel is allowed to warm to room temperature, the products can be eluted with a very polar solution of methanol and dichloromethane to ensure all reaction material is removed from the silica. This ensures that no remaining starting material or side degradation product can interfere with subsequent reactions. This cycle can then be repeated with a new batch of amine being loaded onto the column to continue the cycle. This method was used to perform three reactions in a row using the same portion of silica gel, all of which gave yields comparable to each other, and to yields observed in previously described batch methods.

1.3.2: Scope of Nitro Products

After these optimized conditions had been obtained, the scope of possible transformations was investigated using standard conditions of -60 °C for 15 mins on silica gel. The first steps we took after optimization were to make sure we were able to achieve similar or improved yields on simple scope example similar to what was demonstrated in Mazur's work. Using the optimized standard conditions for our cooled column reactor (**Scheme 17**).

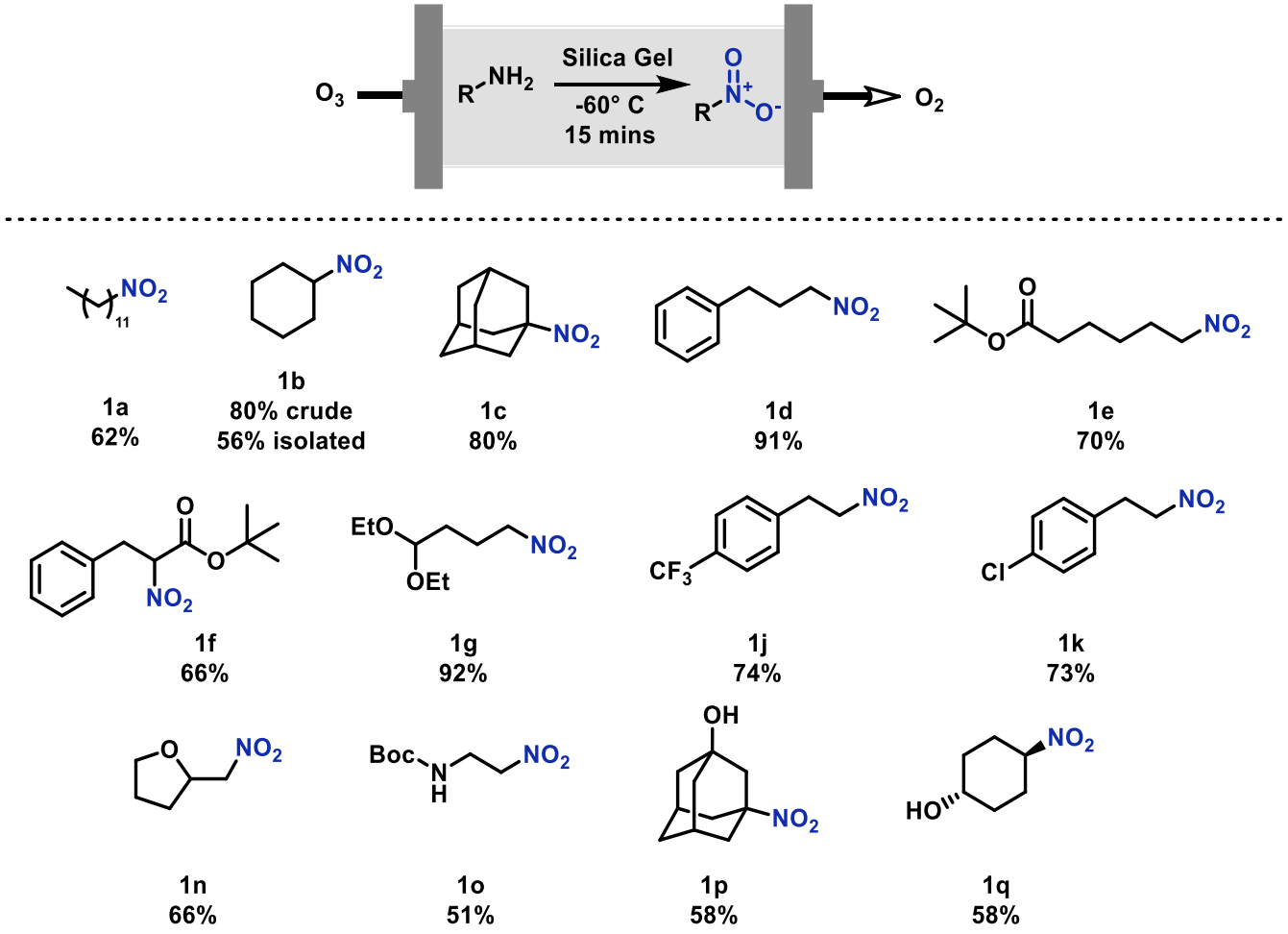

Scheme 17: Standard conditions used to perform amine scope

The first investigations were into molecules similar to what Mazur was able to achieve, which were achieved without trouble (**Figure 2**) and illustrated resistance of this chemistry to aliphatic and aromatic systems.

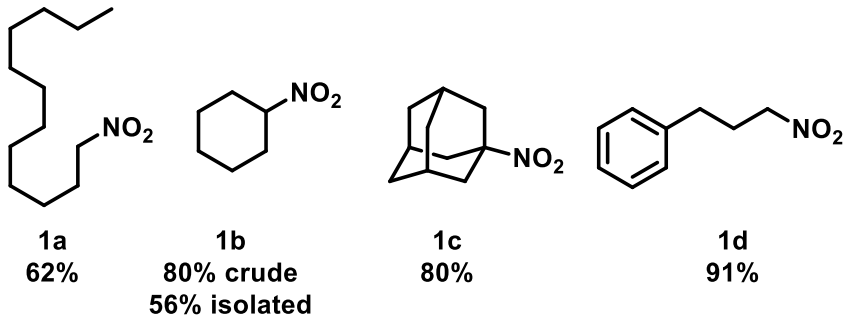

Figure 2: Exclusively aliphatic and aromatic scope examples using standard conditions

After this proof of concept, we sought to target functionality that had not been demonstrated to be tolerated with this method as of yet (**Figure 3**). The easiest, and therefore first, target we identified was esters; as they are already highly oxidized and stable species. We were not let down, and esters proved to be tolerated in good yields. An example of an acetal protecting group was tolerated in excellent yield. We also included in this scope an example of an esterified amino acid, phenylalanine, **1f.**

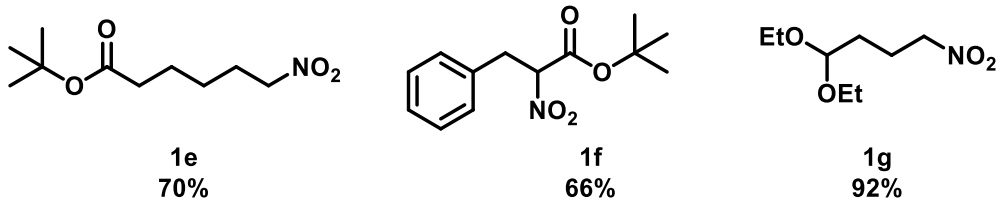

Figure 3: Scope of esters and acetal using standard conditions

Direct oxidation of amino acids often results in degradation products *other* than the nitro acid, often an ammonia salt and the nitrogen free organic moiety.[71] Methods such as ours and the one developed by Rozen[49] (using an acetonitrile and hypofluorous acid complex), offer direct access to these α-nitro esters, which can offer easy access to α-quaternary amino acids. This was also done by Rozen by way of a Henry reaction and alkylation with an alkyl halide, followed by reduction of the nitro group back to an amine. These quaternary amino acid derivatives have been implicated in many bioactive processes notably including prevention of protein aggregation, for example, in Alzheimer's disease.[72]

While we used enantiopure starting materials, we were unable to verify that the nitro esters that resulted from our ozonation maintained their starting conformation. It is our belief that the oxidation step itself would not epimerize the stereocenter, as other results have shown maintenance of stereochemistry (trans nitro cyclohexanol). However, the resulting product has a proton that is alpha to a nitro group and an ester, both with significant electron withdrawing character. The pKa of a proton α to a nitro group alone is around 17, and the pKa of a proton α to an ester is 25 (in DMSO). With a nitro ester containing both of these functionalities, it would be quite acidic, and thus, prone to racemization. With this being the case, it is uncertain whether these species would spontaneously epimerize or not. In any case, we have been unable to successfully view separate isomers via HPLC (see section **1.4.2:**

With the encouraging results obtained thus far, we decided to explore electronic effects on aromatic ring tolerance. It is known that direct ozonation of aromatic rings can form 'ozobenzene',[73,74] an extremely hazardous substance with "furiously explosive properties" (**Scheme 18**). However, this reaction requires low temperatures to avoid decomposition of the product and elongated reaction times on the scale of 10-12 hours, meaning it was not a concern for our undecorated aromatic rings.

[71] Rawalay, S. S.; Shechter, H. *J. Org. Chem.* **1967**, *32*, 3129–3131.
[72] Gilead, S.; Gazit, E. *Angew. Chem. Int. Ed.* **2004**, *43*, 4041–4044.

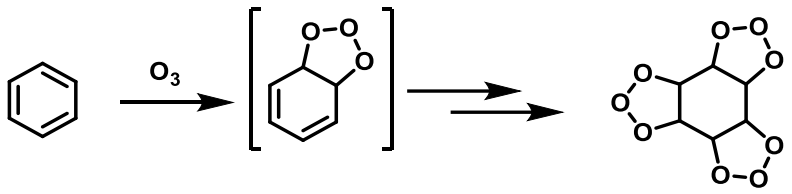

Scheme 18: Proposed structure and formation of ozobenzene

However, when we tried to expose 2-(3,4-dimethoxyphenyl)ethylamine (**Figure 4 1h**) to our ozonation conditions, no discernible products or recovery of starting material could be observed by any attempted analytical method (NMR, GC-MS, GC-FID, or TLC).

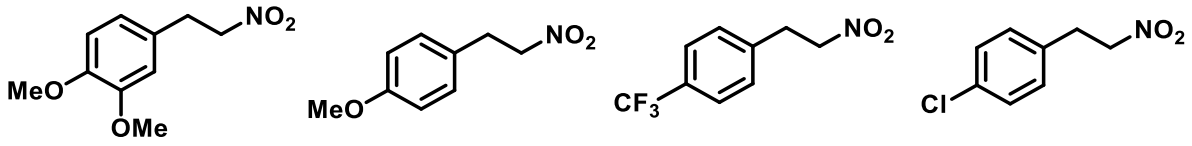

1h 0%

1i 0%

1j 74%

1k 73%

Figure 4: Tolerance of electronic groups on aromatic ring using standard conditions

We theorized that perhaps the presence of two electron donating groups were responsible for the disappearance and probable degradation of all material. But a similar, if less dramatic, result was observed when 2-(4-methoxyphenyl)ethylamine (**Figure 4 1i**) was also tested. By having only one electron donating group we hoped it would be tolerated better and, to a certain extent, it was. By NMR we observed signals indicative of the α-nitro protons, as well as the protons of the benzylic position. We also saw signals indicating the methoxy group was still present, with its integration matching the previous two signals. However, we saw no trace of any aromatic protons at all, leading

[73] Harries, C.; Weiss, V. *Berichte Dtsch. Chem. Ges.* **1904**, *37*, 3431–3433.

[74] Kaye, S. *Encyclopedia of Explosives and Related Items*; US Army Armament Research and Development Command: Dover, NJ, 1978; Vol. 8.

us to believe that the aromatic ring indeed is still oxidized, perhaps to form the di-ozonated version of ozobenzene. We sought no further characterization of the reaction products however and cannot report data beyond the fact that the desired product was not obtained. Fortunately, while the presence of electron donating groups did not seem to allow for the formation of the desired product, amines with aromatic rings bearing electron withdrawing groups yielded their nitro derivatives with little to no issues and in good yields (**Figure 4 1j**). This is presumably due to the electron deficient nature of the aromatic ring preventing attack on the ozone to form the molozonide adduct.

Still, more ambitious substrates were selected to push the limits of what we could tolerate (**Figure 5**). These limitations were quickly identified when substrates with multiple amines were attempted; 3-morpholinopropyl-1-amine yielded no product when subjected to our reaction conditions (**Figure 5 1l**). We were unable to determine if this was due to its heterocyclic nature, or simply the presence of a second nitrogen which could also be able to react with ozone.

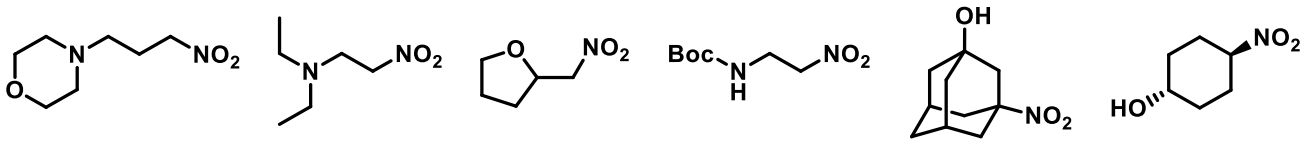

Figure 5: Scope of most decorated amines using standard conditions

To test this hypothesis we tried two additional substrates, one with an additional tertiary amine, and one with a tetrahydrofuran ring (**Figure 5**, **1m** and **1n**). While the

tetrahydrofuran ring yielded a moderate yield of the corresponding nitro compound, no product, starting material or discernable side product was observed when just the additional amine was present (similarly to the electron rich scope examples). Therefore, we concluded that due to the large excess of ozone employed, all amines are able to undergo this oxidation and that the reaction cannot proceed selectively when multiple amines are present on the same molecule. These multiple oxidations most likely cause an increase in side chain oxidations, as was discussed in **Scheme 14:** Side chain oxidations . This would lead to the rapid degradation of the molecule and explain why no discernable products were observed. Fortunately, this can be circumvented through use of a BOC protecting group, which can allow this reaction to proceed in moderate yields while leaving the BOC group intact (**Figure 5 1o**). Finally, two substrates showing tolerance of alcohols were prepared. With ozone being known to perform alcohol oxidation under certain conditions, we were pleased to see moderate yields of our desired nitro compound.[68] In addition to demonstrating tolerance of alcohols, **1q** shows the reaction can proceed stereo selectively. The exclusively trans starting amine was used, and the exclusively trans nitro product was observed via NMR.[75] While far from perfect selectivity or yields, we have demonstrated an appreciable and significant expansion in the scope that was able to be achieved by Mazur.

1.3.3: Additional Oxidations

During the course of this research, a focus was made on primary amine oxidation to nitroalkanes. However, we also wanted to illustrate that this system is generalizable to a diverse range of ozone-mediated processes. For this reason, three additional oxidative transformations were performed, and small scopes were prepared.

1.3.3.1: *N*-oxide formation

Pyridines and related heterocycles can be oxidized to form *N*-oxides. This transformation can be facilitated by relatively mild oxidants, such as *m*-CPBA, or hydrogen peroxide.[76] Without reoptimization, we were able to apply identical conditions from the amine oxidation previously described to synthesize these pyridine *N*-oxides in moderate to excellent yields (**Scheme 19**).

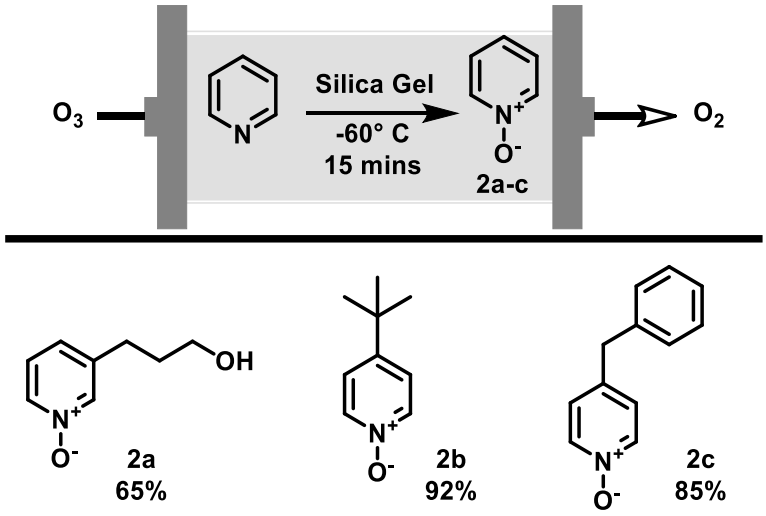

Scheme 19: Pyridine oxidation scope using standard conditions

[75] Janda, K. D.; Ashley, J. A. *Synth. Commun.* **1990**, *20*, 1073–1082.
[76] Palav, A.; Misal, B.; Ernolla, A.; Parab, V.; Waske, P.; Khandekar, D.; Chaudhary, V.; Chaturbhuj, G. *Org. Process Res. Dev.* **2019**, *23*, 244–251.
[77] Durland, J. R.; Adkins, Homer. *J. Am. Chem. Soc.* **1939**, *61*, 429–433.

1.3.3.2: Tertiary C-H Oxidation

Use of ozone to perform tertiary C-H hydroxylation was first discovered by Durland and Adkins as an accidental side product.[77] It can also be facilitated using mixtures of nitric and sulfuric acid[78] or various transition metal catalysts,[79,80] but these cannot compete with the atom economy and affordability that ozone can provide. Resistance to these tertiary C-H bonds being oxidized in our amine scope indicated that this transformation required harsher conditions. Thus, optimized conditions of -20 °C for an ozonation time of 60 mins were obtained by Dr. Jaya Kishore Vandavasi before his departure of the Newman group (**Scheme 20**). Notably, both of these substrates bear two oxidizable tertiary C–H bonds. The acetate group of **3a** presumably deactivates the nearest methine, and the electronegative oxygen atom in alcohol **3b** causes the product to be less reactive than the starting material. No recovery of starting material was seen in either case. While a thorough optimization was performed on these substrates, it is possible that cryogenic conditions for multiple hours (conditions that we are unable to obtain with our reactor) could yield improved results.

[78] Politino, M.; Cadin, M.; Skonezny, P.; Chen, J. Process for Preparing Dipeptidyl Peptidase IV Inhibitors and Intermediates Therefor. EP3000893A3, 2016.
[79] Canta, M.; Font, D.; Gómez, L.; Ribas, X.; Costas, M. *Adv. Synth. Catal.* **2014**, *356*, 818–830.
[80] Shibuya, M.; Osada, Y.; Sasano, Y.; Tomizawa, M.; Iwabuchi, Y. *J. Am. Chem. Soc.* **2011**, *133*, 6497–6500.

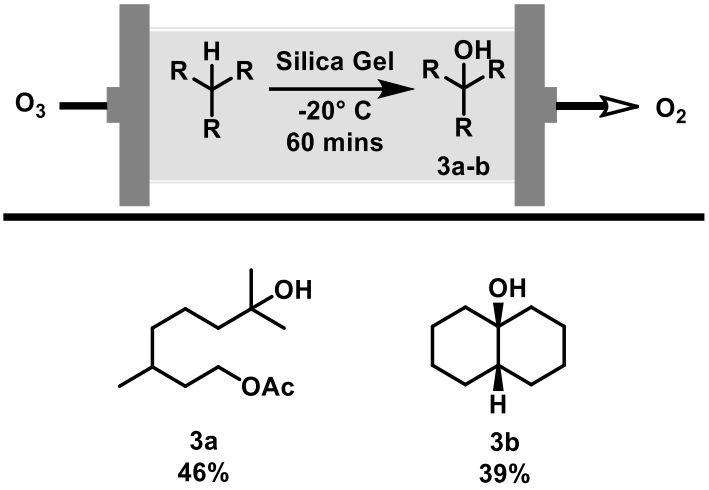

Scheme 20: C-H oxidation scope using altered time and temperature for standard conditions

1.3.3.3: Arene Oxidation

A relatively uncommon, but powerful transformation of alkyl-aryl C-C bonds to carboxylic acids was the fourth and final transformation explored in this project (**Scheme 21**. First identified by Sharpless upon investigation of lower valent ruthenium oxidants,[81] this transformation was also performed by Klein in 1975 using Mazur's dry ozonation method.[82] Arenes were left untouched in the low temperature and short reaction times described for amine oxidation, indicating more aggressive conditions would be needed again. Using the same conditions as for C–H bond hydroxylation enabled direct conversion of phenyl substituents into aliphatic acids in modest yields. When multiple alkyl aryl bonds were tested in the same molecule (e.g tetralin), no product or recovery of starting material was observed. Since identical conditions to the C-H hydroxylation

[81] Carlsen, P. H. J.; Katsuki, T.; Martin, V. S.; Sharpless, K. B. *J. Org. Chem.* **1981**, *46*, 3936–3938.

were applied, the same suggestion made above concerning reoptimization with extended cryogenic conditions could be beneficial here as well.

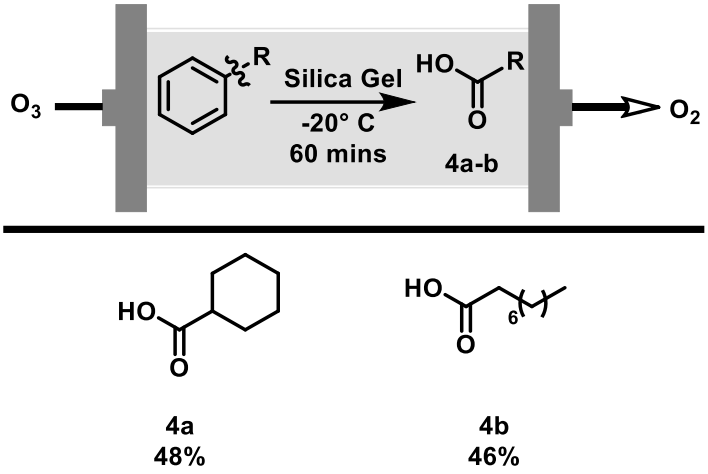

Scheme 21: Aryl C-C bond oxidation scope using altered time and temperature for standard conditions

1.3.4: Limitations

No perfect chemical pathway exists and there must always be advantages and drawbacks. Our method is no exception to this, and while the upsides have been extensively discussed, these ozone-mediated oxidation reactions are not without problems and limitations.

We were unable to improve on the loading capacity/concentration of the amine suspended on silica gel and, unlike Mazur, we are limited to a maximum amount of silica gel in our reactor. Due to the small size of the Vapourtec cooled column reactor platform used for this chemistry, the system is not immediately applicable to larger scale synthesis without acquiring different equipment. There is a possibility a wider diameter of column

[82] Klein, H.; Steinmetz, A. *Tetrahedron Lett.* **1975**, *16*, 4249–4250.

could facilitate larger scale reactions to proceed smoothly, but we were unable to test this due to lack of larger equipment. Our efforts to implement automation was targeted at providing a workaround to these limits of reaction size and still ending up with a process that has improved throughput over time; however this also falls short of a truly scalable process.

Mazur reported performing a C-H hydroxylation of adamantane on 6 g scale, requiring 500 g of silica gel and a total reaction time of 9 hours (2 h for suspension, 2 h for cooling, 2 h for ozonation, and 3 h for warming before the product can be eluted and purified). This represents a total throughput of around 5 mmol per hour. If we were to apply our automation system to our own C-H hydroxylation, we could assume that we would require ~5 mins for loading, 30 minutes for drying, 5 minutes for cooling, 60 minutes for reaction, and 5 minutes for warming and elution. That consists a total reaction time of just under 2 hours for only a 0.1 mmol scale reaction. This is a far cry from what Mazur was already able to attain. However, some areas where our method still holds the advantage is that once set up, it would require minimal oversight in an industrial setting and could operate all hours of the day. Additionally, the required times for Mazur's 6 g scale reaction will continue to get worse and worse as scale increases. There currently is no data for how long it would take to suspend, cool, blow ozone, and warm a 1 mol reaction with ~10 kg of silica gel, if it even could be done, but inefficiency would likely render it extremely impractical.

1.4: Issues to be Addressed

There are a series of topics which were not explored within the scope of this research, either due to lack of time, or access to equipment.

1.4.1: Silica Gel Mesh Size Affecting Scale

The use of silica gel provides a solid matrix for the reaction to proceed. Mazur proposed that the maximum efficient loading concentration of 1% (w/w) is due to the silica gel being saturated with monolayer. Thus, additional amine would be 'free' and able to interfere in neighboring reaction intermediates, having a doubly negative impact on the observed yield. Mazur specified the silica gel he used as Merck, Kieselgel 60, 70-230 mesh. The silica gel we had access to was Silicycle F60 40-63 μm, 230-400 mesh which, due to the larger mesh size would have a higher surface area to volume ratio than what Mazur used. If the monolayer theory is the correct model for this reaction, then we should be able to have more starting material adsorbed onto the silica gel than Mazur. Despite this, we saw no significant improvement to the loading scale we were able to achieve. However, one series of tests that we did not run would be to purchase a larger mesh size of silica gel available and once again screen loading concentrations of starting material. This would potentially give the best chance to see significant improvement to reachable reaction concentrations on the silica gel.

1.4.2: HPLC of Nitro Esters

The amino ester starting material used for scope examples **1f** was enantiopure. However, when we attempted to observe if epimerization had occurred via chiral HPLC, we were unable to resolve the respective isomers after they had been subjected to the reaction conditions. Further time spent developing HPLC conditions to cleanly identify and resolve product isomers would be required to make any conclusions regarding preservation or elimination of enantiomeric excess. Additionally, any other method of enantiomeric resolution could be employed to achieve this, such as optical rotation, or forming diastereomers and measuring coupling constants via ^{1}H NMR.

1.5: Conclusion

At the inception of this project, the goal was to develop a process that was able to control the extreme reactivity of ozone and harness it for appreciable synthetic use. Some notable improvements we wanted to make were in areas of scalability, functional group tolerance, and atom economy. This project succeeded in only two of these three areas: atom economy and functional group tolerance. We were able to drastically increase the scope of molecules amenable to this transformation far beyond what Mazur was able to display. This was accomplished by converting the 'batch' method of ozonation to a more flow based 'cooled column' approach to enable finer control over the reaction conditions. However, the limitations we still face in this area of ozonation pose a significant challenge to further development of this research. In its current state, the scale of operation for this

reactor makes it incredibly impractical to obtain any synthetically useful amount of product. Therefore, I believe if further time is to be invested in this area of research, it should be directed at methods to make this process more amenable to scale up via larger columns, or differing silica gel mesh sizes. The possibility of using prefunctionalized silica gel should not be discarded.

Chapter 2: Organolithium Generation and Use via Challenging Deprotonations

2.1: Introduction

2.1.1: Generation of Organolithium Species

Organolithium species are very important reagents in organic chemistry. Their strongly anionic character have found them significant use as nucleophiles, strong bases and metalating agents, which are known to aggregate in solution.[83] The exact degree of this aggregate depends heavily on the exact identity of both the organolithium and the solvent it is dissolved in. For instance, *n*-BuLi has been observed as a hexamer in hexanes,[84] a tetramer in ether,[85] and a mixture of a tetramer and a dimer in THF.[86] This de-aggregation can conversely be viewed as an increase in solubility, and plays a significant role in the reaction kinetics for organolithium species by affecting both effective concentration and reactivity (see **Figure 6**).[87,88]

[83] Reich, H. J. *Chem. Rev.* **2013**, *113*, 7130–7178.
[84] Kottke, T.; Stalke, D. *Angew. Chem. Int. Ed. Engl.* **1993**, *32*, 580–582.
[85] Lewis, H. L.; Brown, T. L., *J. Am. Chem. Soc.* **1970**, *92*, 4664–4670.
[86] McGarrity, J. F.; Ogle, C. A. *J. Am. Chem. Soc.* **1985**, *107*, 1805–1810.
[87] Gessner, V. H.; Däschlein, C.; Strohmann, C. *Chem. Eur. J.* **2009**, *15*, 3320–3334.
[88] Reich, H. J. *J. Org. Chem.* **2012**, *77*, 5471–5491.

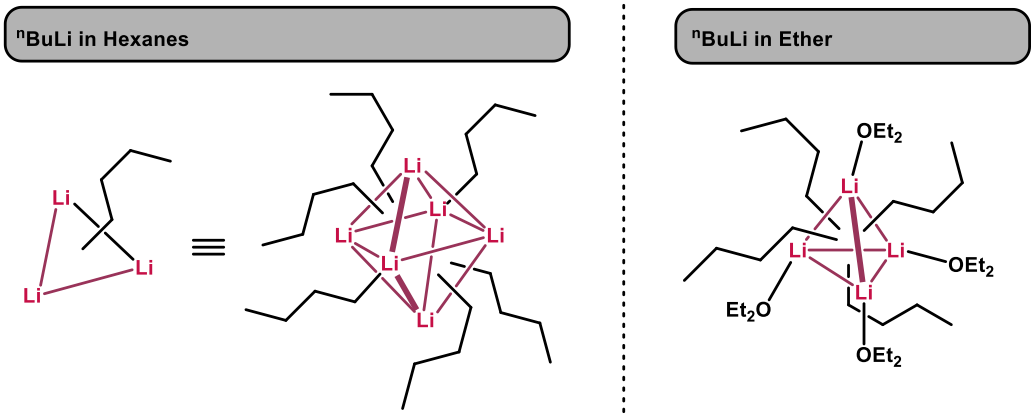

Figure 6: Structure of *n*-BuLi in hexanes and ether

2.1.1.1:Lithium Halogen Exchange

The first method of organolithium generation that will be discussed is through lithium-halogen exchange. This involves, as the name suggests, the exchange of a halogen on one material for a lithium from another.

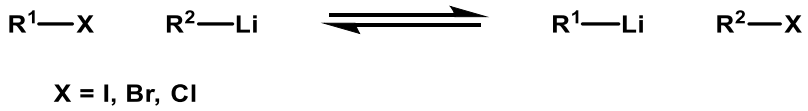

Scheme 22: Lithium halogen exchange general outline

The exact mechanism of this process is not fully agreed upon and a variety of hypothesis are currently entertained.[89] The lithium source can come in the form of lithium (0) metal, or a previously obtained organolithium reagent.[90] The rate of this reaction is extremely quick and has even been observed to outcompete proton transfer in some

[89] Bailey, W. F.; Patricia, J *J. Organomet. Chem.* **1988**, *352*, 1–46.
[90] Gilman, Henry.; Langham, Wright.; Jacoby, A. L. *J. Am. Chem. Soc.* **1939**, *61*, 106–109.

cases, even at cryogenic temperatures (**Scheme 23**).[91] However, this is very case dependent on the exact identity of the reagents.

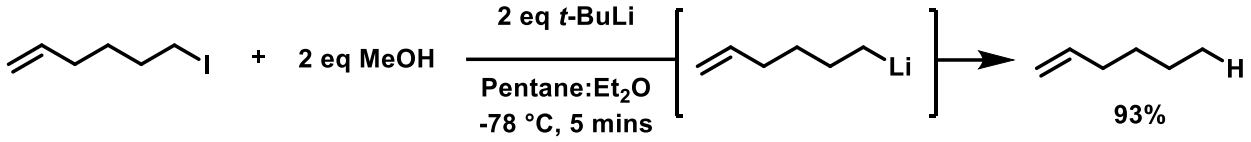

Scheme 23: Lithium-halogen exchange is sufficiently quick to outcompete proton transfer

Exchange rates follow the same trend as S_N2 reactions with iodides being the fastest and chlorides being the slowest. Alkylfluorides are generally unreactive towards this pathway, most likely due to the very strong carbon-fluorine bond being resistant to cleavage.[92] The identity of the carbon bearing the halogen also has a large impact on the rate of reaction. Since this formally represents a reduction from the carbon's perspective, a greater capacity to accept and disperse extra electrons facilitates a faster reaction.[93] Thus, access to resonance, inductive effects and orbital identity play a key role in reaction rate, and trends identical to acidity can be drawn wherein: Aryl sp^2 is the fastest, with sp being faster than sp^2, while sp^3 centres are the slowest. In addition to the identity of the halogen and the carbon on which it is situated, the exact identity of the lithium source can also have a large impact on the rate of this reaction. This trend again follows classical S_N2 chemistry, wherein the order of decreasing reactivity would be *t*-BuLi > *s*-BuLi > *n*-

[91] Bailey, W. F.; Patricia, J. J.; Nurmi, T. T.; Wang, W. *Tetrahedron Lett.* **1986**, *27*, 1861–1864.
[92] Gilman, H.; Moore, F. W. *J. Am. Chem. Soc.* **1940**, *62*, 1843–1846.
[93] Carey, F. A.; Sundberg, R. J. Organometallic Compounds of Group I and II Metals. In *Advanced Organic Chemistry*; Advanced Organic Chemistry; Springer US: Boston, MA, 2007; pp 619–673.

BuLi > MeLi > PhLi. Additionally, this exchange has been performed stereoselectivity in both vinyl[94] and alkyl[95] systems with retention of stereochemical information. As stated previously, lithium metal is also able to perform lithium halogen exchange, and in fact, this is how the above commercially available organolithiums are synthesized industrially.[96] This requires more aggressive conditions (such as elevated temperatures) than use of an organolithium, and if sensitive functional groups are present, incompatibilities may arise.

2.1.1.2:Directed Metalation

Directed metalation is the second method of forming organolithiums that will be discussed. This involves the use of a directing group on an aromatic ring to coordinate the organolithium and perform a stereoselective deprotonation, replacing a hydrogen with a lithium. This reaction can take two different forms depending on the targeted lithiation site. In either case, the use of a directing group ensures a high degree of regioselectivity making it a very attractive reaction. There is a strong suggestion in literature that many metalation reactions proceed via a Complex-Induced Proximity Effect (CIPE) mechanism.[97,98] Schemes in this section are only intended to illustrate potential reactivity using this concept, not supply mechanistic proposals.

---

[94] Neumann, H.; Seebach, D. *Tetrahedron Lett.* **1976**, *17*, 4839–4842.
[95] Freeman, P. K.; Hutchinson, L. L *J. Org. Chem.* **1983**, *48*, 4705–4713.
[96] Rathman, T. 'Li'; Schwindeman, J. A. *Org. Process Res. Dev.* **2014**, *18*, 1192–1210.
[97] Whisler, M. C.; MacNeil, S.; Snieckus, V.; Beak, P. *Angew. Chem. Int. Ed.* **2004**, *43*, 2206–2225.
[98] Chadwick, S. T.; Ramirez, A.; Gupta, L.; Collum, D. B. *J. Am. Chem. Soc.* **2007**, *129*, 2259–2268.

Ortho Metalation:

Ortho Metalation, as the name suggests, uses coordination of the lithium to target a site that is ortho to the directing group (**Scheme 24**). The resulting organolithium can be quenched with an electrophile to furnish new functionalized products. This provides a more attractive version of an electrophilic aromatic substitution reaction, due to its high regioselectivity.

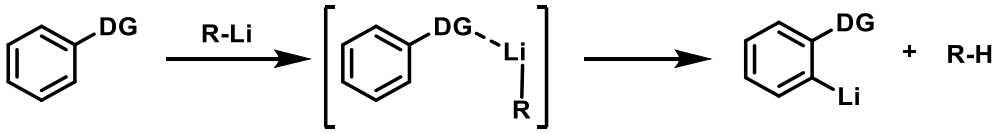

Scheme 24: General proposal of directed ortho metalation

Many diverse classes of directing groups have been identified and explored extensively, but only three classes will be discussed herein: aromatic ethers, benzamides and heterocycles.[99]

Benzamides are the most activating of these three classes with two heteroatoms conveying an almost doubly activating nature (**Scheme 25**). The oxygen represents an extremely Lewis basic functionality, assisted by the conjugation from the nitrogen. This strong coordinating ability is further enhanced by the overall electron withdrawing nature of the benzamide acidifying the protons of the ring. This double activation results in extremely cold conditions often being employed, and very rapid reaction rates.[100]

---

[99] Snieckus, V. Directed Ortho Metalation. *Chem. Rev.* **1990**, *90*, 879–933.
[100] Bowles, P.; Clayden, J.; Helliwell, M.; McCarthy, C.; Tomkinson, M.; Westlund, N. *J. Chem. Soc. Perkin* **1997**, *17*, 2607–2616.

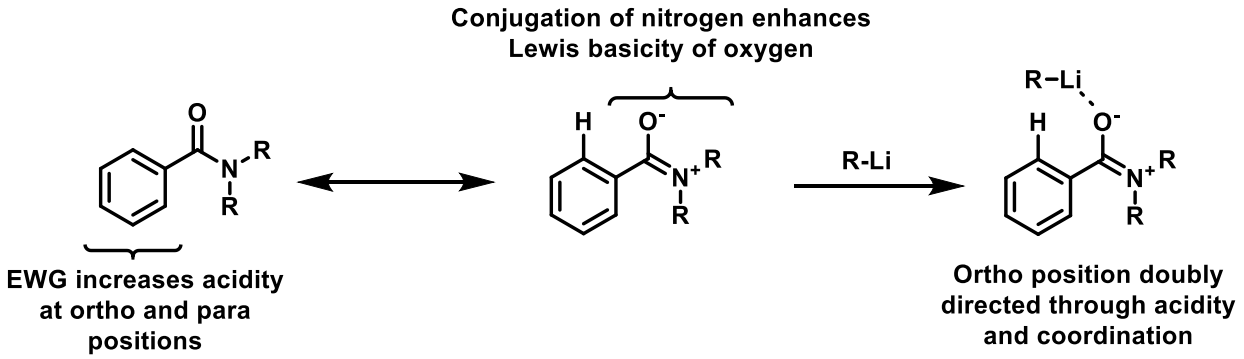

Scheme 25: Amides as directing groups

The electrophilicity of these benzamides is a distinct benefit, but can also acts as a hindrance for this type of reaction. The electrophilic functionalities open up the possibility of direct attack on the amide by the lithiating agent. However, this can be relatively easily solved by using tertiary, sterically hindered, amides.

Ethers can also act as directing groups and function much the same as the above amide directing groups (**Scheme 26**). The electron withdrawing ability acidifies nearby protons on the ring, while the long pairs of the oxygen are able to coordinate the lithium and direct it to the ortho position. As they only have one heteroatom working at this goal, they are less reactive than the amide directing groups and as such require either longer or hotter reaction conditions.[101] In addition, their lack of an electrophilic carbonyl means they cannot be attacked by the lithiating agent. While less reactive than other directing groups, they are still often employed due to their synthetic utility. They are extremely

[101] Slocum, D. W.; Jennings, C. A. *J. Org. Chem.* **1976**, *41*, 3653–3664.

simple and easily accessible through a variety protecting groups which, in a few cases, can enhance the reactivity through addition of a second heteroatom to facilitate coordination.

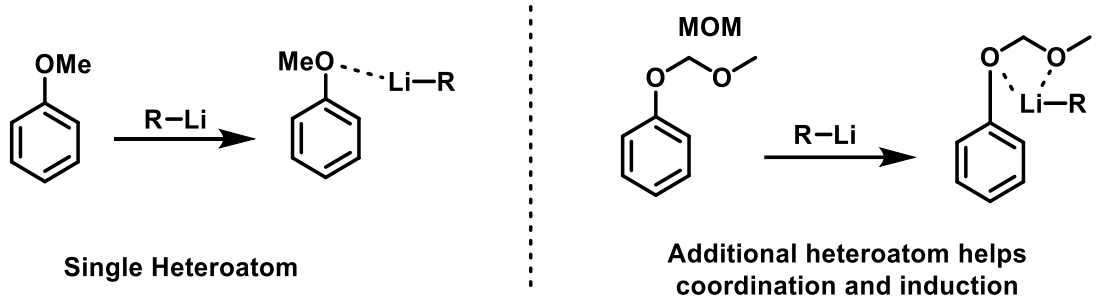

Scheme 26: Ethers as directing groups

The directing group doesn't need to be an additional decoration on the aromatic ring, but can also be built into the structure of the aromatic ring, such as heterocycles. For example, *N*-methylpyrrole,[102] furan[103] and thiophene[104] heterocycles have all been shown to undergo facile metalation at the alpha position. Heterocycles are arguably the most problematic of the directing groups, as they often more prone to electrophilic attack than deprotonation.[105] However, they can work in conjunction with additional directing groups present on the ring to achieve greater reactivity or direct to alternate positions. Though, for the sake of this overview only simple unfurnished heterocycles have been mentioned.

---

[102] Shirley, D. A.; Gross, B. H.; Roussel, P. A. *J. Org. Chem.* **1955**, *20*, 225–231.
[103] Joule, J. A.; Mills, K.; Smith, G. F. *Heterocyclic Chemistry*, 3. ed.; Chapman & Hall: London, 1995.
[104] Schlosser, M. Organoalkali Chemistry. In *Organometallics in Synthesis*; Schlosser, M., Ed.; John Wiley & Sons, Inc.: Hoboken, NJ, USA, 2013; pp 1–222.
[105] Clarke, A. J.; McNamara, S.; Meth-Cohn, O. *Tetrahedron Lett.* **1974**, *15*, 2373–2376.

The most glaring disadvantage that all of these methods share is the requirement for a directing group. While use in a total synthesis is far from impossible, this adds complication and extra steps to a synthesis to add, modify or remove these directing groups. Additionally, this only enables activation of sp^2 sites, which are inherently more activated and accessible than sp^3 sites.

Lateral Metalation:

Lateral lithiation is the term to be employed when the target site of lithiation is an alkyl benzylic position that is, itself, ortho to the directing group.[106]

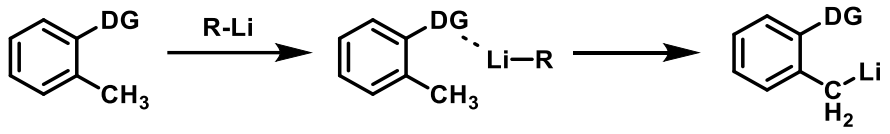

Scheme 27: General overview of lateral lithiation

While still bearing large similarity to directed ortho metalation,[107] lateral metalation facilitates deprotonation of sp^3 sites; transformations that otherwise would be exceedingly difficult (see **Scheme 28**). This is despite the fact that the pKa of an aromatic ring is higher (pKa = 43) than a typical benzylic CH_3 group (pKa = 41). For example, the benzylic deprotonation of toluene by *n*-BuLi is favourble by pKa's (pKa = 50), yet kinetically is extremely slow to occur due to lack of activation. Large excesses of *n*-BuLi

[106] Clark, R. D.; Jahangir, A. Lateral Lithiation Reactions Promoted by Heteroatomic Substituents. In *Organic Reactions*; John Wiley & Sons, Inc., Ed.; John Wiley & Sons, Inc.: Hoboken, NJ, USA, 1995; pp 1–314.
[107] Clayden, J. *Organolithiums: Selectivity for Synthesis*, 1st ed.; Tetrahedron Organic Chemistry; Pergamon, 2002; Vol. 23

along with extended reaction times have only produced yields around 25% without the use of a directing group.[108]

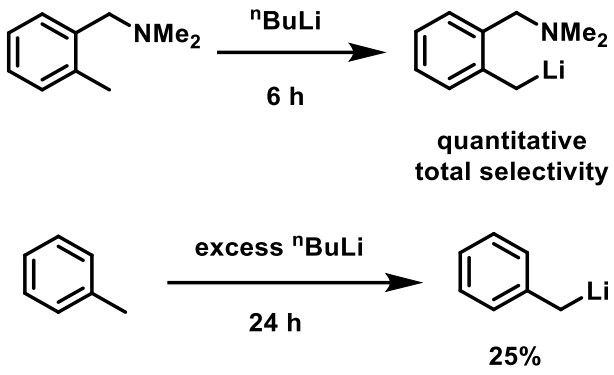

Scheme 28: Deprotonation of toluene with and without a directing group

Deprotonation of these sites without the use of directing groups will be more thoroughly covered later on in section 2.1.2: Superbases.

Comparison of Ortho and Lateral Metalation:

If a competition were to arise between ortho and lateral lithiation, then the specific conditions of the reaction would need to be carefully tailored to reach the desired outcome. Whereas ortho lithiation benefits mainly from inductive effects and coordination, lateral lithiation is mostly encouraged by conjugation and acidification of benzylic positions. This is due to the location and orbital alignment relative to the lithium atom. In ortho lithiation, the lithium is in the plane of the ring, preventing it from benefitting from the direct conjugation with the aromatic ring and consequently, the directing group (see **Figure 7A**). Therefore, the main benefit arises from inductive effects

[108] Gilman, H.; Gaj, B. J. *J. Org. Chem.* **1963**, *28*, 1725–1727.

from the directing group in the form of coordination. (Note: this is not to say that conjugation has no benefit for ortho lithiation, only that the *main* source of direction comes from coordination). In lateral lithiation the lithium is aligned with the orbitals of the aromatic ring and therefore also the directing group (see **Figure 7B**). Thus, direct conjugation and acidification provide the strongest source of stabilization.

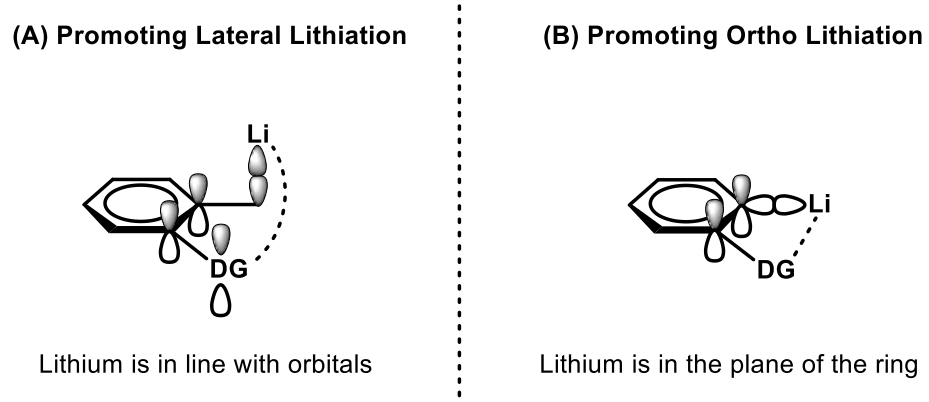

Figure 7: Orbital alignment of lateral lithiation vs. ortho lithiation

The effects of this directing preference can be seen in **Scheme 29**.[107] In equation (**1**) and equation (**2**) the most stable product is formed at the lateral benzylic site. This is because the strong acidification in concert with the coordination effect of the amide directs more strongly to the lateral site than the ortho aryl site. In equation (**3**) it can be seen that when a *p*-methyl group is present instead of an *o*-methyl group, super bases such as *s*-BuLi/TMEDA will deprotonate at the ortho site, benefiting more from coordination and leaving the methyl group untouched. However, LDA at warmer temperatures will direct entirely to the remote methyl group, as conjugation and acidification still prefer this site. This can be viewed as a type of kinetic vs thermodynamic

control, with the colder and irreversible base forming the kinetic product (benzylic deprotonation) while the warmer and reversible base forms the thermodynamic product (lateral deprotonation).

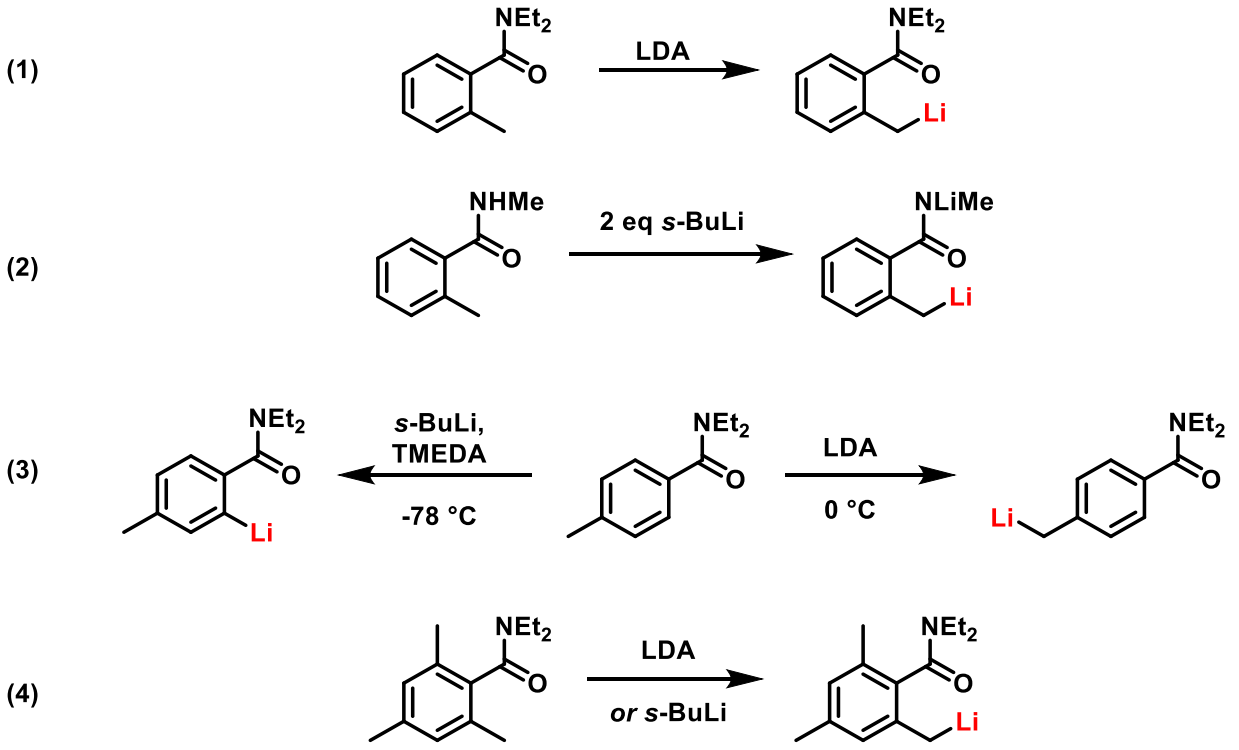

Scheme 29: Regioselectivity between ortho and lateral lithiation[107]

2.1.2: Superbases

The term "superbase" is unlike the tern "superacid" in that it does not refer to being above or below a specific pK_a or strength.[109] Rather, the generally accepted definition for a superbase was coined by Paul Caubère in 1993 who defined it as: "…a basic reagent [that] is created by combining the characteristics of several different

[109] Himmel, D.; Goll, S. K.; Leito, I.; Krossing, I. A. *Angew. Chem. Int. Ed.* **2010**, *49*, 6885–6888.

bases".[110] Two main classes of superbases dominate the literature: LiCKOR superbases, and coordinating amine superbases.

2.1.2.1: LiCKOR Superbases

"Lochman – Schlosser bases" (often referred to simply as Schlosser's base) are formed by mixing potassium *tert*-butoxide with *n*-butyllithium, and bears the name of its inventors, Lubomir Lochman, and Manfred Schlosser.[111] This generates a superbasic mixture, which has been reported to perform a number of difficult deprotonations with a surprising degree of selectivity.[111–114] These classes of reagents can be more generally referred to as LiCKOR bases, owing to the nature of ingredients being an organolithium (Li-C) and a potassium alkoxide (K-OR). While not entirely accurate or consistent with literature findings presented in **Figure 9** and **Figure 10** below, a simplified version of this superbase is presented in **Figure 8**, which can be used to conceptualize or understand the interactions of these reagents.

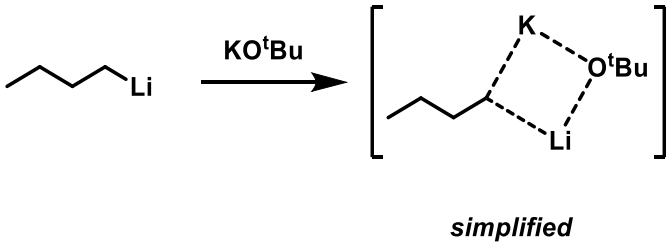

Figure 8: Simplified Schlosser's base

[110] Caubere, P. *Chem. Rev.* **1993**, *93*, 2317–2334.
[111] Schlosser, M. *J. Organomet. Chem.* **1967**, *8*, 9–16.
[112] Schlosser, M.; Strunk, S. *Tetrahedron Lett.* **1984**, *25*, 741–744.
[113] Schlosser, M. *Pure Appl. Chem.* **1988**, *60*, 1627–1634.
[114] Faigl, F.; Schlosser, M. *Tetrahedron Lett.* **1991**, *32*, 3369–3370.

Upon its discovery, initial hypotheses of its exact structure of Schlosser's base ranged from a simple organopotassium to an ate–complex, defined by Georg Wittig in 1958 as a complex anion $[ZR_n]^{(n-z)-}$ in association with a cationic partner to form a structure of $M_{n-z}[ZR_n]$. While exploring anionic polymerization methods, Lochman and Lim determined the product that precipitates from this mixture of organolithium and potassium alkoxide to be an organopotassium.[115] However, Schlosser hypothesized that if the reactive species of this superbase was truly a simple organopotassium, reactivity between varying components of this reagent should produce identical results. He found the opposite was true, and that the exact identity of the LiCKOR reagent played a large role in its reactivity and selectivity, with fresh *n*-BuLi and KO^{t}Bu being the overall best performing candidate.[112]

The uncertainty surrounding the exact nature or identity of this reagent wasn't resolved until many years later, when Strohmann obtained crystal structures indicative of a pair of complexes for the metalation of toluene by KO^{t}Bu and *n*-BuLi.[116]

[115] Lochmann, L.; Pospíšil, J.; Lím, D. *Tetrahedron Lett.* **1966**, *7*, 257–262.
[116] Unkelbach, C.; O'Shea, D. F.; Strohmann, C. *Angew. Chem. Int. Ed.* **2014**, *53*, 553–556.

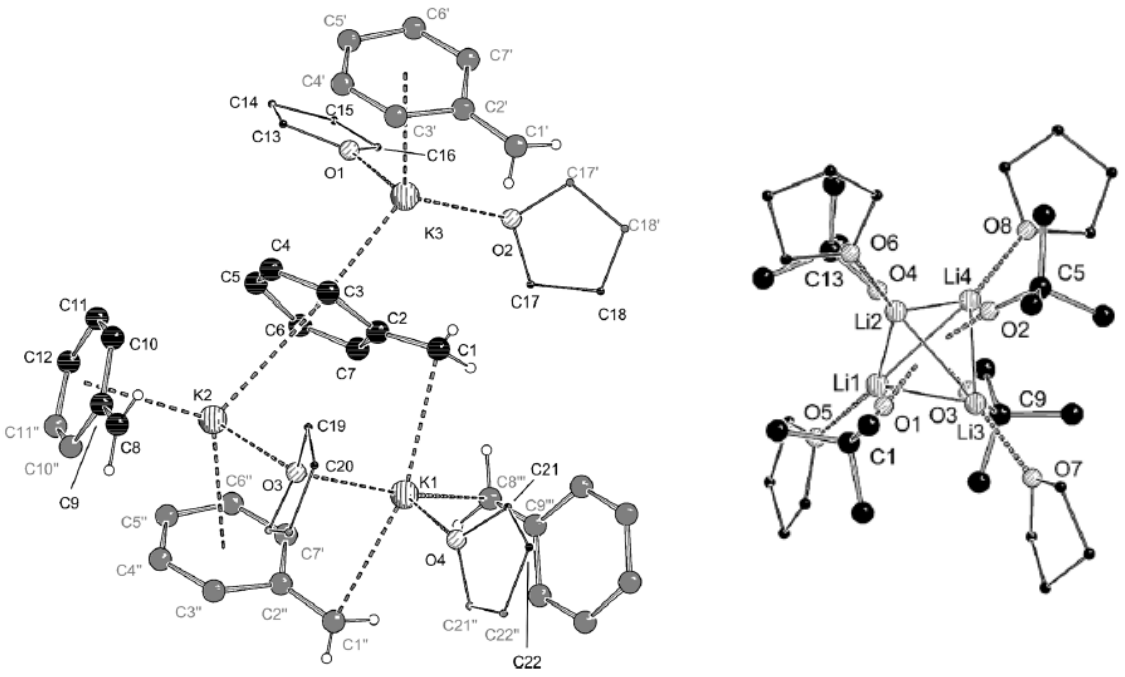

Figure 9: Crystal structures of Schlosser's base complexes during metalation of toluene. This work was reproduced from John Wiley and Sons with approval from the publisher

Stohmann also studied the metalation of toluene through an initial metalation of benzene to form phenyllithium. He found this complex (**Figure 10**) coordinates and metalates toluene via the illustratesd transition state below.[116]

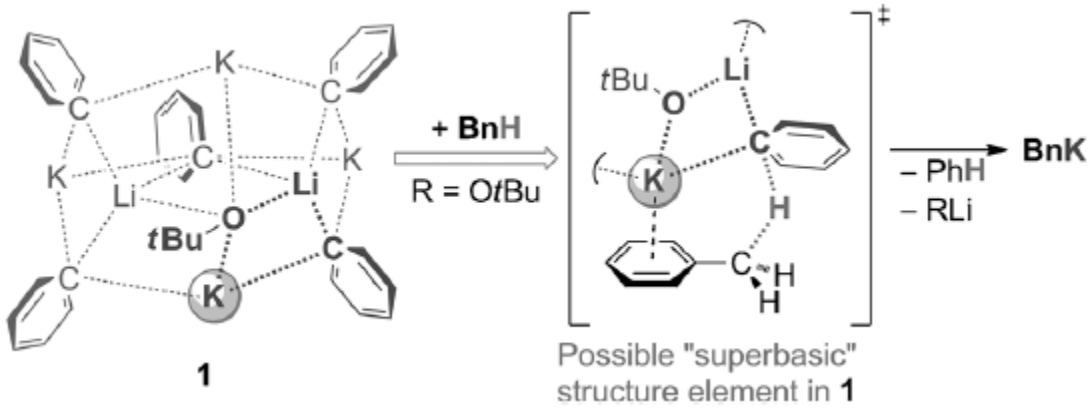

Figure 10: Proposed structure and transition state of active metalating complex and transition state of toluene metalation. This work was reproduced from John Wiley and Sons with approval from the publisher

2.1.2.2: Coordinated-Amine Superbases

As mentioned in section **2.1.1**, the structure and aggregation state of organolithium species plays a critical role in reactivity: as aggregation decreases, reactivity increases. Initial investigations by Gilman *et. al.*[117,118] discovered that THF delivered the best metalation results when compared to other ethereal solvents such as diethyl ether or THF-diethyl ether mixtures. However, it was quickly found that this mixture lacked stability, and decomposition of the THF was often observed (**Scheme 30**).[119–121] This created a need for a more stable metalating complex which was more resistant to decomposition.

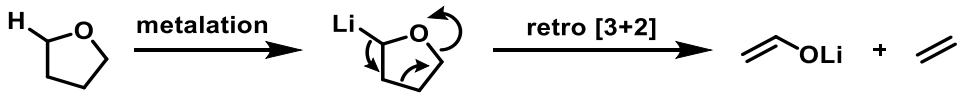

Scheme 30: Decomposition of THF

While investigating anionic polymerization methods, Eberhardt and Butte along with A.W Langer Jr. independently investigated the use of chelating/ligand bases such as TMEDA (*N,N,N′,N′*-tetramethylethylenediamine) and DABCO (1,4-diazabicyclo[2.2.2]octane) with *n*-BuLi. Alklyllithium polymerization methods before this period typically yielded very low MW oligomers when used to polymerize ethylene. Langer found that this mixture of *n*-BuLi and TMEDA used in catalytic amounts was stable under intense

[117] Gilman, H.; Gray, S. *J. Org. Chem.* **1958**, *23*, 1476–1479
[118] Gilman, H.; Gorsich, R. D. *J. Org. Chem.* **1958**, *23*, 550–551.
[119] Gilman, H.; Gaj, B. J. *J. Org. Chem.* **1957**, *22*, 1165–1168.
[120] Stanetty, P.; Mihovilovic, M. D. *J. Org. Chem.* **1997**, *62*, 1514–1515.
[121] Clayden, J.; Yasin, S. A. *New J. Chem.* **2002**, *26*, 191–192

reaction conditions and yielded high MW plastics on par with standard polymerization methods such as Phillips or Zeigler catalysis.[122] Both of these researchers postulated that the increased metalating power of the *n*-BuLi/TMEDA complex resulted primarily from coordination of the ligands to the lithium centre, providing stabilization, elongating, and weakening the carbon-lithium bond (**Figure 11**). This results in an increase in ionic character and a stronger localization of negative charge on the carbon atom.[98,123,124]

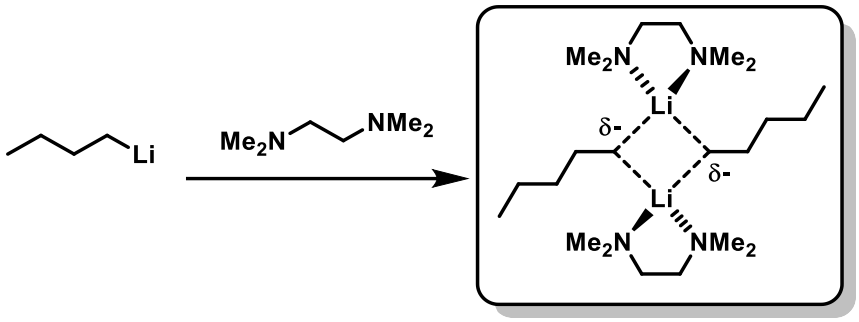

Figure 11: Structure of *n*-BuLi/ TMEDA dimer

Later on, the synthetic utility of this superbasic mixture to perform more difficult metalations was tested. When *n*-BuLi alone is mixed with benzene, little to no metalation can be observed, even after extended reaction times. However, addition of a chelating agent such as TMEDA facilitate near quantitative metalation after 3 h at room temperature (**Scheme 31**).[125]

[122] Langer, A. W. *Trans. N. Y. Acad. Sci.* **1965**, *27*, 741–747.
[123] Nichols, M. A.; Williard, P. G. *J. Am. Chem. Soc.* **1993**, *115*, 1568–1572.
[124] Strohmann, C.; Gessner, V. H. *J. Am. Chem. Soc.* **2008**, *130*, 11719–11725.
[125] Rausch, M. D.; Ciappenelli, D. J. *J. Organomet. Chem.* **1967**, *10*, 127–136.

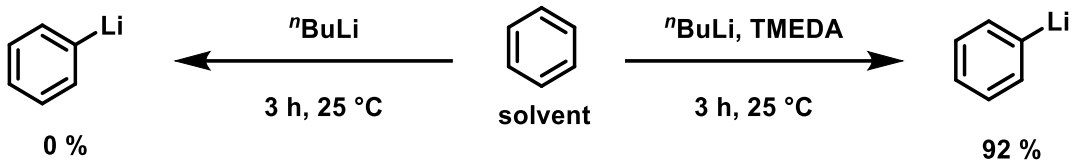

Scheme 31: Metalation of Benzene by *n*-BuLi alone vs. *n*-BuLi/TMEDA

Deprotonation of benzylic positions can also be achieved using this mixture at or above room temperature. This occurs with about 90% selectivity, with the remaining 10% being undesired deprotonation of the aromatic ring, mainly at the meta position.[126]

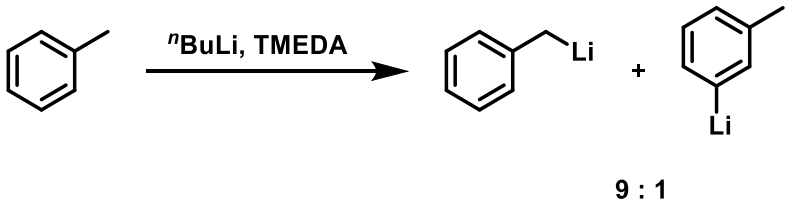

Scheme 32: Selectivity of *n*-BuLi/TMEDA deprotonation of toluene

A variety of acceptable conditions are used to deprotonate benzylic positions with amine coordinating superbases. For instance, the groups of Taylor[127] and Klein[128] both perform deprotonations at 0 °C for an unspecified amount of time, while the groups of Gates[129] and Ichikawa[130] perform deprotonations at 90 °C for 2 h and room temperature for 30 mins respectively.

---

[126] Broaddus, C. D. *J. Org. Chem.* **1970**, *35*, 10–15.
[127] Furber, M.; Herbert, J. M.; Taylor, R. J. K. *J. Chem. Soc. Perkin 1* **1989**, *4*, 683.
[128] Klein, J.; Medlik, A.; Meyer, A. Y. *Tetrahedron* **1976**, *32*, 51–56.
[129] Siu, P. W.; Serin, S. C.; Krummenacher, I.; Hey, T. W.; Gates, D. P. *Angew. Chem. Int. Ed.* **2013**, *52*, 6967–6970.
[130] Fuchibe, K.; Jyono, H.; Fujiwara, M.; Kudo, T.; Yokota, M.; Ichikawa, J. *Chem. Eur. J.* **2011**, *17*, 12175–12185.

2.2: Project Goals

Feringa *et al's* establishment of organolithiums as compatible nucleophiles for Pd-catalyzed cross coupling reactions in his 2013 *Nat. Chem*. publication served as the central motivation for this project (**Scheme 33**).[131] In this publication, Feringa demonstrated the first example of an effective organolithium coupling, which avoided significant issues of lithium halogen exchange, which have previously limited this reactions applicability.[132] This was achieved through the use of a slow addition, which allowed the oxidative addition adduct of this reaction to build in concentration; making transmetalation with organolithium the rate limiting step, and able to outcompete lithium halogen exchange.

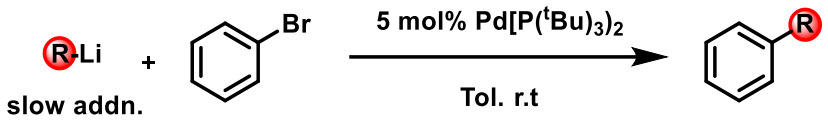

Scheme 33: Feringa's organolithium coupling

We noted that his source of organolithium nucleophiles he employed was limited to those made by either simple lithium halogen exchange, directed ortho metalation or those that were already commercially available. The ability to synthesize and couple custom or varied organoliothiums would represent a significant improvement to this work.

[131] Giannerini, M.; Fañanás-Mastral, M.; Feringa, B. L. *Nat. Chem.* **2013**, *5*, 667–672.
[132] Murahashi, S.; Yamamura, M.; Yanagisawa, K.; Mita, N.; Kondo, K. *J. Org. Chem.* **1979**, *44*, 2408–2417.

However, where Feringa was limited in this access to novel nucleophiles, Patrick Walsh's 2018 *J. Am. Chem. Soc.* focused entirely on generation of nucleophiles via a Pd/KHMDS enabled C-H activation of toluene derivatives (**Scheme 34**).[133]

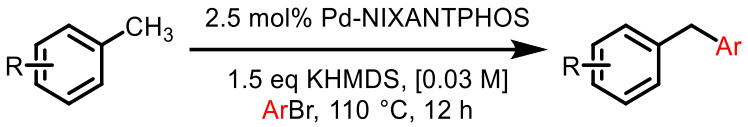

Scheme 34: Walsh's activation of toluene derivatives for coupling

However, this methodology has many limitations associated with it. Firstly, solvent quantities of toluene derivatives are required. This introduces extreme limitations to the applicability of this very powerful reaction, as the scope of reasonable starting materials is reduced to cheap commercially available compounds such as toluene, xylene or mesitylene. The requirement for solvent quantities of starting material also implicitly necessitates that the starting material is a liquid at the reaction temperature. For room temperature or cooled reactions, this would mean that even if any substrates could be sourced in large enough quantities, they would have to be lacking any decoration that might significantly raise the melting point.

Secondly, Walsh's deprotonation requires activation of the aryl ring via η^6 coordination of KHMDS, their base of choice (see **Figure 12**). This KHMDS is also

[133] Sha, S.-C.; Tcyrulnikov, S.; Li, M.; Hu, B.; Fu, Y.; Kozlowski, M. C.; Walsh, P. J. *J. Am. Chem. Soc.* **2018**, *140*, 12415–12423.

coordinated to the ligand binding the Pd centre, allowing immediate transmetalation once deprotonation has occurred.

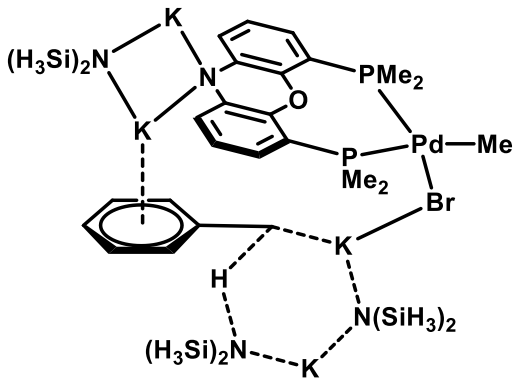

Figure 12: Walsh's proposed transition state

However, this entire coordination complex is quite bulky and results in steric clashing if decoration is present on the toluene derivative. The authors noted this as a drastic reduction in the rate constant of deprotonation from toluene to 4-^{t}Bu toluene to diphenylmethane.[133] Finally, minor criticisms involve the requirement for a sophisticated and expensive catalyst and ligand, along with the use of elevated temperatures to push the reaction forward.

With the limitations highlighted between the work of Feringa and Walsh, we hypothesized that the use of superbases presented an ideal solution to merge these excellent methodologies and end with a facile C-H activation via deprotonation followed by an efficient coupling.

Both Schlosser's and coordinated amine superbases are known to perform this deprotonation rather efficiently, but while the identity of the amine superbases is known

to be an organolithium-amine dimer[83] the exact identity of the direct Schlosser's base product is complex (see section **2.1.2.1: LiCKOR Superbases**). Our initial goals involved the generation and direct use of these species, and as such, we determined to proceed with the amine superbases in lieu of Schlosser's base for a variety of reasons. These reasons were based primarily off the assumption that both the Schlosser's base reactive species and product would behave somewhat similarly to an organopotassium. Firstly, to our knowledge, the direct cross coupling of organopotassiums has never been reported. This is most likely due to the extremely high reactivity of organopotassiums compared to other nucleophiles. For example, they are strong enough bases that they can undergo ortho deprotonation of aryl halides to form benzyne: In an experiment where BnK was isolated and subjected to coupling conditions with 2-chloronaphthalene with and without catalyst, two isomers were observed by GC, indicating significant benzyne formation, followed by substitution without specificity. Furthermore, they are only stable at cryogenic temperatures in ethereal solvents. If these temperatures are exceeded, they will begin to react and decompose whatever they are dissolved in.[113] These issues together presented a serious incompatibility that we were unprepared to try and solve when a potentially more facile alternative existed. Therefore, we decided to proceed with the *n*-BuLi/TMEDA mixture.

A wide variety of conditions have been reported to deprotonate benzylic positions with amine coordinating superbases (see **2.1.2.2: Coordinated Amine Superbases**).

However, one requirement that they all share is the use of solvent quantities of substrate, the same limitation that was faced by Walsh.[133] This presented a challenging outlook, with multiple literature sources indicating that solvent quantities of substrate were indeed required. However, the limitations faced by these researchers did not deter us, and we began investigation of optimal deprotonation conditions to ideally arrive at a process that could quickly and efficiently generate organolithium species from a variety of toluene derivatives and use them as nucleophiles in palladium catalysed cross coupling reactions.

2.3: Results and Discussion

As stated at the beginning (see Statement of Contributions:), this research was planned and executed in conjunction with Garrett P. R Freure, who performed all aspects of the research concerning coupling optimization and use of generated benzyllithium species. This will be discussed only in minimal detail as it impacts and shapes my own research and decisions regarding optimization or reaction conditions.

2.3.1: Initial Optimization of Deprotonation

The first steps that we took in the initiation of this project was to conduct our own investigation and reoptimization of the benzylic deprotonation conditions.

We decided not to perform our initial investigation with toluene itself, as we wanted to immediately establish our conditions as more generalizable. Thus, a solid (at room temperature) toluene derivative, 4-phenyltoluene, was chosen (**Table 5**). Using this substrate, it was found that elevated reaction temperatures enable reaction times as low

as 5 mins while maintaining good yields (**Table 5** Entry 1 and 2. Lower temperatures required longer reaction times (**Table 5** Entry 3 and 4). While longer reaction times did show higher conversion, the shorter reaction times were chosen as optimal to keep overall reaction time lower.

Table 5: Initial Optimization Using 4-Phenyltoluene[a]

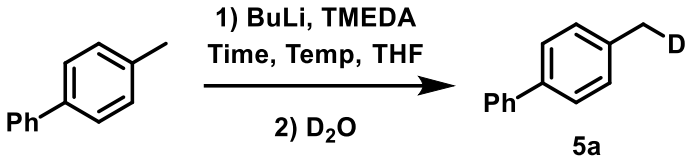

5a

Entry	Temperature (°C)	Time	% Deuteration[b]
1[c]	**60**	**5 min**	**75%**
2[c]	60	60 min	80%
3[c]	25	5 min	40%
4[c]	25	60 min	100%
5	25	5 min	20%

[a] 4-Phenyltoluene (0.5 mmol), TMEDA (0.4 mmol), and *n*-BuLi (1.6 M in hexanes, 0.4 mmol) are stirred for listed temperature and time. D_2O (0.8 mmol) is then added to quench the deprotonation.
[b] Deuteration determined by ^1H NMR by integration suppression relative to the aromatic protons
[c] Dry TMEDA over sieves

However, a control experiment without TMEDA revealed that this deprotonation could proceed in the presence of only *n*-BuLi. This is likely due to the increased level of resonance and conjugation available to 4-phenyltoluene that toluene alone cannot achieve. With this new finding, we thought it best to proceed further with the optimization using toluene itself, which is known to be much more inert to *n*-BuLi alone.[108] Still, we required an alternative quantification method as deuterated toluene

would be too volatile to reliably observe accurate ratios after workup and sample preparation. Thus, we turned to literature to find an acceptable method of quantification for these reactive intermediates and found precedent for a quench with benzophenone to yield benzyldiphenylcarbinol in 85% yield.[134]

Despite the change in both substrate and quantification method, we still thought our findings of high temperatures and low reaction times would hold true and attempted the same conditions with a slight increase in time to compensate for the less activated nature of toluene (**Scheme 35**). The yield of this experiment was, unsurprisingly, much lower than with 4-phenyltoluene at 45%.

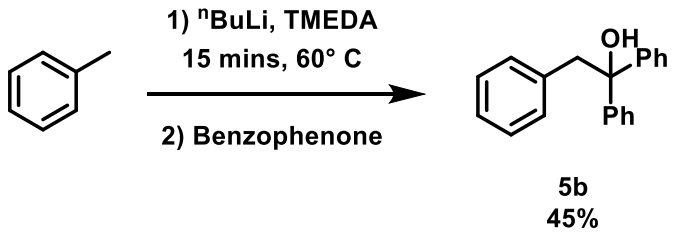

Scheme 35: Application of partially optimized conditions to toluene

Still, these conditions were used to begin investigation into the second step of the project: cross-coupling. It was at this point that we discovered a key limitation with TMEDA when we began observing *N*,*N*-dimethyl-2-naphthylamine in the product mixtures (**Scheme 36**).

[134] Eberhardt, G. G.; Butte, W. A. *J. Org. Chem.* **1964**, *29*, 2928–2932.

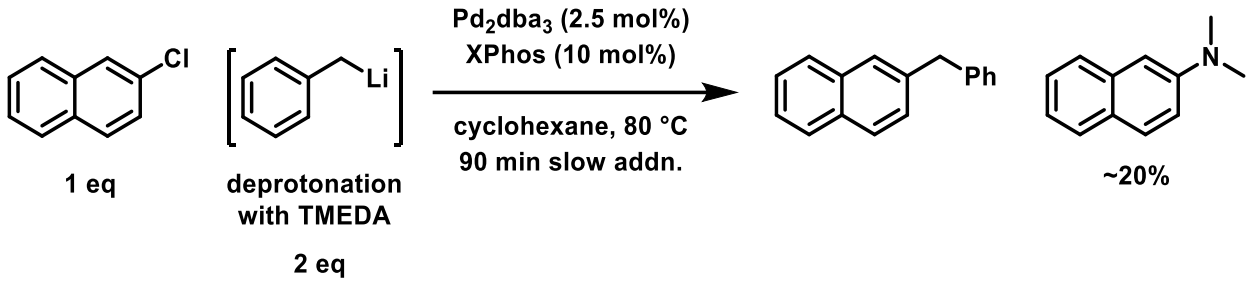

Scheme 36: Formation of *N*,*N*-dimethylaniline products by Garrett P.R Freure

TMEDA is known to undergo decomposition when subjected to aggressive reaction conditions with organolithiums to produce lithium *N*,*N*-dimethylamide (**Scheme 37**).[134] We hypothesized that this decomposition was responsible for the generation of this side product, which most likely resulted from a Buchwald-Hartwig amination between the aryl halide and *N*,*N*-dimethylamide.

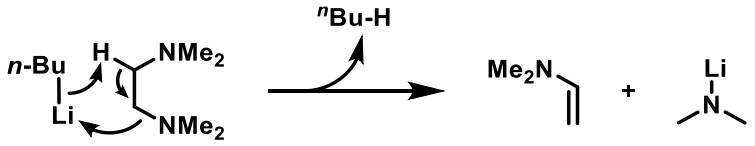

Scheme 37: Proposed TMEDA decomposition pathway

We hypothesized and arrived at two possible solutions: milder reaction conditions, or an alternative to TMEDA that would be more resistant to decomposition. Milder conditions would mean longer reaction times which, as stated above, we wanted to avoid if possible. That left seeking an alternative to TMEDA. As it happens, trans-*N*,*N*,*N*′,*N*′-tetramethylcyclohexane-1,2-diamine (TMCDA, see **Scheme 38**) is a known, though relatively less common alternative to TMEDA for this super base chemistry.[83] As seen in **Scheme 37**, the decomposition path for TMEDA arises from an E_2 type reaction,

whereupon the flexibility of the carbon backbone enables rotation and adoption of geometry that permits this elimination. A rigid backbone could lock the amine in a conformation that is unfavourable to undergo elimination, but still facilitates coordination and reactivity. Thus, we thought TMCDA would be a perfect candidate for our needs.

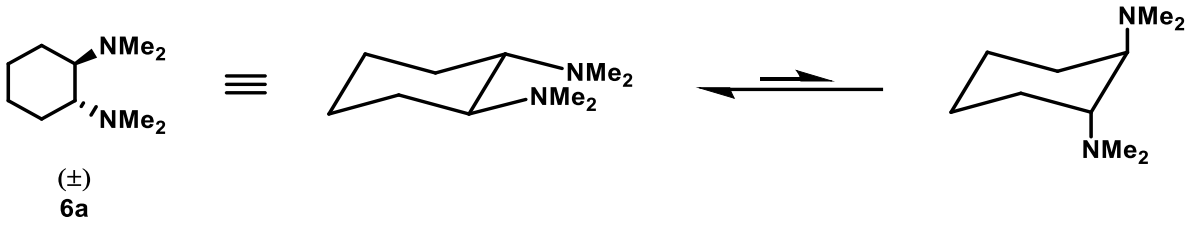

Scheme 38: TMCDA structure and rigid backbone discourages decomposition

By adopting a chair conformation with a (racemic) trans substitution pattern, the substituents would preferentially adopt the di-equatorial orientation. This drastically reduces the possibility of elimination as axial geometry is required for E_2 reactions to proceed in a ring. Even if a chair flip to the di-axial geometry were to occur, statistically there would only be a single proton available for each amine group to be eliminated. After an easy one step synthesis from a commercially available starting material, we began optimization of the reaction using TMCDA (**Table 6**).

Table 6: Optimization of Deprotonation with TMCDA[a]

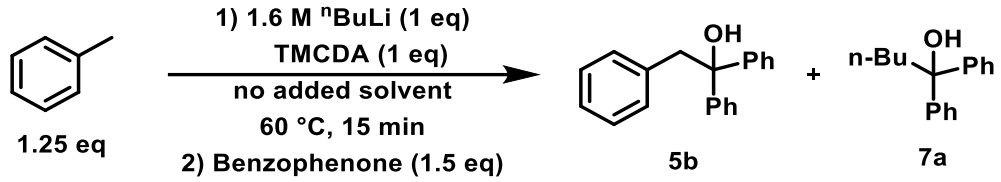

Entry	Deviation from Standard Conditions	Yield[b]	
		5a	7a
1	**none**	**55%**	**0%**
2	TMEDA instead of TMCDA	45%	0%
3	Room Temperature	22%	24%
4	Room Temperature for 1 h	50%	4%
4	Diluted with cyclohexane [0.3M]	37%	7%
5	Diluted with cyclohexane [0.3M] for 30 mins	42%	trace

[a] Toluene (0.5 mmol), TMCDA (0.4 mmol), and *n*-BuLi (1.6 M in hexanes, 0.4 mmol) are stirred at 60 °C for 15 minutes. Benzophenone (1M in THF, 0.6 mmol) is then added to quench the deprotonation.
[b] Yields are reported by GC-MS using a 5-point calibration curve relative to 1,3,5-trimethoxybenzene as an internal standard

Conditions of 60 °C for a time of 15 mins with no additional solvent were found to be optimal, and delivered a yield of 55% by GC-MS, an immediate 10% improvement from TMEDA (**Table 6** Entries 1 and 2). Furthermore, when these conditions were applied to the coupling, it was immediately seen that the dimethylamino product (seen in **Scheme 36**) had disappeared entirely. If lower temperatures were employed, the reaction proved to be quite slow, and could not go to completion, even after elongated reaction times (**Table 6** Entries 3 and 4). Finally, the usage of additional solvent did

nothing to benefit the reaction, even with longer reaction times to make up for slower kinetics (**Table 6** Entries 5 and 6).

With these optimized conditions, our yields remained around 50%, and so all coupling reactions performed with these deprotonation conditions were done using 2 equivalents of benzyllithium. These conditions feature a path to directly couple the resulting organolithium (**Scheme 39** Path A), or perform a transmetalation to obtain the corresponding organozinc followed by an optimized Negishi coupling (**Scheme 39** Path B).

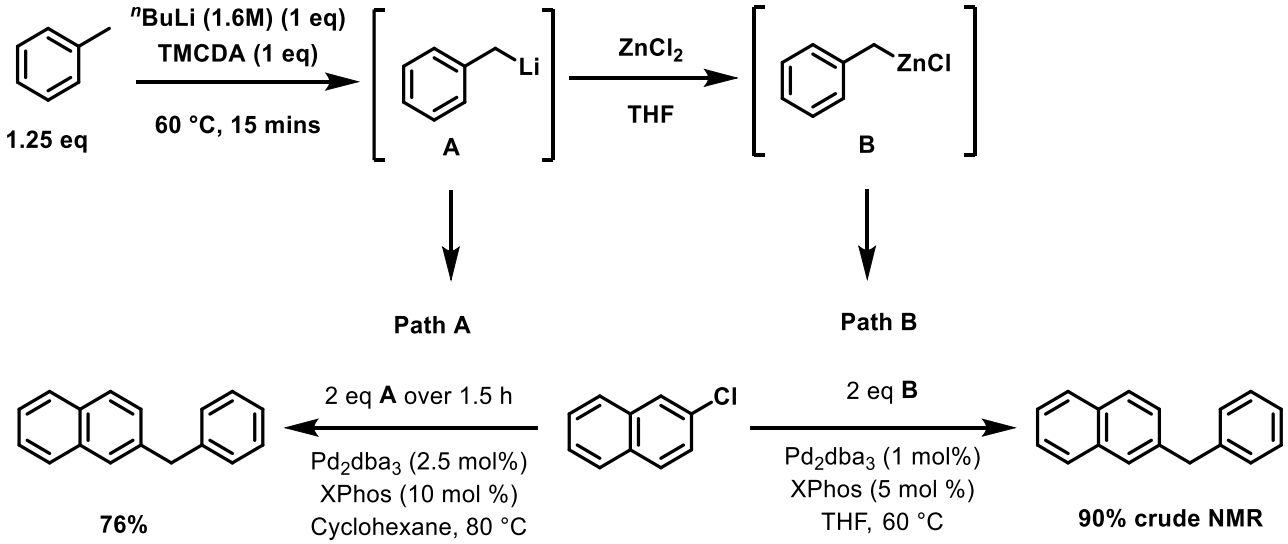

Scheme 39: Coupling conditions developed by Garrett P. R. Freure for generated organolithiums and organozincs

2.3.2: Scope of Deprotonation

Having a greater appreciation and understanding of the reaction, we decided to try and investigate whether our initial goal of generalizable conditions for benzylic deprotonation had been realized. As the logical extension of the deprotonation conditions

are for use in subsequent coupling, data will be presented regarding the final coupled product in lieu of quenched and isolated intermediates.

2.3.2.1: Ethylbenzene Selectivity

The first new substrate that was attempted was ethylbenzene. This secondary benzylic position is known to be more difficult to deprotonate, leading to significant selectivity issues arising from aryl ring deprotonation.[126] Despite this, we attempted a variety of conditions hoping to alter the product distribution by manipulating reaction length, concentration and temperature (see **Table 7**). While our conditions did seem to offer a significant improvement to previous literature attempts,[126] we observed that when these conditions were used in the coupling, an inseparable mixture of isomers was still obtained. Since Schlosser's base is already known to perform this deprotonation with a much higher degree of selectivity,[114,126] we abandoned further attempts to make these conditions more selective. New conditions to perform this deprotonation and coupling selectively with Schlosser's base instead are currently under development by other members of the group.

Table 7: Selectivity of Ethylbenzene Deprotonation[a]

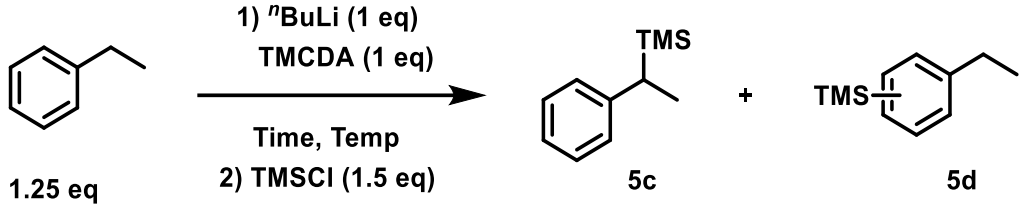

Entry	Temperature	Time	Selectivity	
			5c	5d
1	60	1.5 h	75	24
2	60	3 h	76	31
3	25	1.5 h	74	25
4	0	1.5 h	76	23
5[c]	60	1.5 h	73	26

[a] Ethylbenzene (0.5 mmol), TMCDA (0.4 mmol), and *n*-BuLi (1.6 M in hexanes, 0.4 mmol) are stirred at specified temperature for specified time. TMSCl (0.6 mmol) is then added to quench the deprotonation.
[b] **5c** was synthesized independently to verify elution time by GC-MS (see Figure **S1**)
[c] Reaction diluted to [0.3 M] with cyclohexane

2.3.2.2: Other Scope Investigations

The scope of compatible toluene derivatives with this deprotonation is quite narrow. Any electrophilic functionalities such as nitriles, esters, ketones, aldehydes or alkyl halides are automatically disqualified, as we are generating a highly nucleophilic species. If these functionalities were present, the product would be consumed as soon as it is formed. Thus, our initial examples include only a handful of decorated toluene derivatives with a single available benzylic position (see **Scheme 40**).

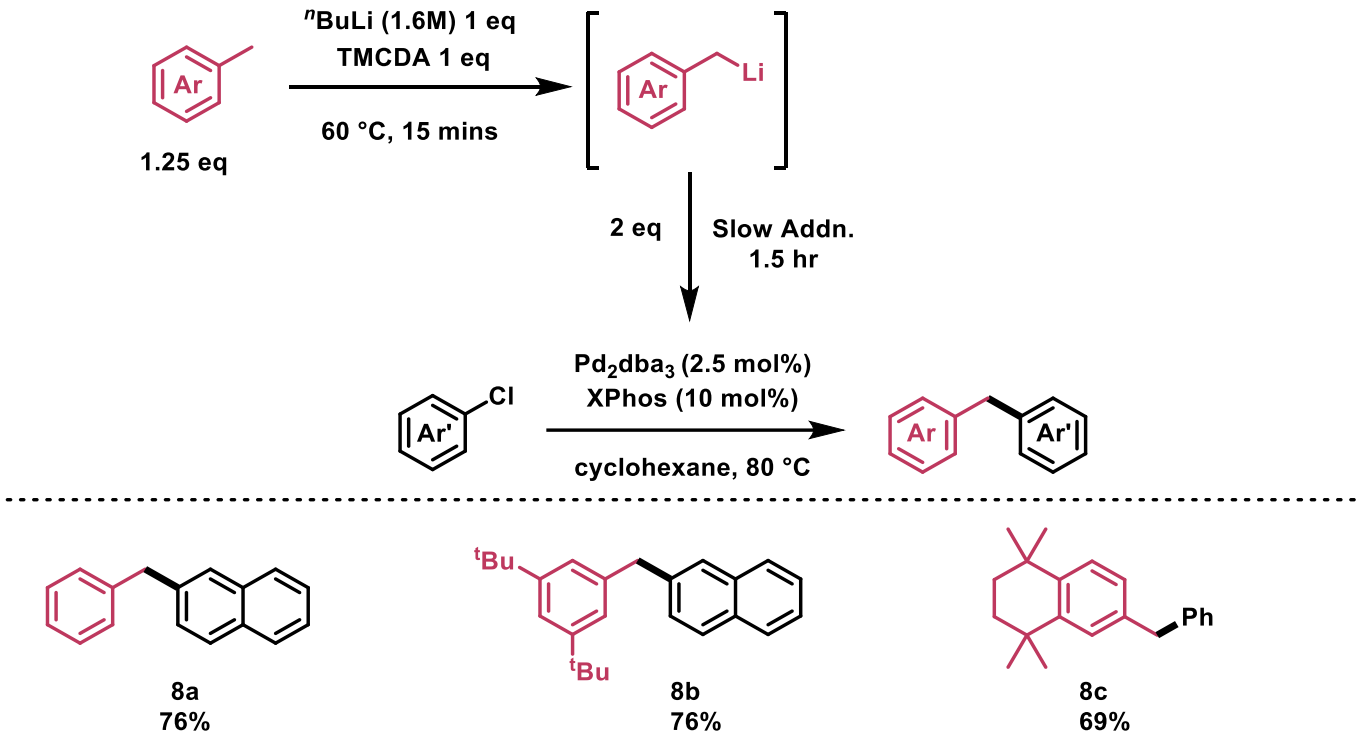

Scheme 40: Scope of coupling reactions performed by Garrett P.R Freure using developed deprotonation conditions

Following this success more ambitious toluene derivatives were attempted including substrates bearing altered ring electronics, acidic protons, acetals, carbamates and ethers. Unfortunately, each one of these examples either failed to yield product at all, or was susceptible to an alternative reaction path such as directed ortho metalation or deprotection, making them unfeasible (see **Scheme 41**).

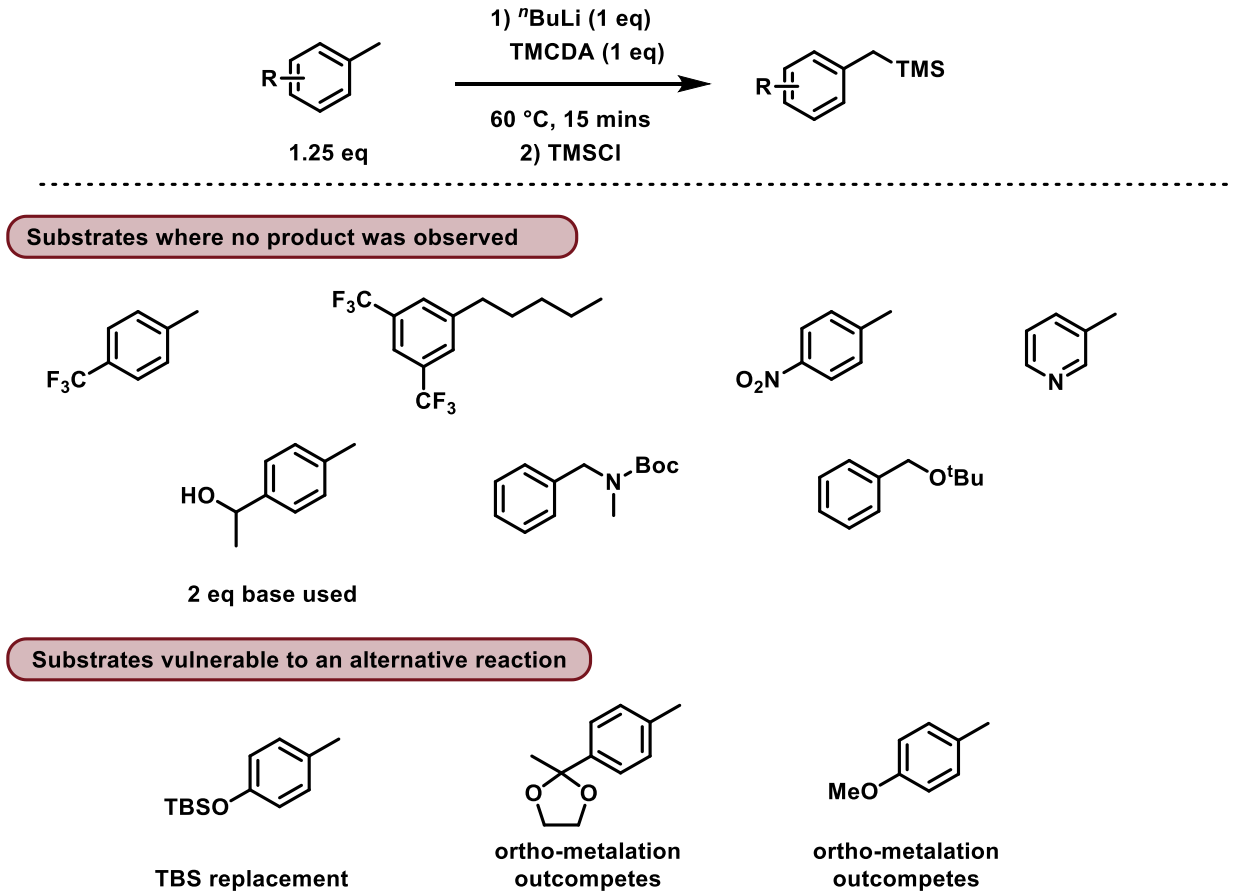

Scheme 41: Failed scope examples

After these ambitious scope attempts, a return to simple hydrocarbons was chosen; this time with a focus on multiple possible sites of deprotonation, as can be seen in **Scheme 42**. Methylnaphthalene and *p*-cymene both were immediately amenable to the deprotonation conditions; both showing two peaks with a mass corresponding to a TMS adduct by GC-MS in greater than 95:5 ratio. We hypothesized that these peaks might be the result of deprotonation and quench at both the benzylic position and the aromatic ring. However, when *m*-xylene and mesitylene were subjected to the reaction conditions, a slightly different observation was noted. In the crude GC-MS of *p*-xylene, two peaks of interest were seen. These peaks corresponded to the molecular weight of the starting

material with a single TMS group added, and the molecular weight of the starting material with two TMS groups added (93 : 7 ratio). This trend was continued with in the crude GC-MS of mesitylene, where three peaks corresponding to the mass of a mono, di and tri-silylation were observed (91 : 7 : 1 ratio).

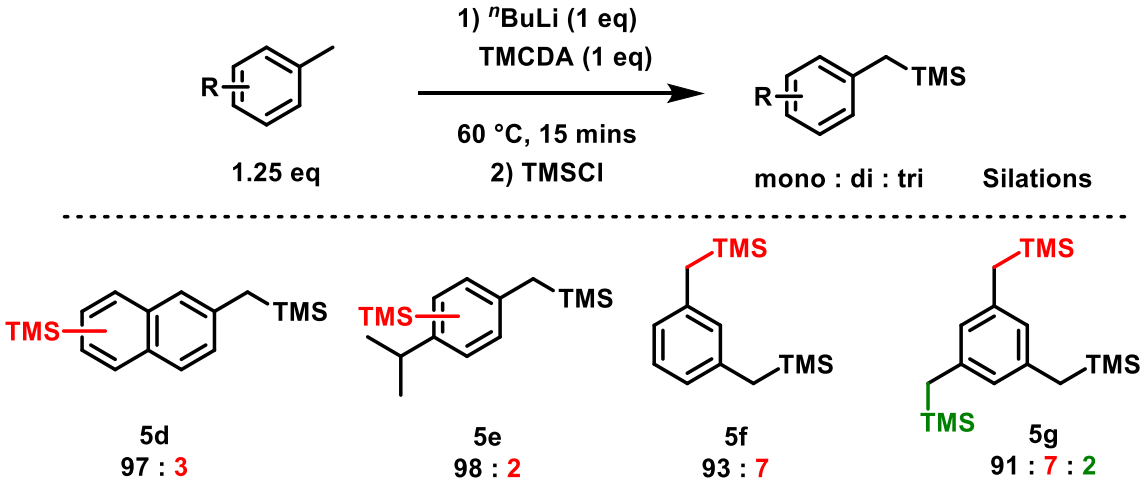

Scheme 42: Ratios of silylated products by GC-MS showing scope of tolerated toluene derivatives with multiple sites of deprotonation.

In order to avoid potential multiple deprotonations interfering with the coupling results, a quick reoptimization was performed (**Table 8**). By using a slower addition of *n*-BuLi to the reaction mixture and a slightly larger excess of starting material (**Table 8** Entries 2 and 3), the ratios of likely TMS adducts was shifted away from multiple silylations.

Table 8: Reoptimization for Multiple Primary Benzylic Positions[a]

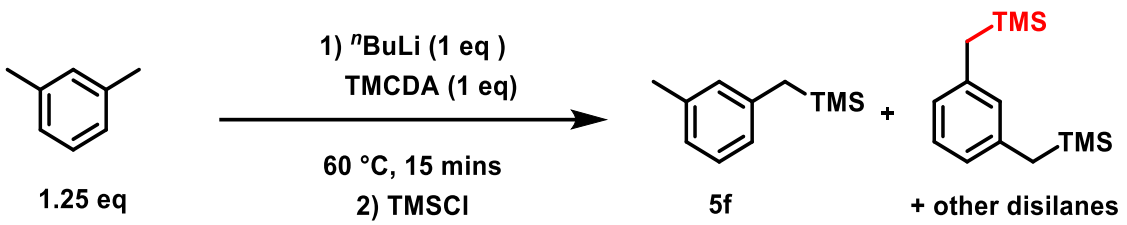

Entry	Deviation from standard conditions	Selectivity[b] (mono : di : [tri])
1	none	93 : 7
2	*n*-BuLi added over 10 mins	98 : 2
3	2.5 eq of starting material used	97 : 3
4	2.5 eq of Mesitylene with *n*-BuLi added over 10 mins	98 : 1 : 0

[a] Substrate (0.5 mmol), TMCDA (0.4 mmol), and *n*-BuLi (1.6 M in hexanes, 0.4 mmol) are stirred at 60 °C for 15 minutes. TMSCl, 0.6 mmol) is then added to quench the deprotonation

[b] Selectivity determined by GC-MS using reported mass of starting material with multiple TMS groups added

As we did not conduct any thorough characterization of these reactions, the structures and sites of deprotonation presented are only logical hypotheses up to this point. Structure verification and characterization was performed after these intermediates were used in the subsequent coupling reaction to verify deprotonation site and selectivity.

The next round of coupling reactions using the above developed substrates and conditions was performed using previously mentioned "Path B" conditions (see **Scheme 39**). This involved the identical generation of the benzyllithium species, followed by a

transmetalation with $ZnCl_2$ to obtain the benzylzinc (**Scheme 43**). These resulting nucleophiles are much milder and more selective, enabling higher yields, lower catalyst loading and a *drastically* improved and diverse scope of compatible aryl halides, all without the use of a slow addition.

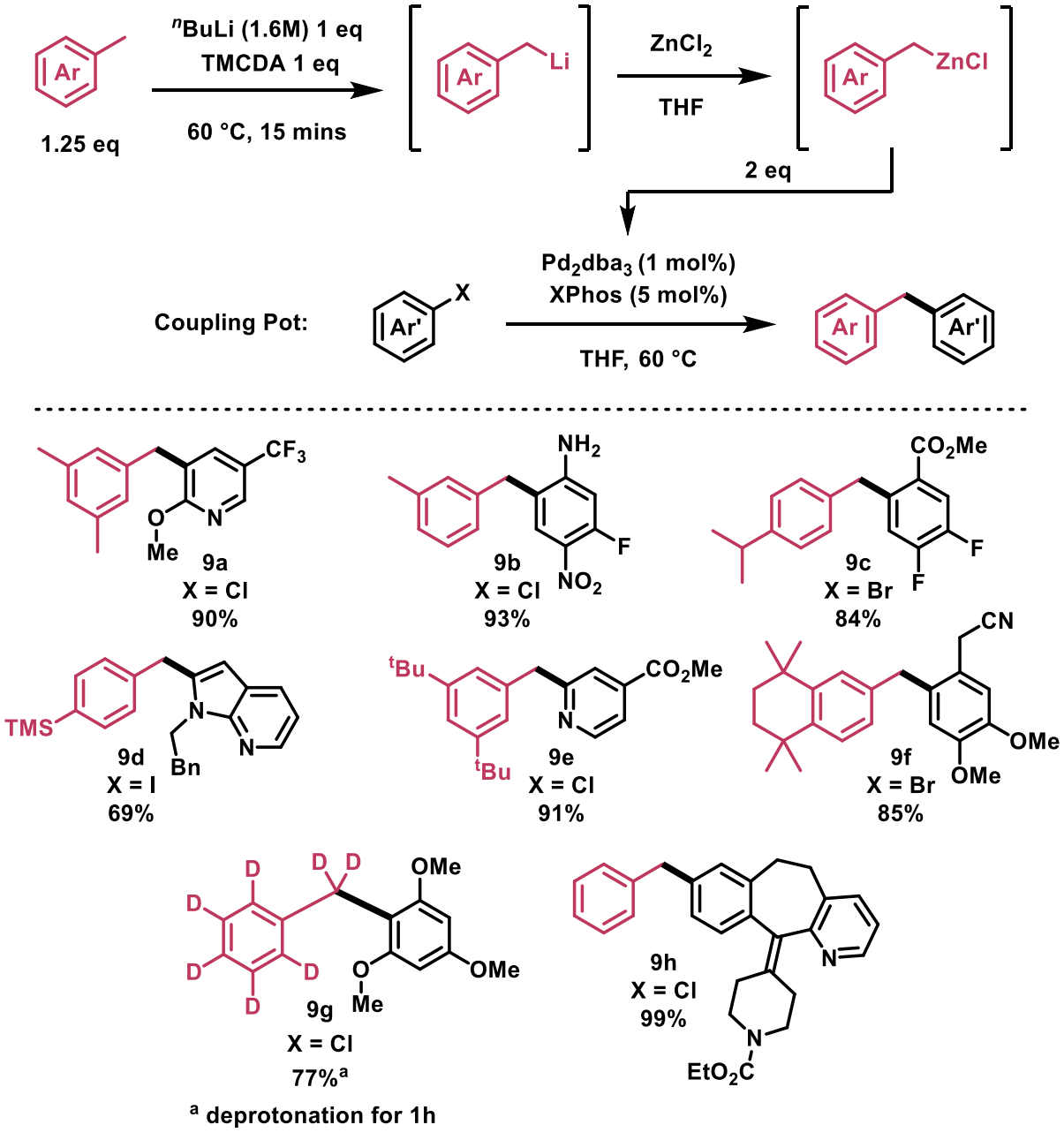

Scheme 43: Coupling reactions performed by Garrett Freure using optimized deprotonation conditions

As can be seen in **Scheme 40** and **Scheme 43**, the isolated products from the coupling support earlier hypotheses about site selectivity.

2.4: Deprotonation of Toluene Derivatives in Flow

One limitation of the deprotonation conditions in batch is that when scaled up it would involve a large volume of very reactive superbase being handled all at once, which could lead to significant safety risks. Flow chemistry is a well established method to provide facile and safe scale up of reactions with hazardous intermediates, such as this one.[135] This methodology has been previously applied to using Schlosser's base in flow to synthesize ibuprofen in three superbase facilitated steps.[136] Our goal was to develop a facile adaptation of our optimized batch deprotonation to flow, and utilize continuous generation to slowly add this nucleophile to our coupling pot at increased scale. With this method, only a small amount of the superbase exists at any given time, before it is added to the coupling pot. This would circumvent the necessity to manipulate large amounts of our superbase in a syringe, thus avoiding potential safety hazards.

To this end, a flow apparatus was set up such that we mirrored our optimal conditions in batch with a residence time of 15 mins at 60 °C (**Scheme 44**). We found that a back pressure regulator was important for preventing formation of bubbles, presumably from generated butane.

---

[135] Plutschack, M. B.; Pieber, B.; Gilmore, K.; Seeberger, P. H. *Chem. Rev.* **2017**, *117*, 11796–11893.
[136] Lee, H.; Kim, H.; Kim, D. *Chem. – Eur. J.* **2019**, *25*, 11641–11645.

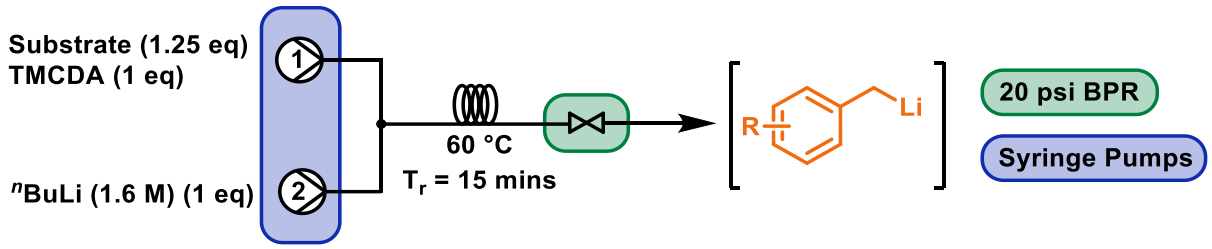

Scheme 44: Initial flow apparatus

We decided to assemble the flow apparatus such that the substrate and TMCDA are contained in **Syringe 1**, while [1.6 M] *n*-BuLi is contained in S**yringe 2** (see **Figure 13**). This way we can prevent formation of the superbase until the solutions meet. If the desired substrate is not liquid at room temperature *and* not soluble in TMCDA alone, a slight modification can be made to this setup. Using [2.5 M] *n*-BuLi in lieu of 1.6 M, would mean a smaller volume would be required to add the same molar amount. This difference in volume can be added to **Syringe 1** as cyclohexane to help solubilize a substrate (proper adjustments must be made to flow rates to account for this alteration of volumes and concentration).

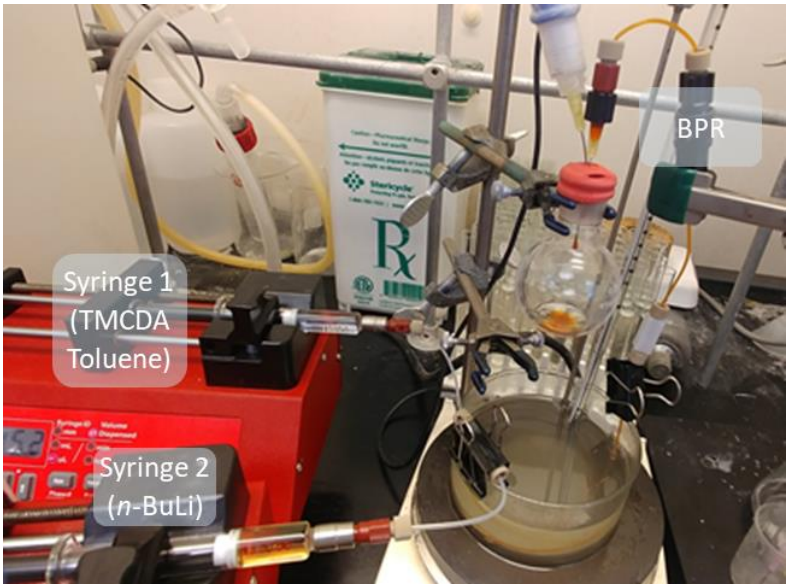

Figure 13: Picture of flow apparatus

With the flow apparatus assembled and tested, we next wanted to use it to perform our optimized coupling at 10 mmol scale (relative to aryl halide). However, since an improved coupling was achieved with a transmetalation of the organolithium to the organozinc, we wanted to replicate this in flow as well using a [0.25 M] solution of $ZnCl_2$ in THF. This reaction produces an organozinc, along with LiCl precipitate. While this precipitate did not present a problem in batch, solid precipitates in flow are very prone to cause fouling of reaction tubes and ultimately lead to clogging, especially at T-mixing junctions where solutions first contact each other. To prevent this issue, we came up with two solutions to try and prevent this clogging issue: a Tube-in-Tee style mixer, or a quench pot style collection.

2.4.1: Tube-in-Tee Mixer

This Tube-in-Tee style approach works on the premise that T-mixers have extremely narrow passages, which are prone to fouling and clogging (see **Figure 14 A**). Therefore, by using an efflux tube with a larger internal diameter and extending the tubing of one reagent inside this inner diameter of the efflux tube (see **Figure 14 B**), a much larger volume is permitted for precipitate to form and be swept away before it can settle and block flow.

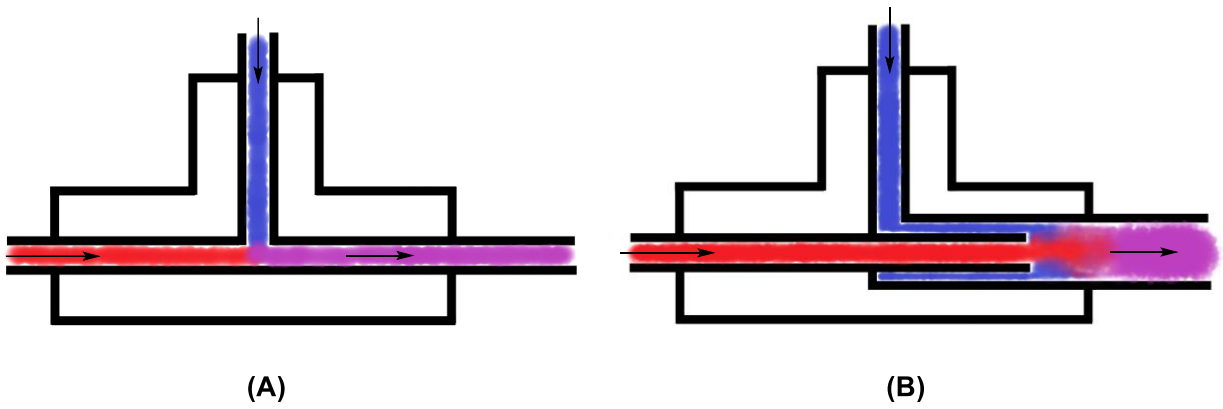

Figure 14: Regular t-mixer (A) compared to a "Tube-in-Tee" style mixer (B)

This Tube-in-Tee style mixer was employed at the junction of the benzyllithium meeting the $ZnCl_2$ solution, in an attempt to prevent LiCl from building up and clogging the tubes (**Scheme 45**). To our pleasure, this system worked rather well, and all evidence of clogging disappeared once it was implemented.

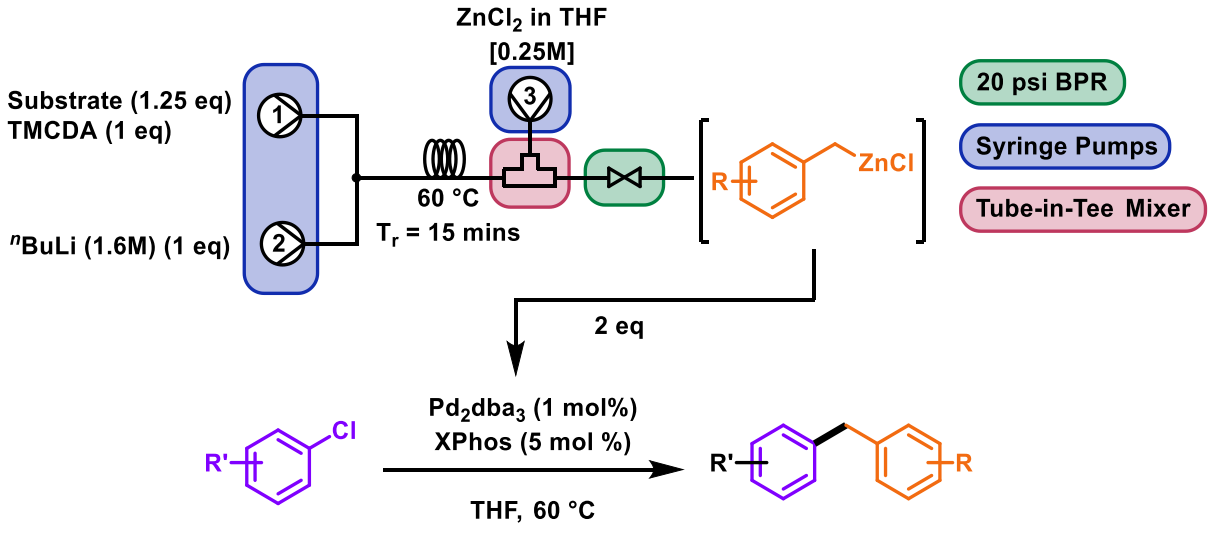

Scheme 45: Flow setup using Tube-in-Tee Mixer

2.4.2: $ZnCl_2$ Quench Pot

The second, and simpler, idea we came up with was to simply generate the benzyllithium in flow and collect it in a pot containing our $ZnCl_2$ solution (**Scheme 46**).

This would still allow generation of our desired organozinc while eliminating the possibility of its formation causing fouling entirely. This collected organozinc can then be dosed with aryl halide and catalyst, and heated for the second part of the reaction to take place.

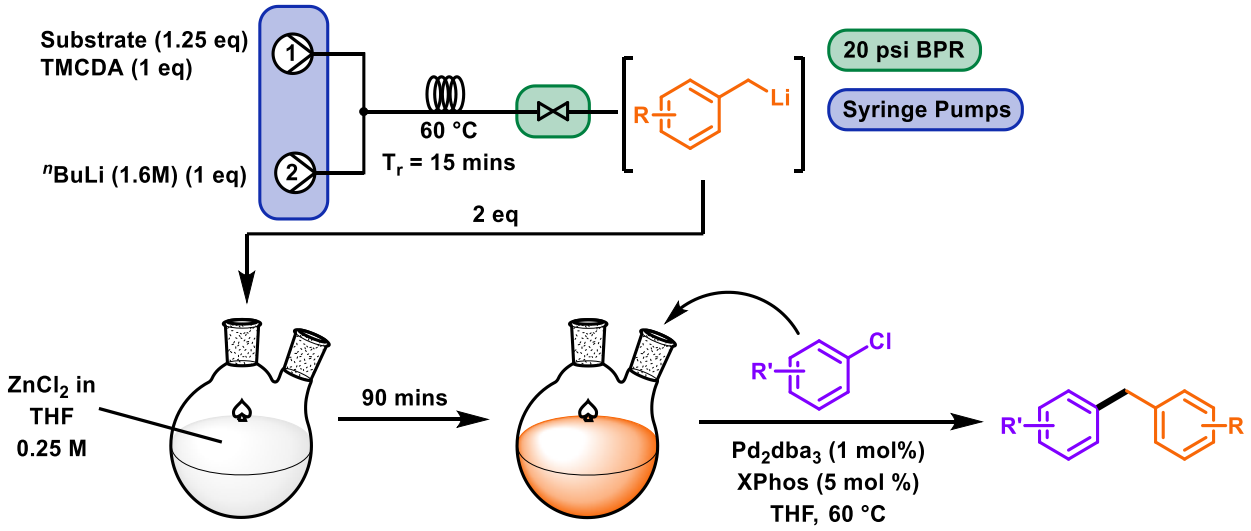

Scheme 46: Collection of benzyllithium in a $ZnCl_2$ pot

Both of the above strategies were assembled and tested using 3,5 ditertbutyltoluene as a nucleophile, with a variety of aryl halides. Unfortunately, both methods ultimately failed to match the results that could be obtained in batch, as significant new problems began to arise.

Firstly, we began to recover aryl halide after the reaction was supposed to have reached completion and 2 eq of nucleophile had been added. In addition, we observed incomplete conversion of *n*-BuLi, as its coupled product was observed by GC. Both of these problems hadn't presented in batch reactions since optimization had been completed. Upon closer analysis of crude GC's, 2 new side products were observed which

could explain these findings. These products corresponded to a benzyl alcohol and a benzaldehyde derivative of our nucleophiles. These findings were consistent across multiple nucleophile and electrophile pairings . No characterization or isolation of these products was performed, and as such, we cannot be totally confident in their accuracy.

Our best hypothesis to explain these findings lies in the permeability of PFA tubing we employed to assemble the flow apparatus. It is known that PFA tubing's permeability to gasses increases with rising temperatures.[137] This increase in permeability, to oxygen in particular, could be the mechanism by which oxygen is introduced to this system. This would explain the recovery of aryl halide, as degradation of nucleophile would mean that less than the required 2 equivalents would be delivered to the coupling mixture. This would also explain why this issue is so present in flow, but not in batch. These issues together presented a significant issue when considering yield and ease of purification of the final product.

As time was a limiting factor in the conduct of this research, there are possible solutions that were unable to be attempted. If further attempts were to be made, the main issues that should be addressed are replacing the PFA tubing with alternate materials such as PEEK or possibly stainless steel. These materials would not have the same issues of gas permeability as PFA and could provide a simple solution to test our hypothesis.

2.5: Conclusions

Organolithium species are extremely reactive, and as such, have been utilized to perform a variety of transformations that would otherwise be impossible or drastically less practical. However, this reactivity has historically proved too uncontrollable for the world of transition metal catalysed cross coupling chemistry. Feringa changed this through implementation of slow addition technology, making organolithiums useful reagents to perform coupling of sp^3 hybridized carbon centred nucleophiles. Sp^3 functionalization remains an extremely difficult challenge, with only a handful of options available all with stringent requirements such as solvent quantities of substrate, intramolecular reactivity, or use of directing groups.

Our goal at the inception of the project was to develop a methodology that circumvents these restrictions and allows generation and use of diverse benzylic sp^3 hybridized nucleophiles using stoichiometric quantities of starting material without the use of a directing group. This was ultimately achieved through means of C-H activation via deprotonation with superbases followed by coupling to facilitate complex functionalization of extremely simple starting materials in two steps.

Limitations that are still faced is the adaptation of this deprotonation methodology to flow chemistry, most likely due to the PFA tubing currently used being permeable to oxygen at elevated temperatures. Potential solutions that should be investigated are the use of other materials such as PEEK. The next steps that should be taken in the

development of this chemistry is the application of this C-H activation methodology to other starting materials such as olefins, ethers or secondary benzylic positions.

Chapter 3: Supporting information

3.1: Ozone Mediated Amine Oxidation

3.1.1: General Experimental Details

Unless otherwise indicated, reagents were obtained from Sigma Aldrich, Fisher Scientific or Combi-Blocks and used as received. Silicycle F60 40-63 μm silica gel was used for amine suspension and column chromatography. The silica gel was stored at room temperature and dried in a 140 °C oven for ~24 hours prior to use in the packed bed reactor. Analytical thin layer chromatography (TLC) was conducted using aluminum-backed EMD Millipore Silica Gel 60. Visualization of developed plates was performed under UV light (254 nm) and/or using $KMnO_4$ stains.

3.1.1.1: Instrumentation and Flow Reactor Details

^{1}H NMR and ^{13}C NMR were recorded on a Bruker AVANCE 400 MHz spectrometer and referenced to residual solvent signals. Data for ^{1}H NMR are reported as follows: chemical shift (δ ppm), multiplicity (s = singlet, d = doublet, t = triplet, q = quartet, m = multiplet), coupling constant (Hz), integration. Yields for optimization were determined by NMR or GC analysis of the crude reaction mixture using 1,3,5-trimethoxybenzene as an internal standard. FTIR spectra were collected on a Varian 640-IR spectrometer equipped with an attenuated total reflectance accessory (ATR, Pike MIRacle) in the 4000-400 cm^{-1} range with 64 scans per sample. Unless otherwise indicated, continuous flow experiments were performed using 1/16" O.D., 1.0 mm I.D. PFA. PEEK fittings were used for all PFA tubing. PEEK fittings and parts were purchased from Upchurch Scientific. Vapourtec V3 pumps with blue tubing and built-in Tee joints were used for pumping and reagent selection.

3.1.1.2: General Procedure A

To a clean round-bottom flask was added the corresponding amine (0.3 mmol), followed by pentane (20 mL). 3 g of silica gel (stored in a 140 °C oven overnight) was added to form a slurry (0.1 mmol of substrate per gram of silica). The solvent was slowly evaporated under reduced pressure (no lower than 800 mbar to avoid silica bumping as it dries) to yield silica gel loaded with starting material. 1 g of this impregnated silica gel was added to an omnifit column measuring 150 mm long with an I.D of 10 mm (Part number# 006EZ-10-15-AF). The silica plug measured around 3 cm long inside the column. This assembly was connected to a Vapourtec E-series (easy-Medchem) reactor and cooled

down to -60 °C using the with Vapourtec Cooling Module (#50-1314) under a constant flow of oxygen through the reaction vessel (10 psi). Once the reactor was cooled, the in-line ozone generator (Oxidation Technologies, VMUS-DG1) was turned on. This was operated at maximum power with an approximate flow rate of 0.12 L/min of oxygen. This corresponds to an approximate production of 1.75 g/h or 0.6 mmol of O_3 per minute. Ozone exit tubing from the reaction led to a solution of sodium metabisulfite in water to quench any remaining excess.

After 15 minutes, the ozone generation was turned off while allowing oxygen to continue to flow. After the remaining ozone is purged from the silica gel (~10 seconds; loss of blue color), the reactor is allowed to warm to room temperature. Silica gel was harvested from the reactor and the column was cleaned with acetone before repeating above procedure again. Two combined 1 g reactions were directly dry-loaded to a column of silica gel for purification following a pentane wash to remove excess grease.

3.1.1.3: General Procedure B

Identical to General Procedure A, but reactor is cooled to -20 °C and ozone is applied for 60 min.

3.1.1.4: Reaction 'Automation' Procedure

Amine was dissolved in 10% MeOH/DCM solution (0.1 mmol amine per 10 mL of solution). 1 g of dried silica gel was added to our omnifit column, and attached to the Vapourtec built in pumps. Using the Vaportec V3 pumps, a total of 10 mL of this solution was drawn added to the omnifit column. The Vapourtec interface was then used to select oxygen flow to remove the solvent and dry the column for a total of 20 mins. Reaction was then cooled and ozonated as described in General Procedure A. Following reaction completion, Vapourtec V3 pumps were used to draw and pump 20 mL of a 1:1 MeOH/DCM solution. These steps could then be repeated from the beginning.

3.1.2: Starting Material Synthesis

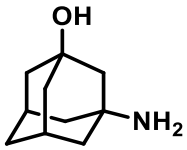

3-Aminoadamantol: Synthesized according to literature precedent.[1] Adamantanamine (1 g, 5.33 mmol) was added to a pot of premixed H_2SO_4 (10.3 mL) and nitric acid (1 mL) at 0 °C and yielded the title product as a white solid (0.6987 g, 78%). ^{1}H NMR: (400 MHz, $CDCl_3$) δ 2.28-2.19 (m, 4H), 1.68-1.59 (m, 4H), 1.56 (s, 2H), 1.52-1.48 (m, 6H). ^{13}C NMR (100 MHz, $CDCl_3$) δ 69.8, 53.9, 50.4, 44.9, 44.1, 34.8, 31.1.

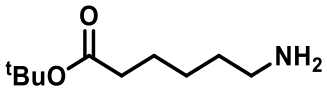

6-aminohexanoic acid tert-butyl ester: Synthesized according to literature precedent.[2] 6-aminohexanoic acid (0.6560 g, 5.0 mmol) was mixed with thionyl chloride (1.63 mL, 22.5 mmol) and *t*-BuOH (2.7 mL) to yield the title compound as an off white solid (0.4064 g, 44%). ^{1}H NMR: (400 MHz, $CDCl_3$) δ 2.63 (t, J= 7.0 Hz, 2H), 2.19 (s, 2H), 2.13 (t, J= 7.4 Hz, 2H), 1.51 (quin, J= 7.4 Hz, 2H), 1.42 (quin, J= 7.4 Hz, 2H), 1.35 (s, 9H), 1.31-1.22 (m, 2H). ^{13}C NMR (100 MHz, $CDCl_3$) δ 172.9, 79.4, 41.6, 35.3, 32.7, 28.0, 26.2, 24.7.

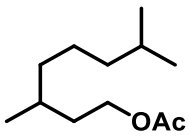

3,7-dimethyloctyl acetate: Synthesized according to literature precedent.[3] 3,7-Dimethyloctanol (0.96 mL, 5.0 mmol) and acetyl chloride (0.43 mL, 6.0 mmol) were mixed to yield the title compound as a colourless oil (0.7712 g, 77%). ^{1}H NMR: (400 MHz, $CDCl_3$) δ 4.15-4.03 (m, 2H), 2.04 (s, 3H), 1.70-1.60 (m, 1H), 1.57-1.48 (m, 2H), 1.47-1.37 (m, 1H), 1.35-1.08 (m, 6H), 0.89 (d, J=6.5 Hz, 3H), 0.86 (d, J=6.6 Hz, 6H). ^{13}C NMR (100 MHz, $CDCl_3$) δ 171.2, 63.1, 39.1, 37.1, 35.5, 29.8, 27.9, 24.6, 22.7, 22.6, 21.0, 19.5.

3.1.3: Characterization Data for Products:

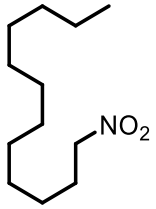

1-Nitrododecane (1a): The title compound was synthesized according to general procedure A using dodecylamine (0.0370 g, 0.2 mmol) and 2 g of dry silica gel. After reaction, the product was isolated using flash chromatography (5% EtOAc/Hexanes, R_f: 0.43). The title compound was isolated as a yellow oil (0.013 g, 62%). ^{1}H NMR: (400 MHz, $CDCl_3$) δ 4.38 (t, *J* = 7.1 Hz, 2H), 2.00 (quin, *J* = 7.1 Hz, 2H), 1.42-1.20 (m, 18H), 0.88 (t, *J* = 6.8 Hz, 3H). ^{13}C NMR (100 MHz, $CDCl_3$) δ 75.7, 31.9, 29.7, 29.6, 29.4, 29.3, 29.2, 28.8, 27.4, 26.2, 22.7, 14.1. Spectral data was consistent with literature reports.[4]

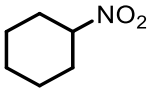

Nitrocyclohexane (1b): The title compound was synthesized according to general procedure A using cyclohexylamine (0.0298 g, 0.3 mmol) and 3 g of dry silica gel. Crude NMR: 80%. After reaction, the product was isolated using flash chromatography (10% EtAOc/Hexanes, R_f: 0.44). The title compound was isolated as a yellow oil (0.0216 g, 56%). ^{1}H NMR: (400 MHz, $CDCl_3$) δ 4.36 (tt, *J*= 10.7, 4.0 Hz, 1H), 2.26-2.19 (m, 2H), 1.91-1.82 (m, 4H), 1.69-1.62 (m, 1H), 1.39-1.23 (m, 3H). ^{13}C NMR (100 MHz, $CDCl_3$) δ 84.6, 30.9, 24.7, 24.1. Spectral data was consistent with literature reports.[5]

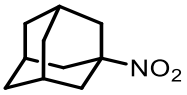

Nitroadamantane (1c): The title compound was synthesized according to general procedure A using adamantylamine (0.0306 g, 0.2 mmol) and 2 g of dry silica gel. After reaction, the product was isolated using flash chromatography (5% EtOAc/Hexanes, R_f: 0.44). The title compound was isolated as a yellowish solid (0.0290 g, 80%). ^{1}H NMR: (400 MHz, $CDCl_3$) δ 2.23 (s, 3H), 2.21 (s, 6H), 1.77-1.66 (m, 6H). ^{13}C NMR (100 MHz, $CDCl_3$) δ 84.7, 40.8, 35.5, 29.7. Spectral data was consistent with literature reports.[6]

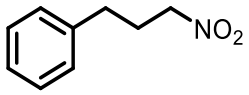

(3-Nitropropyl)benzene (1d): The title compound was synthesized according to general procedure A using 3-phenylpropylamine (0.0270 g, 0.2 mmol) and 2 g of dry silica gel. After reaction, the product was isolated using flash chromatography (5% EtOAc/Hexanes, R_f: 0.26). The title compound was isolated as a pale-yellow oil (0.0283 g, 85%). ^{1}H NMR: (400 MHz, $CDCl_3$) δ 7.34-7.16 (m, 5H), 4.37 (t, *J*= 6.9 Hz, 2H), 2.73 (t, *J*= 7.4 Hz), 2.37-2.30 (m, 2H). ^{13}C NMR (100 MHz, $CDCl_3$) δ 139.5, 128.7, 128.4, 126.6, 74.7, 32.3, 28.8. Spectral data was consistent with literature reports.[7]

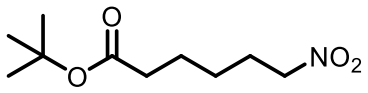

6-Nitrohexanoic acid t*ert*-*b*utyl ester (1e): The title compound was synthesized according to general procedure A using *tert*-butyl-6-aminohexanoate (0.0375 g, 0.2 mmol) and 2 g of dry silica gel. After reaction, the product was isolated using flash chromatography (10% EtOAc/Hexanes, R_f: 0.21). The title compound was isolated as a white solid (0.0294 g, 70%). ^{1}H NMR: (400 MHz, $CDCl_3$) δ 4.38 (t, *J*= 7.0 Hz, 2H), 2.23 (t, *J*= 7.3 Hz, 2H), 2.06-1.99 (m, 2H), 1.67-1.58 (m, 2H), 1.44 (s, 9H), 1.42-1.39 (m, 2H). ^{13}C NMR (100 MHz, $CDCl_3$) δ 172.6, 80.4, 75.4, 35.0, 28.1, 27.1, 25.7, 24.2. IR: 1722, 1554, 1264, 1151, 730. HRMS (ESI+): [M+] m/z Calc'd for $C_{10}H_{19}NO_4Na$: 240.1212; Found: 240.1202.

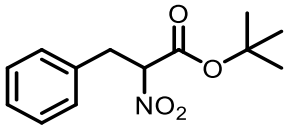

***Tert*-butyl nitrophenylpropanoate (1f):** The title compound was synthesized according to general procedure A using phenylalanine *tert*-butyl ester (0.0443 g, 0.2 mmol) and 2 g of dry silica gel. After reaction, the product was isolated used flash chromatography (5% EtOAc/Hexanes, R_f: 0.35). The title compound was isolated as a white solid (0.0333 g, 66%). ^{1}H NMR: (400 MHz, $CDCl_3$) δ 7.33-7.20 (m, 5H), 5.25 (dd, *J*= 9.3, 5.9 Hz), 3.55-3.40 (m, 2H), 1.46 (s, 9H). ^{13}C NMR (100 MHz, $CDCl_3$) δ 162.9, 134.3, 128.9, 128.8, 127.7, 89.9, 84.8, 36.2, 27.7. IR: 2982, 1742, 1560, 1455, 1370, 1148. HRMS (ESI-H): $[M-H]^-$ m/z Calc'd for $C_{13}H_{16}NO_4$: 250.1079; Found: 250.1075.

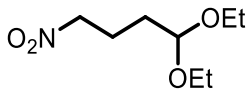

1,1-Diethoxy-4-nitrobutane (1g): The title compound was synthesized according to general procedure A using 1,1-Diethoxy-4-Aminobutane (0.0322 g, 0.2 mmol) and 2 g of dry silica gel. After reaction, the product was isolated using flash chromatography (25% EtOAc/Hexanes, R_f: 0.47). The title compound was isolated as a yellow oil (0.0352g, 92%). ^{1}H NMR: (400 MHz, $CDCl_3$) δ 4.50 (t, *J*= 5.3 Hz, 1H), 4.42 (t, *J*= 7.0 Hz, 2H), 3.68-3.60 (dq, *J*= 9.4, 7.1 Hz, 2H), 3.51-3.44 (dq, *J*= 9.4, 7.1 Hz, 2H), 2.13-2.06 (m, 2H), 1.73-1.68 (m, 2H), 1.20 (t, *J*= 7.1 Hz, 6H). ^{13}C NMR (100 MHz, $CDCl_3$) δ 102.0, 75.4, 61.7, 30.3, 22.6, 15.3. Spectral data was consistent with literature reports.[10]

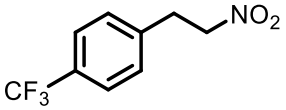

1-(2-Nitroethyl)-4-(trifluoromethyl)benzene (1j): The title compound was synthesized according to general procedure A using 2-(4-trifluoromethylphenyl)ethylamine (0.0378 g, 0.2 mmol) using 2 g of dry silica gel. After reaction the product was isolated using flash chromatography (10% EtOAc/Hexanes, R_f: 0.33). The title compound was isolated as a pale-yellow oil (0.0325 g, 74%). ^{1}H NMR: (400 MHz, $CDCl_3$) δ 7.60 (d, *J*= 7.9 Hz, 2H), 7.34 (d, *J*= 7.9 Hz, 2H), 4.64 (t, *J*= 7.2 Hz, 2H), 3.38 (t, *J*= 7.2 Hz, 2H). ^{13}C NMR (100 MHz, $CDCl_3$) δ 139.7, 129.0, 125.9 (quart), 122.6, 75.6, 33.0. Spectral data was consistent with literature reports.[8]

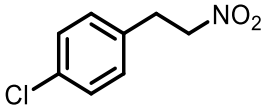

1-(2-Nitroethyl)-4-chlorobenzene (1k): The title compound was synthesized according to general procedure A using 2-(4-Chlorophenyl)ethylamine (0.0311 g, 0.2 mmol) and 2 g of dry silica gel. After reaction, the product was isolated using flash chromatography (5% EtOAc/Hex, R_f: 0.15). The title compound was isolated as a colorless oil (0.0271 g, 73%). ^{1}H NMR: (400 MHz, $CDCl_3$) δ 7.32-7.28 (m, 2H), 7.16-7.13 (m, 2H), 4.60 (t, *J*= 7.13 Hz, 2H), 3.29 (t, *J*= 7.13 Hz, 2H). ^{13}C NMR (100 MHz, $CDCl_3$) δ 134.1, 133.4, 129.9, 129.2, 76.0, 32.7. Spectral data was consistent with literature reports.[9]

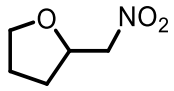

2-(Nitromethyl)tetrahydrofuran (1n): The title compound was synthesized according to general procedure A using Tetrahydrofurfylamine (0.0202 g, 0.2 mmol) and 2 g of dry silica gel. After reaction, the product was isolated using flash chromatography (20% EtOAc/Hex, R_f: 0.29). The title compound was isolated as a colourless oil (0.0174 g, 66%). ^{1}H NMR: (400 MHz, $CDCl_3$) δ 4.60-4.52 (m, 1H), 4.47-4.37 (m, 2H), 3.94-3.80 (m, 2H), 2.20-2.10 (m, 1H), 2.00-1.92 (m, 2H), 1.72-1.62 (m, 1H). ^{13}C NMR (100 MHz, $CDCl_3$) δ 78.9, 75.2, 68.7, 29.0, 25.4. Spectral data was consistent with literature reports.[14]

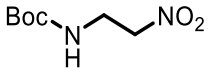

***Tert*-butyl (2-nitroethyl)carbamate (1o):** The title compound was synthesized according to general procedure A using *N*-Boc-Ethylenediamine (0.0320 g, 0.2 mmol) and 2 g of dry silica gel. After reaction, the product was isolated using flash chromatography (20% EtOAc/Hex, R_f: 0.26). The title compound was isolated as a colorless oil (0.0193 g, 51%). ^{1}H NMR: (400 MHz, $CDCl_3$) δ 5.03 (s, 1H), 4.51 (t, *J*= 5.4 Hz, 2H), 3.69 (quart, *J*= 5.4 Hz), 1.44 (s, 9H). ^{13}C NMR (100 MHz, $CDCl_3$) δ 155.6, 80.3, 74.2, 37.8, 28.3. IR: 3449, 2979, 2925, 1703, 1555, 1366. Spectral data was consistent with literature reports.[13]

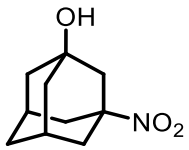

1-Nitro-3-adamantol (1p): The title compound was synthesized according to general procedure A using 3-Aminoadamantol (0.0335 g, 0.2 mmol) and 2 g of dry silica gel. After reaction, the product was isolated using flash chromatography (30% EtOAc/Hexanes, R_f: 0.20). The title compound was isolated as colorless needle-like crystals (0.0227 g, 58%). ^{1}H NMR: (400 MHz, $CDCl_3$) δ 2.46-2.41 (m, 2H), 2.19 (s, 2H), 2.15-2.11 (m, 4H), 1.73 (d, *J*= 3.1 Hz, 4H), 1.61-1.58 (m, 2H). ^{13}C NMR (100 MHz, $CDCl_3$) δ 86.0, 69.7, 48.0, 43.5, 39.7, 34.1, 30.8. Spectral data was consistent with literature reports.[12]

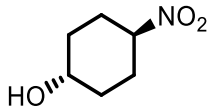

Trans-4-nitrocyclohexanol (1q): The title compound was synthesized according to general procedure A using trans-4-aminocyclohexanol (0.0230 g, 0.2 mmol) and 2 g of dry silica gel. After reaction, the product was isolated using flash chromatography (50% EtOAc/Hexanes, R_f: 0.31). The title compound was isolated as white needle-like crystals (0.0167 g, 58% yield). ^{1}H NMR: (400 MHz, $CDCl_3$) δ 4.39 (tt, *J*=10.8, 4.1 Hz, 1H), 3.76 (tt, *J*=9.9, 4.1 Hz, 1H), 2.35-2.29 (m, 2H), 2.11-2.05 (m, 2H), 2.02-1.91 (m. 2H), 1.47-1.38 (m, 2H). ^{13}C NMR (100 MHz, $CDCl_3$) δ 83.3, 68.3, 32.3, 28.2. Spectral data was consistent with literature reports.[11]

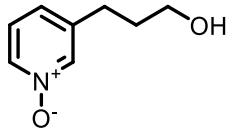

3-Pyridinylpropanol *N*-oxide (2a): The title compound was synthesized according to general procedure A using 3-pyridinylpropanol (0.0274 g, 0.2 mmol) and 2 g of dry silica gel. After reaction, the product was isolated using flash chromatography (20% MeOH/EtOAc, R_f: 0.18). The title compound was isolated as a colorless oil (0.0198 g, 65%). ^{1}H NMR: (400 MHz, $CDCl_3$) δ 8.15 (s, 1H), 8.09-8.05 (m, 1H), 7.23-7.17 (m, 2H), 3.63 (t, *J*= 6.1 Hz, 2H) 2.70 (t, *J*= 7.7 Hz, 2H), 1.88-1.81 (m, 2H). ^{13}C NMR (100 MHz, $CDCl_3$) δ 141.4, 139.1, 136.8, 127.5, 125.7, 60.8, 32.9, 28.9. IR: 3350, 2929, 2855, 1744, 1157. HRMS (ESI-TOF) m/z: $[M+Na]^+$ Calc'd for $C_8H_{11}NO_2Na$ 176.0687; Found: 176.0679.

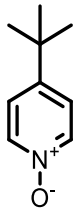

4-*Tert*-butylpyridine *N*-oxide (2b): The title compound was synthesized according to general procedure A using 4-tertbutylpyridine (0.0270 g, 0.2 mmol) and 2 g of dry silica gel. After reaction, the product was isolated using flash chromatography (10% MeOH/EtOAc, R_f: 0.16). The title compound was isolated as a colorless oil (0.3070, 92%). ^{1}H NMR: (400 MHz, $CDCl_3$) 8.11 (d, J= 7.1 Hz, 2H), 7.23 (d, J= 7.1 Hz, 2H), 1.28 (s, 9H). ^{13}C NMR (100 MHz, $CDCl_3$) δ 151.0, 138.5, 123.1, 34.5, 30.5. Spectral data was consistent with literature reports.[15]

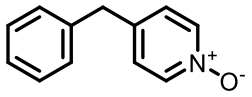

4-Benzylpyridine *N*-oxide (2c): The title compound was synthesized according to general procedure A using 4-benzylpyridine (0.0338 g, 0.2 mmol) and 2 g of dry silica gel. After reaction, the product was isolated using flash chromatography (10% MeOH/EtoAc, R_f: 0.09). The title compound was isolated as a yellow oil (0.0316, 85%). ^{1}H NMR: (400 MHz, $CDCl_3$) δ 8.14-8.10 (m, 2H), 7.35-7.30 (m, 2H), 7.29-7.23 (m, 1H), 7.17-7.12 (m, 2H), 7.08-7.04 (m, 2H), 3.95 (s, 2H). ^{13}C NMR (100 MHz, $CDCl_3$) δ 141.0, 139.0, 138.0, 129.0, 129.0, 128.9, 127.1, 126.3, 40.3. Spectral data was consistent with literature reports.[16]

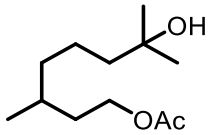

7-Hydroxy-3,7-dimethyloctyl acetate (3a): The title compound was synthesized according to general procedure B using 3,7-dimethyloctyl acetate (0.0401 g, 0.2 mmol) and 2 g of dry silica gel. After reaction, the product was isolated using flash chromatography (10% EtOAc/Hex, R_f: 0.31). The title compound was isolated as a colourless oil (0.0199 g, 46%). ^{1}H NMR: (400 MHz, $CDCl_3$) δ 4.12-4.01 (m, 2H), 2.02 (s, 3H), 1.69-1.24(m, 10H), 1.19 (s, 6H), 1.17-1.09 (m, 1H). ^{13}C NMR (100 MHz, $CDCl_3$) δ 171.23, 71.0, 63.0, 44.1, 37.4, 35.5, 29.8, 29.3, 29.2, 21.6, 21.0, 19.5. Spectral data was consistent with literature reports.[6]

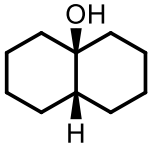

Cis-9-decalol (3b): The title compound was synthesized according to general procedure B using cis-decalin (0.0276 g, 0.2 mmol) and 2 g of dry silica gel. After reaction, the product was isolated using flash chromatography (10% EtOAc/Hex, R_f: 0.27). The title compound was isolated as a colourless oil (0.0118 g, 39%). ^{1}H NMR: (400 MHz, $CDCl_3$) δ 1.80-1.19 (m, 18H). ^{13}C NMR (100 MHz, $CDCl_3$) δ 71.8, 42.8, 29.7, 28.0. Spectral data was consistent with literature reports.[17]

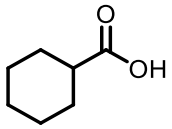

Cyclohexane carboxylic acid (4a): The title compound was synthesized according to general procedure B using Cyclohexylbenzene (0.0320 g, 0.2 mmol) and 2 g of dry silica gel. After reaction, the product was isolated using flash chromatography (20% EtOAc/Hex, 1% AcOH, R_f: 0.32). The title compound was isolated as a colourless oil (0.0122 g, 48%). ^{1}H NMR: (400 MHz, $CDCl_3$) δ 11.1 (br, 1H), 2.33 (tt, *J*= 3.6, 11.2 Hz, 1H), 1.97-1.90 (m, 2H), 1.80-1.73 (m, 2H), 1.68-1.60 (m, 1H), 1.51-1.40 (m, 2H), 1.35-1.20 (m, 3H). ^{13}C NMR (100 MHz, $CDCl_3$) δ 181.6, 42.8, 28.8, 25.7, 25.3. Spectral data was consistent with literature reports.[18]

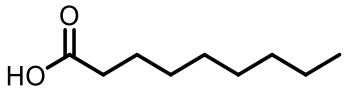

Nonanoic acid (4b): The title compound was synthesized according to general procedure B using Octylbenzene (0.0381 g, 0.2 mmol) and 2 g of dry silica gel. After reaction, the product was isolated using flash chromatography (10% EtOAc/Hex, 1% AcOH, R_f: 0.27). The title compound was isolated as a colourless oil (0.0132 g, 46%). ^{1}H NMR: (400 MHz, $CDCl_3$) δ 2.35 (t, *J*= 7.5 Hz, 2H), 1.63 (quin, *J* = 7.5 Hz, 2H), 1.35-1.22 (m, 8H), 0.88 (t, *J*= 6.9 Hz, 3H). ^{13}C NMR (100 MHz, $CDCl_3$) δ 179.5, 34.0, 31.8, 29.2, 29.1, 24.7, 22.6, 14.1. Spectral data was consistent with literature reports.[19]

3.1.4: NMR Spectra

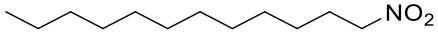

2a - Nitrododecane

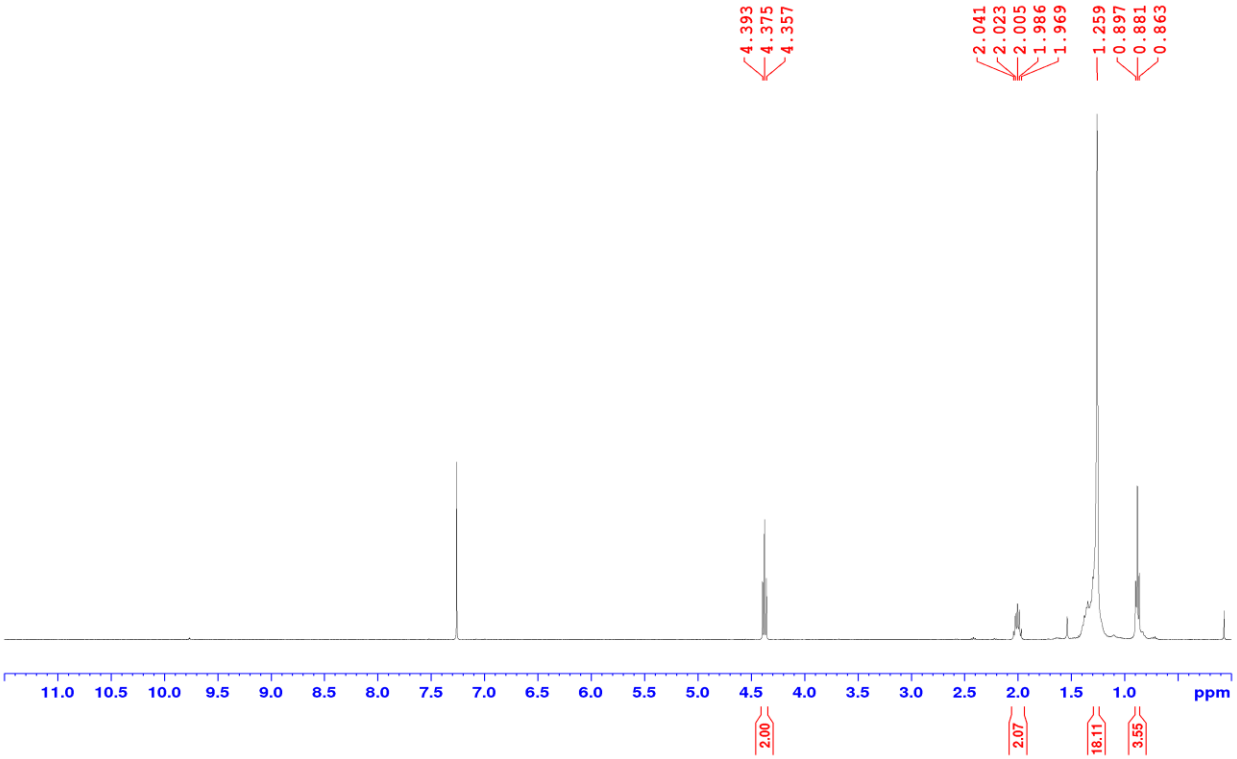

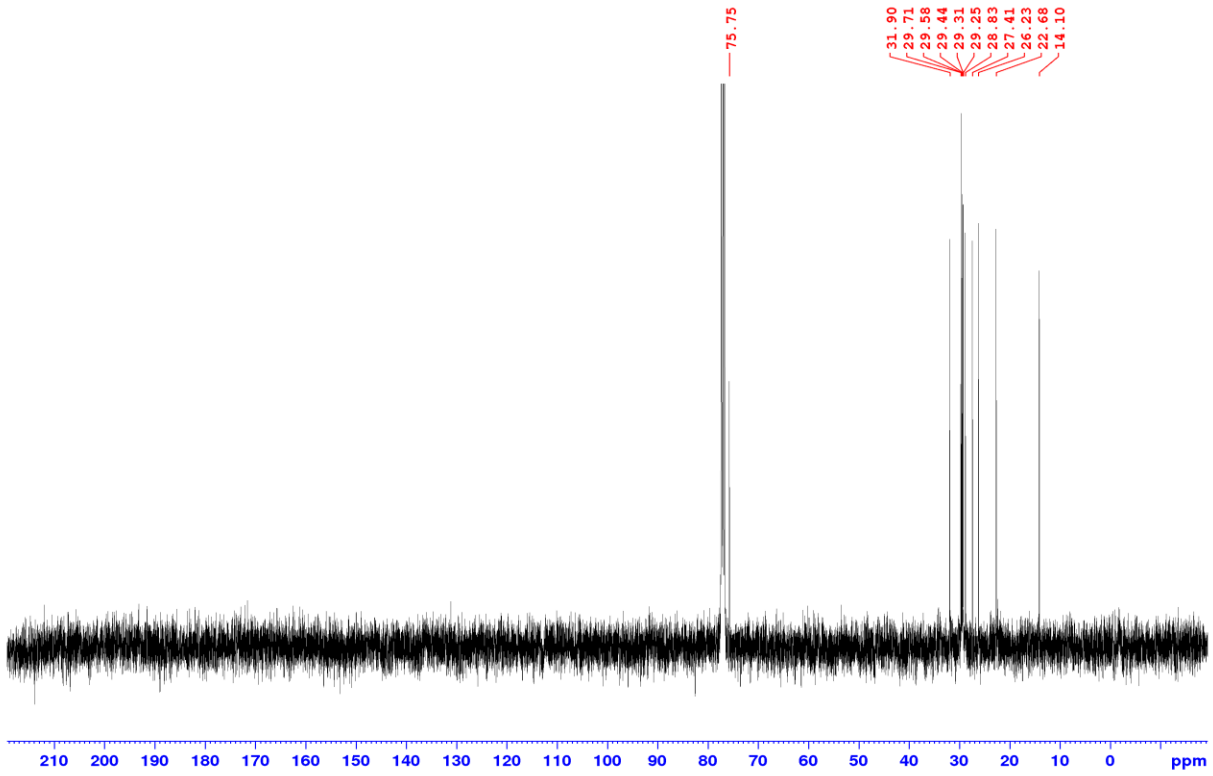

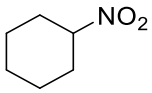

2b - Nitrocyclohexane

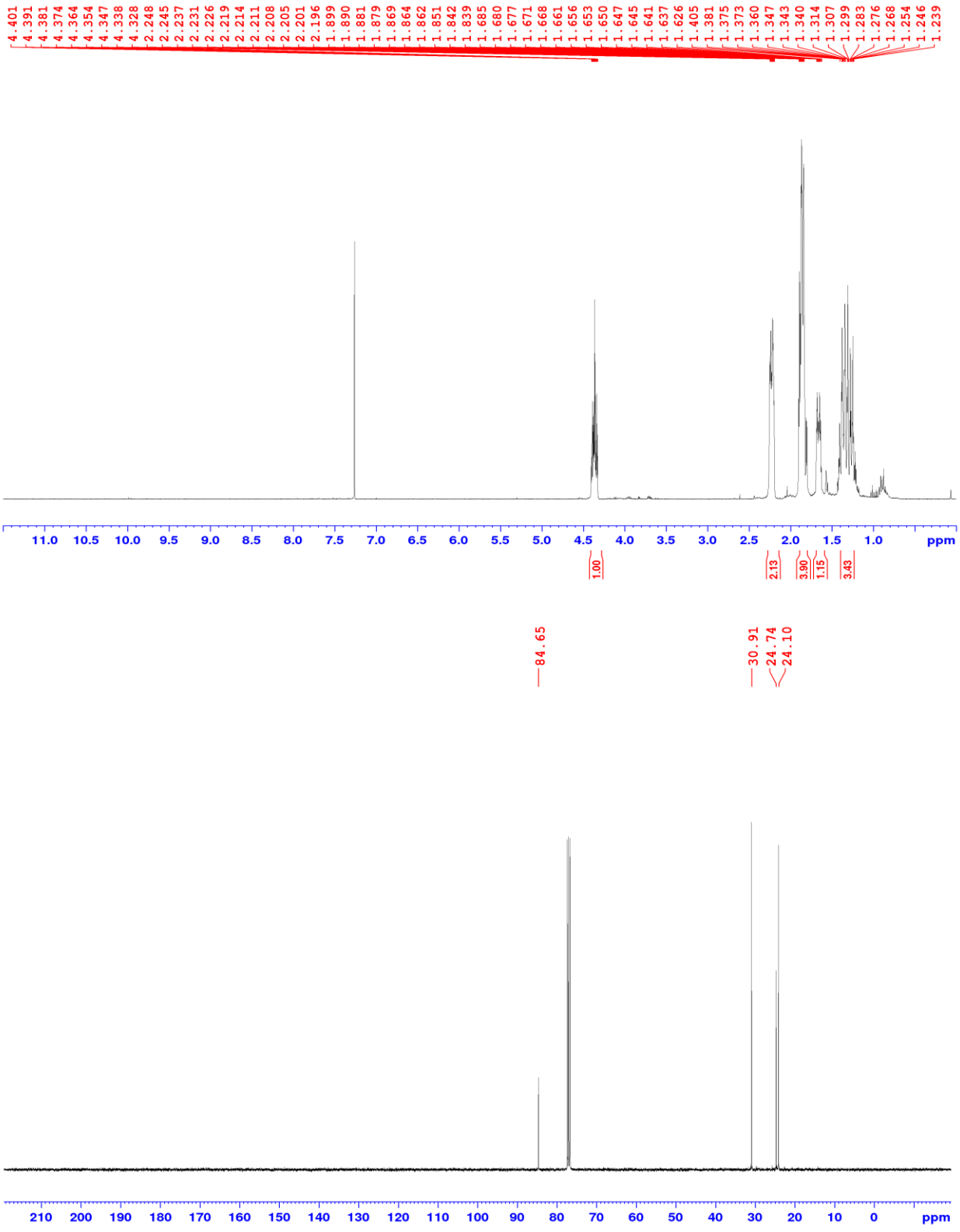

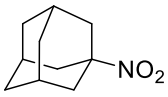

2c - Nitroadamantane

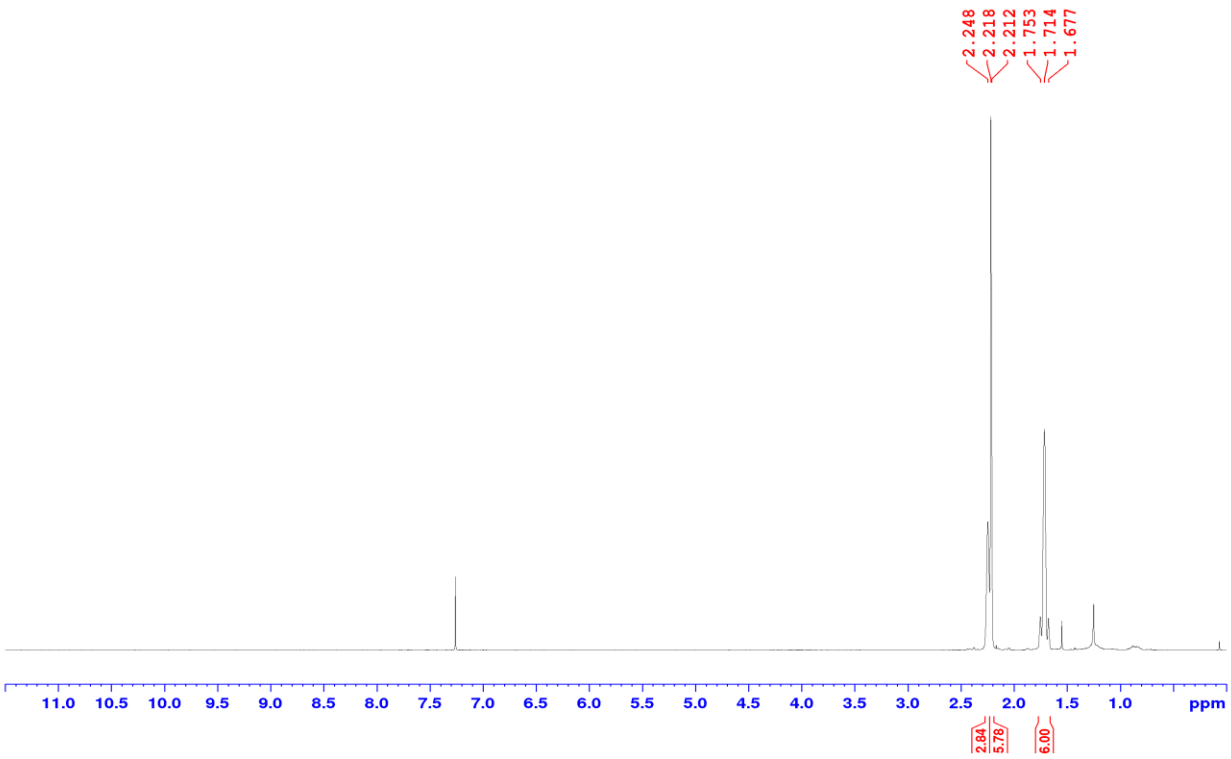

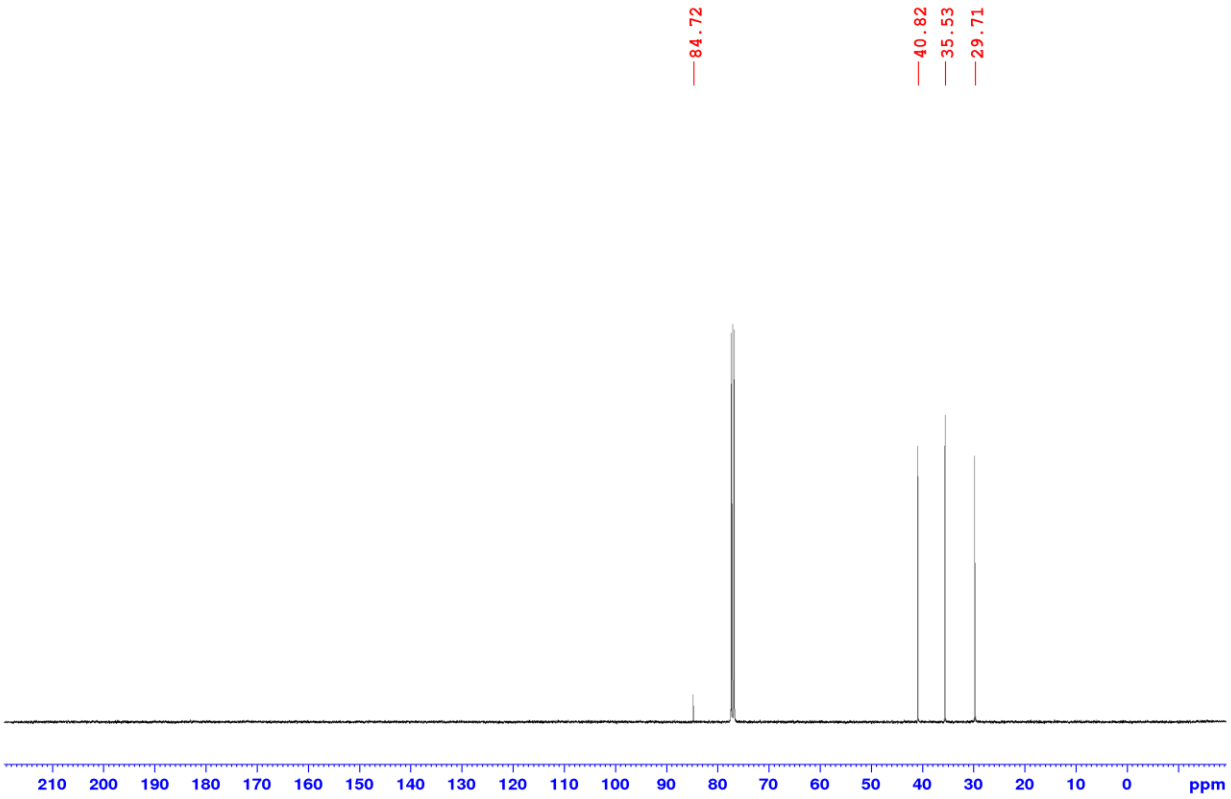

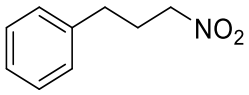

2d - (3-Nitropropyl)benzene

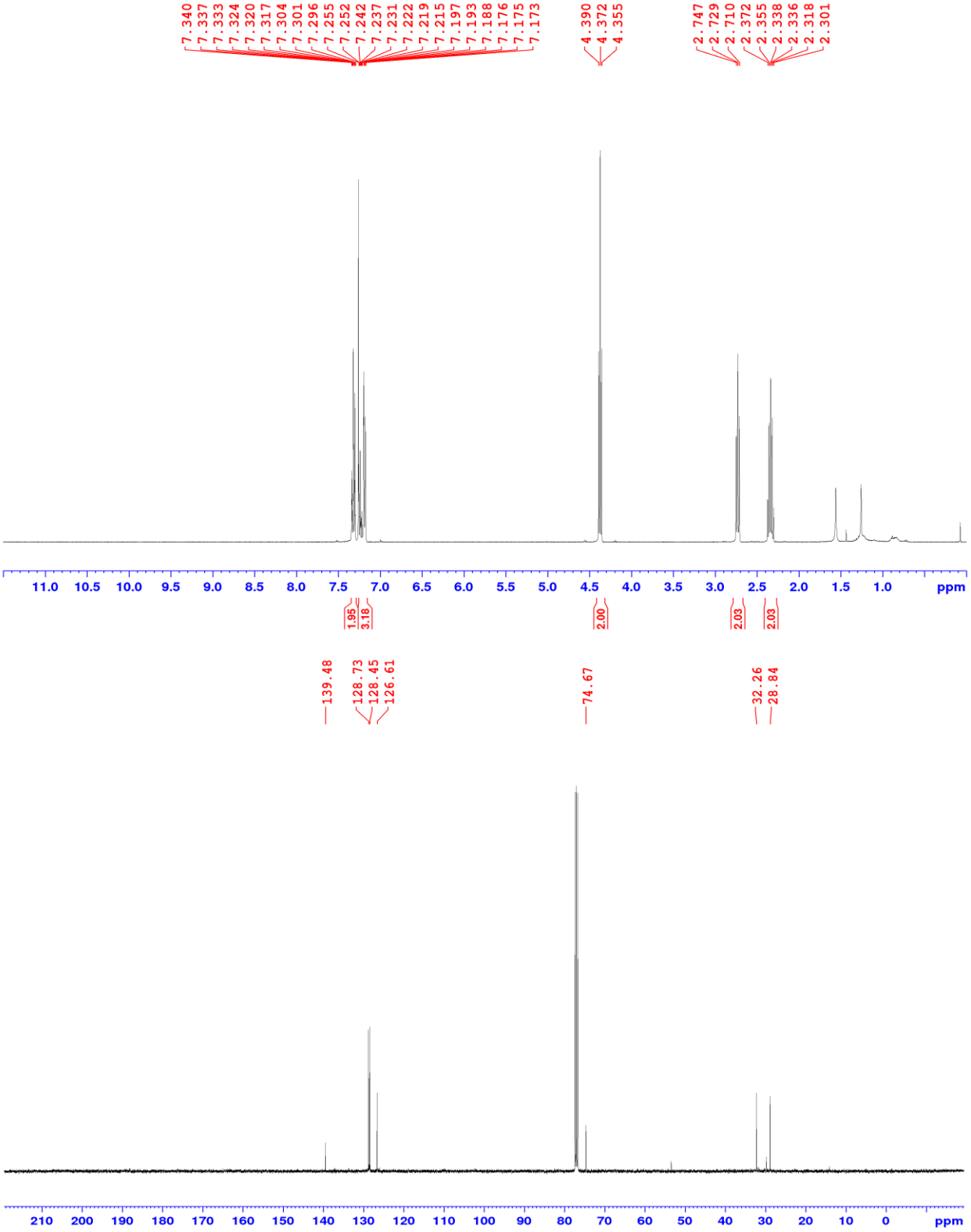

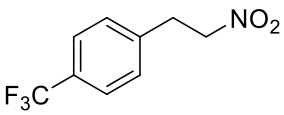

2e - 1-(2-Nitroethyl)-4-(Trifluoromethyl)benzene

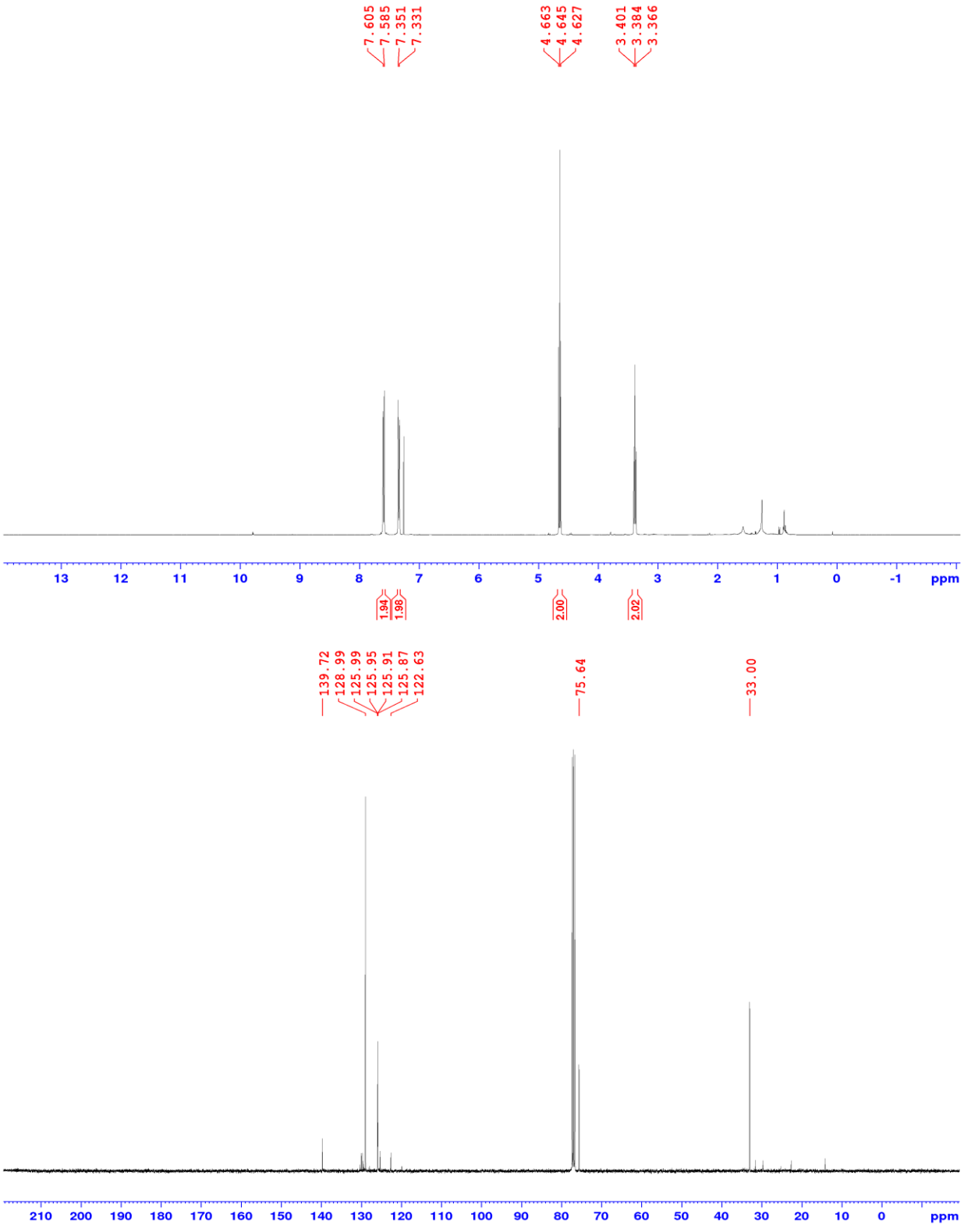

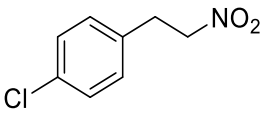

2f - 1-(2-Nitroethyl)-4-Chlorobenzene

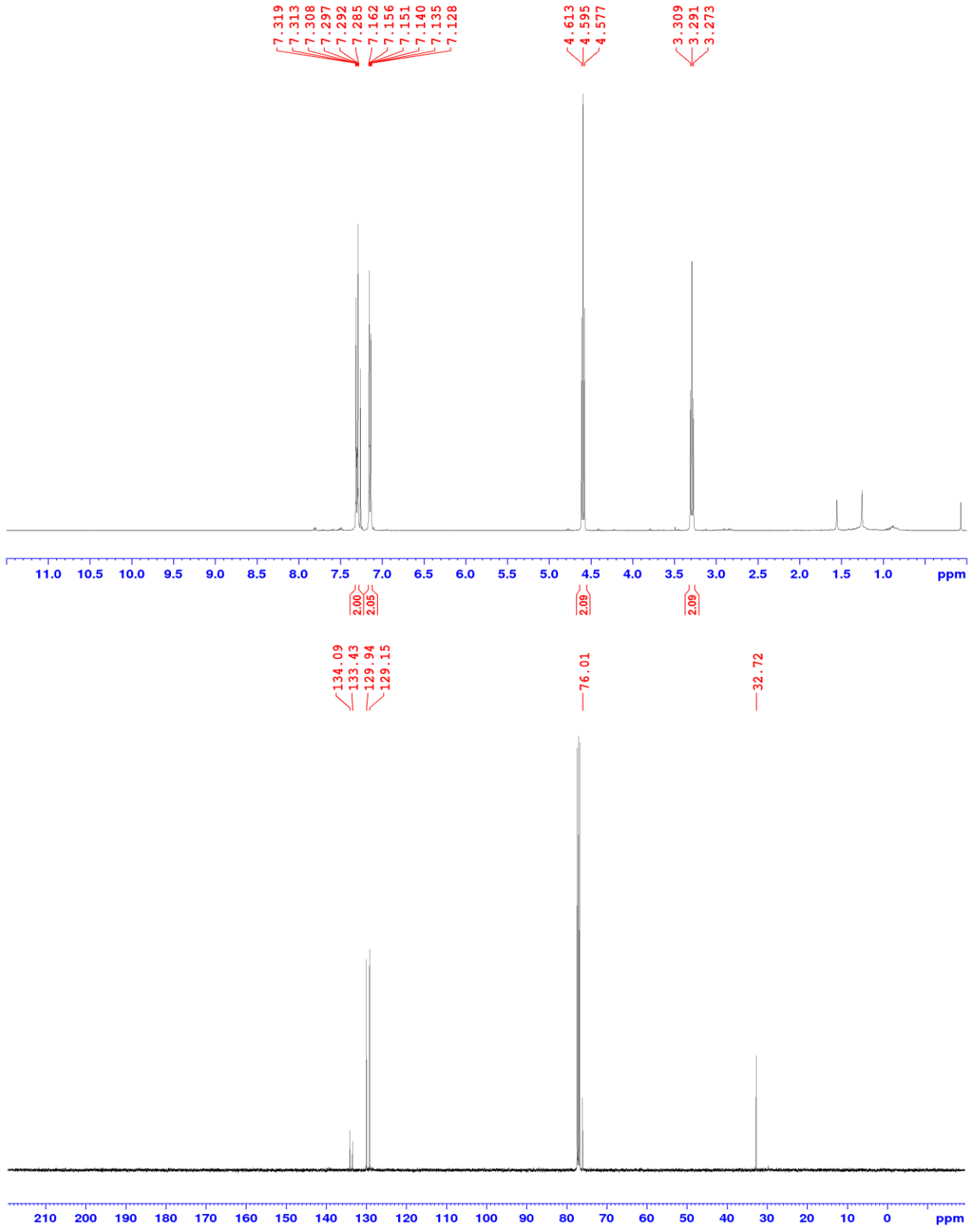

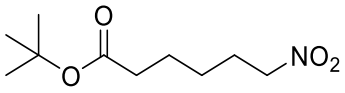

2g - 6-Nitrohexanoic Acid *Tert*-Butyl Ester

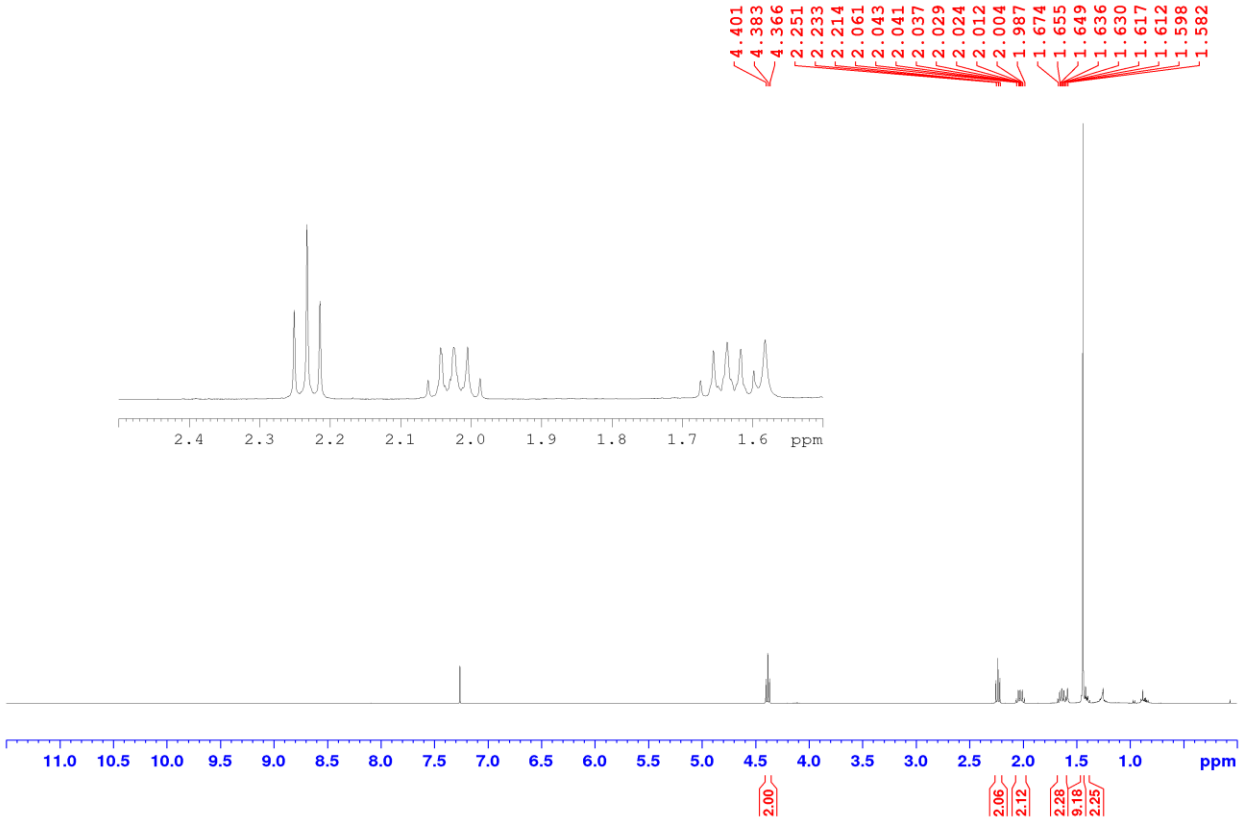

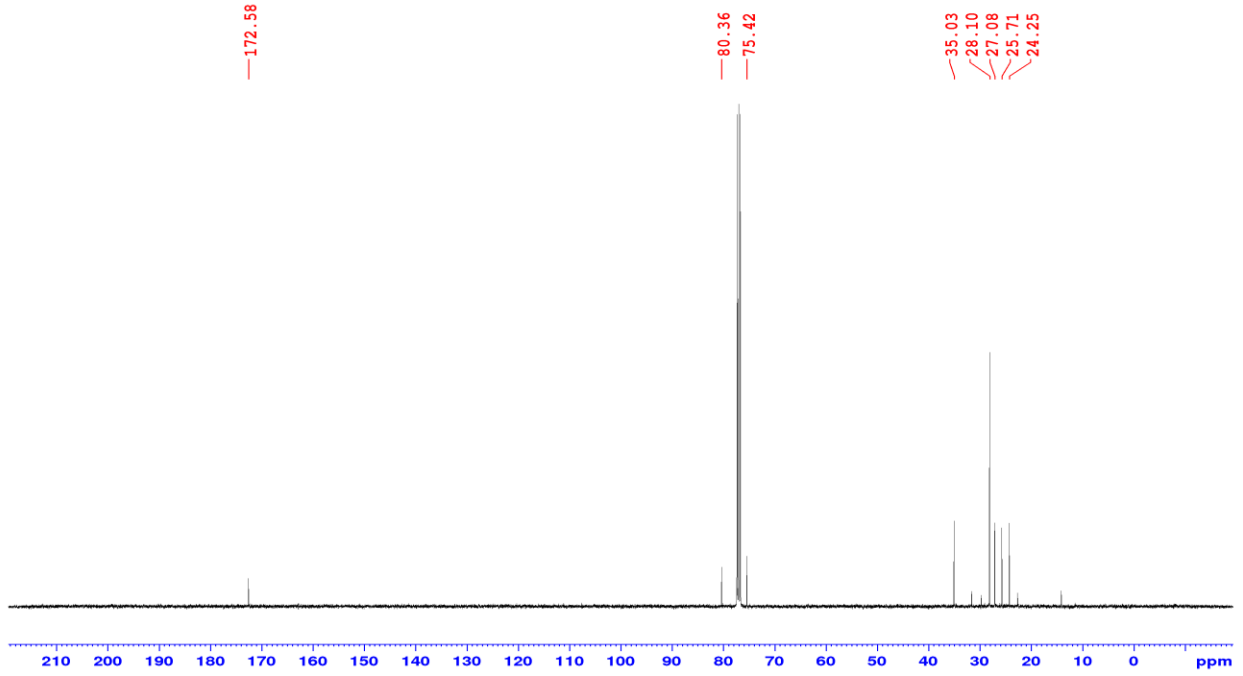

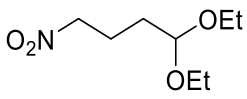

2h - 1,1-Diethoxy-4-Nitrobutane

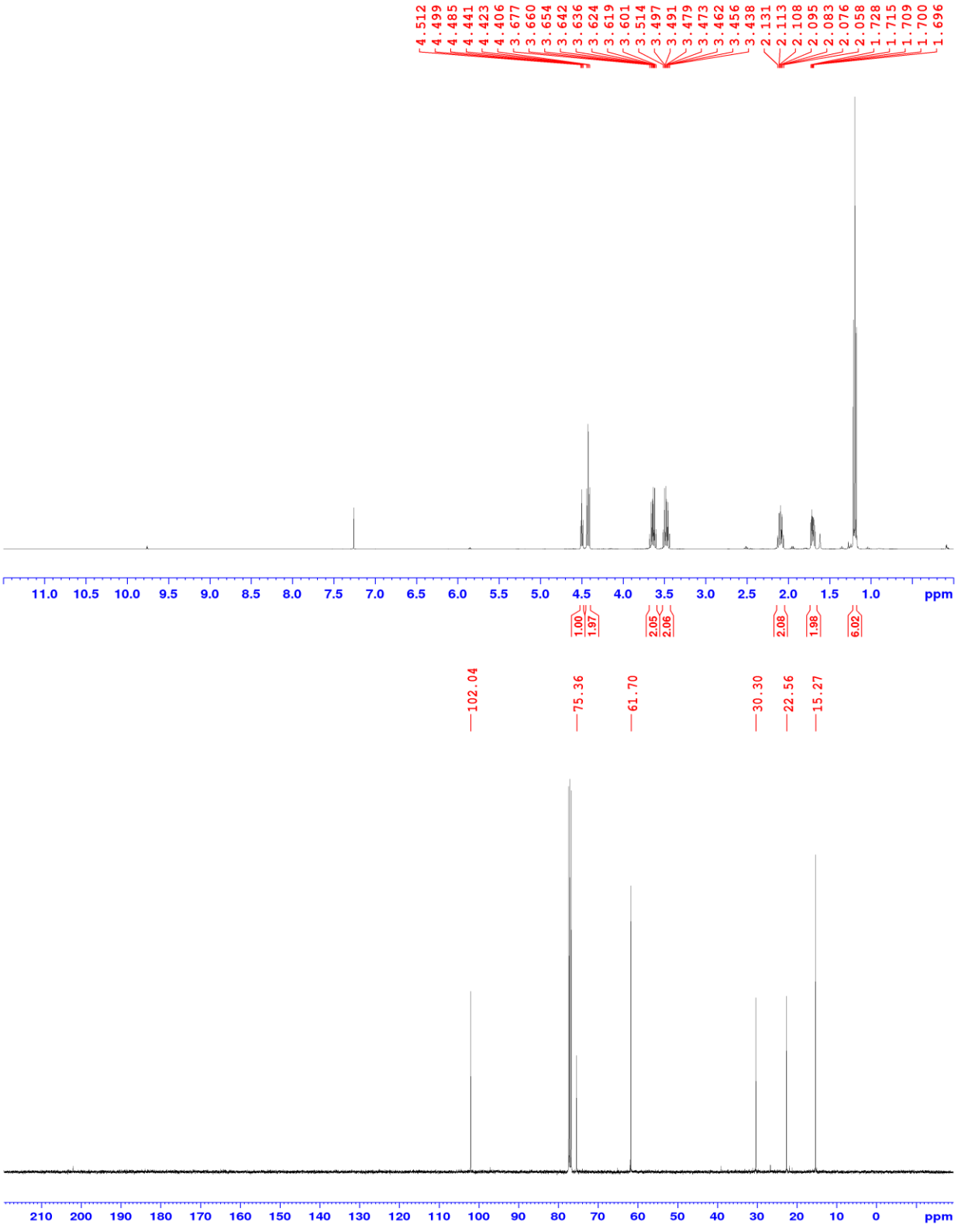

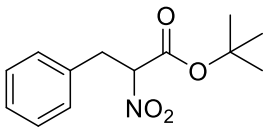

2i - *Tert*-Butyl Nitrophenylpropanoate

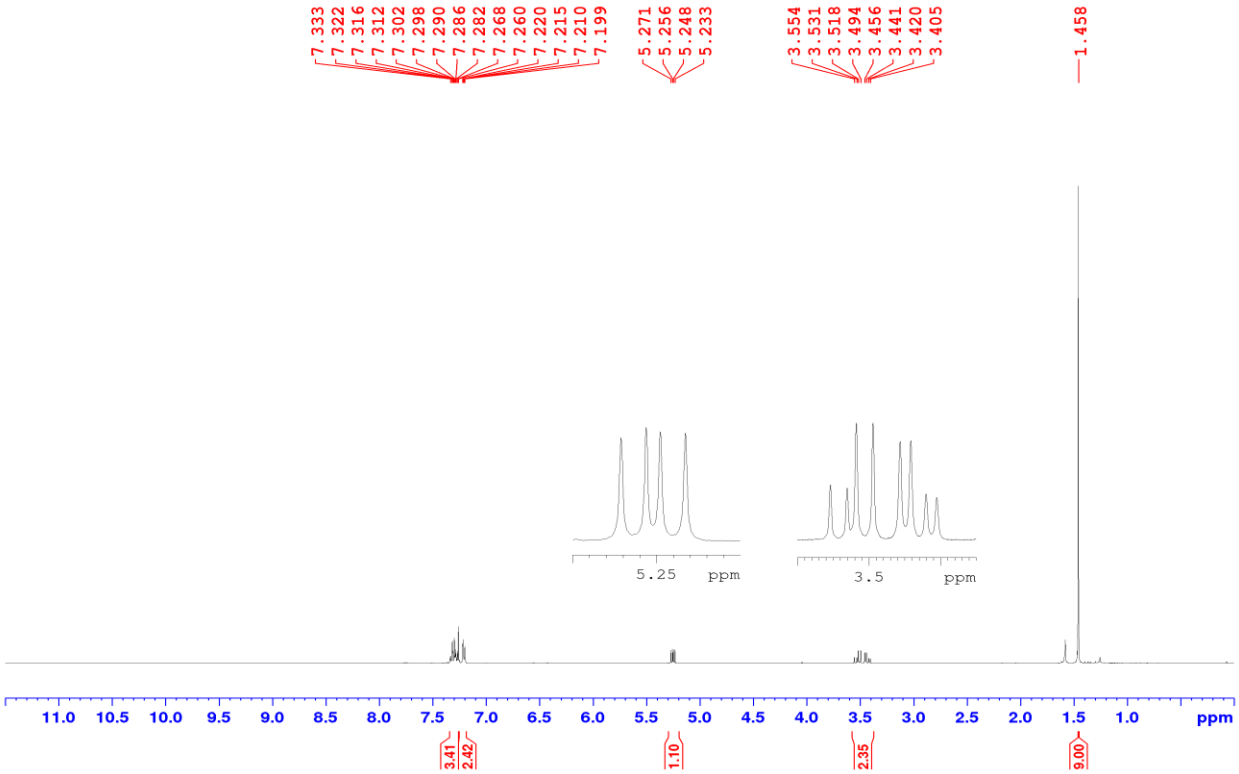

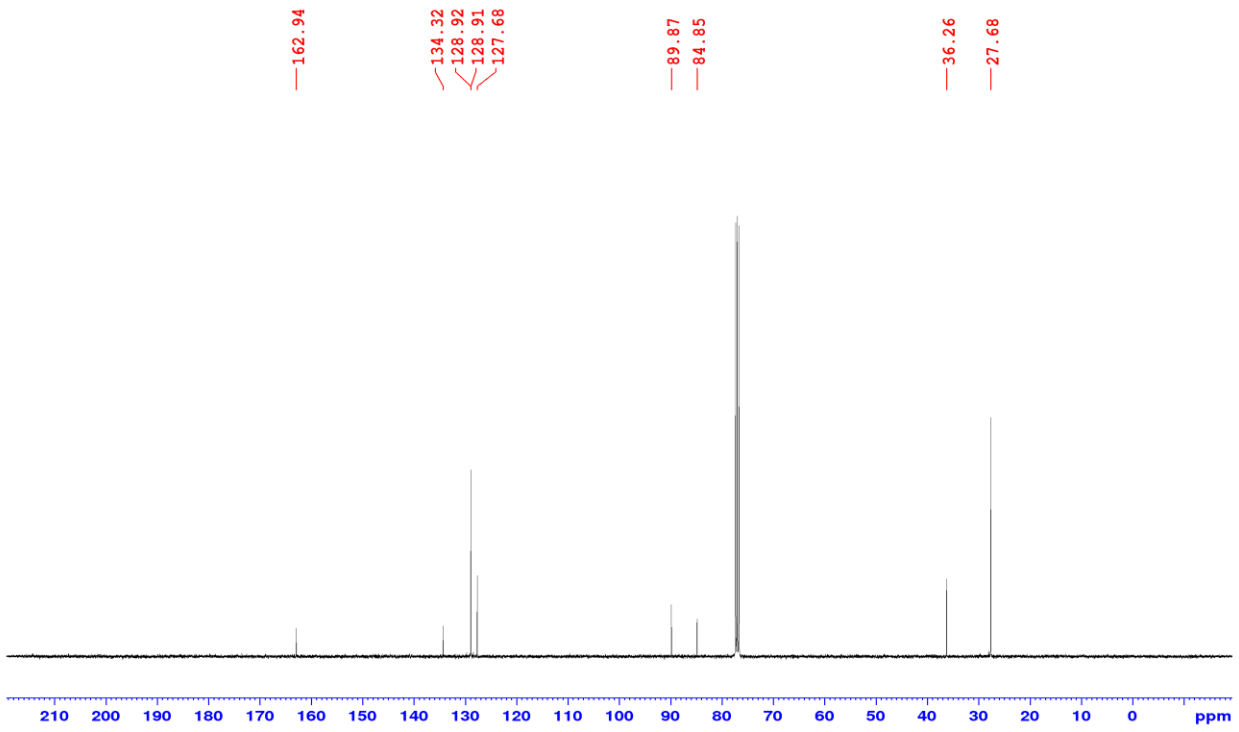

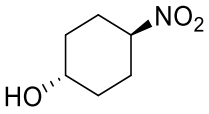

2j - Trans-4-Nitrocyclohexanol

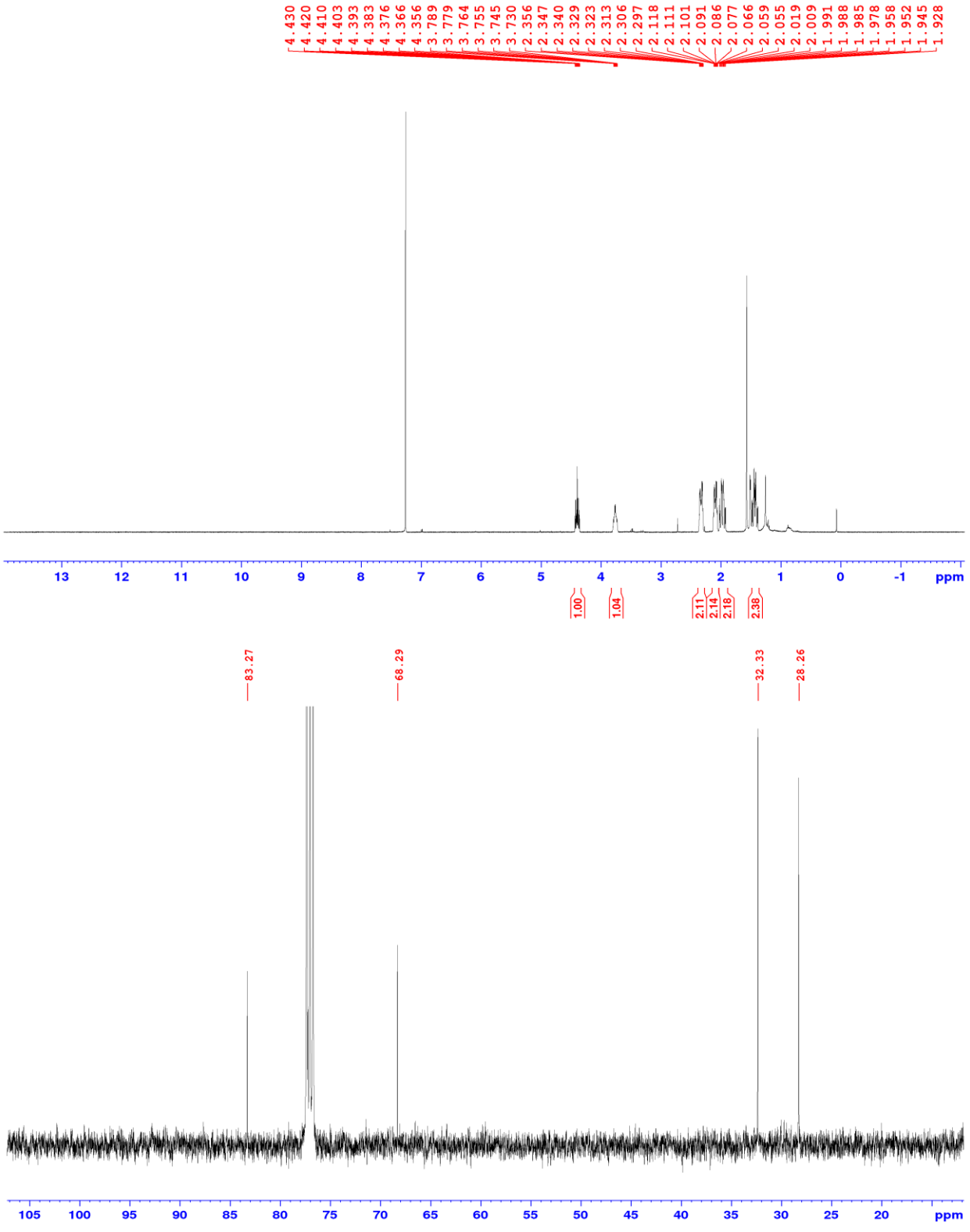

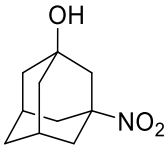

2k - 1-Nitro-3-Adamantol

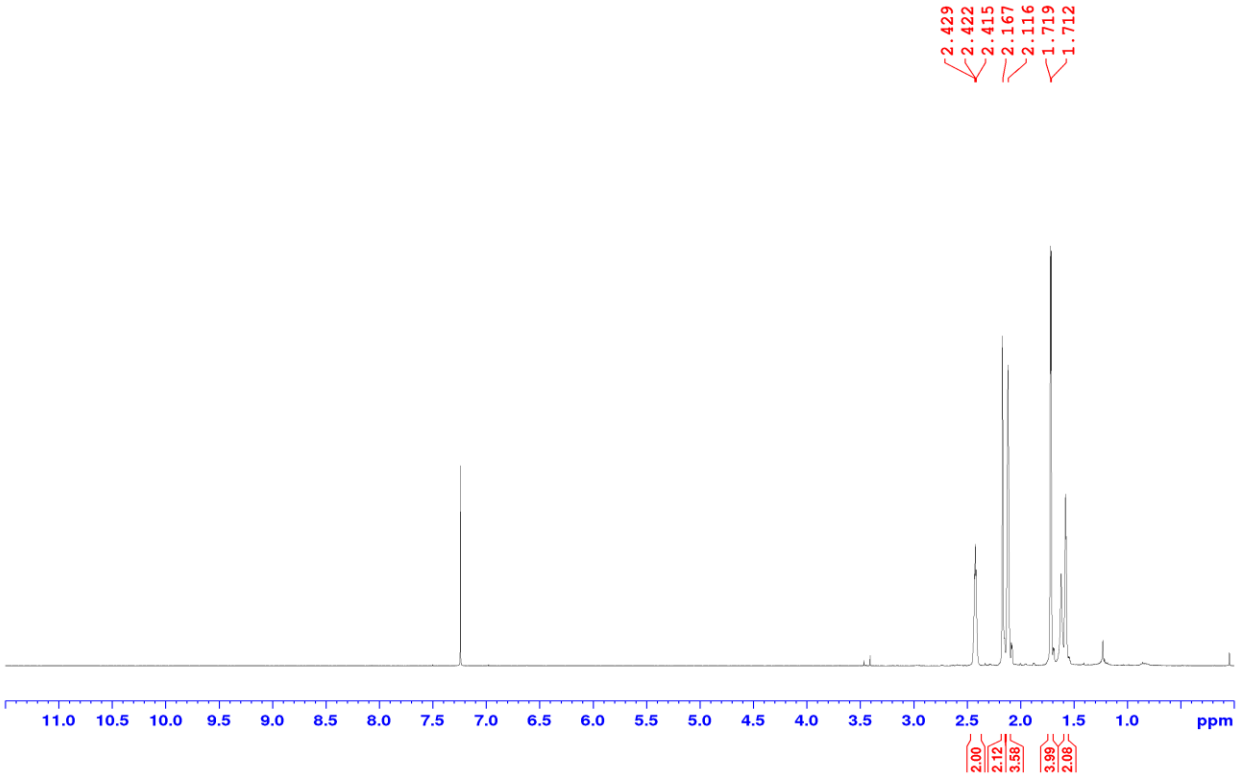

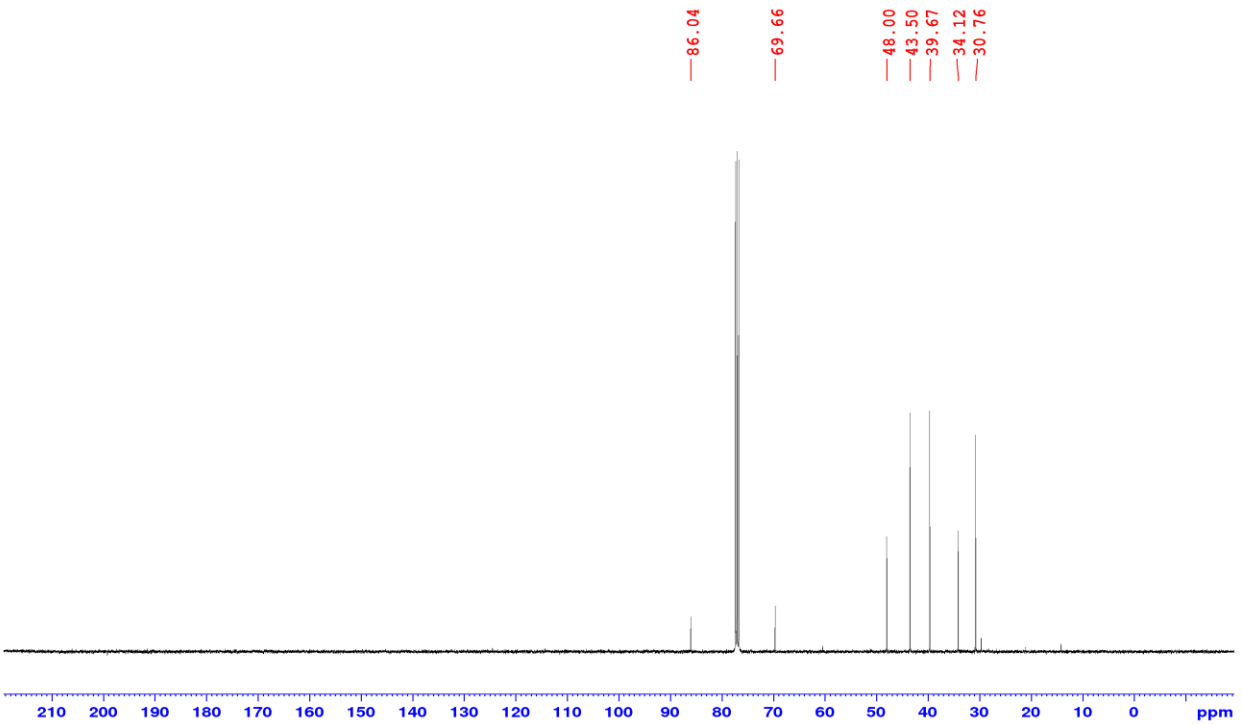

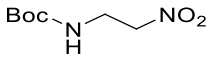

2l - *Tert*-Butyl (2-Nitroethyl)carbamate

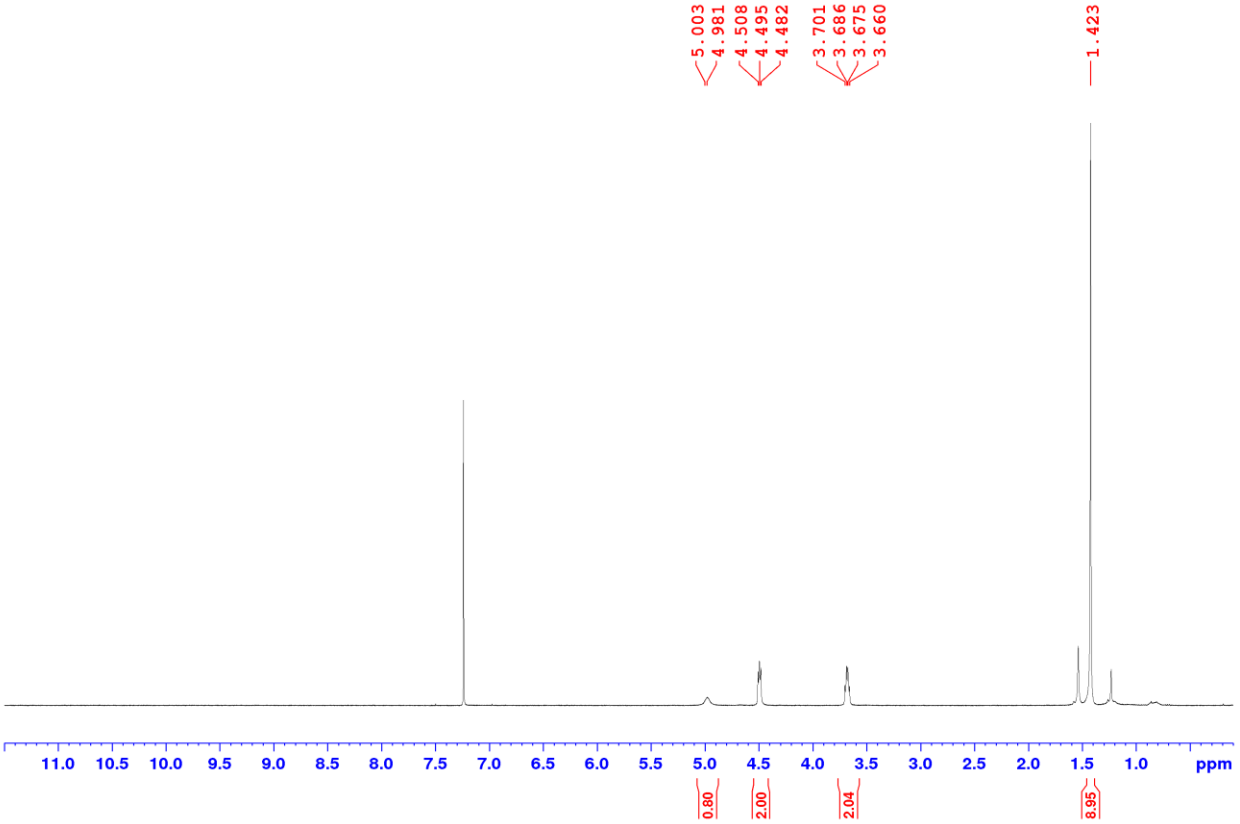

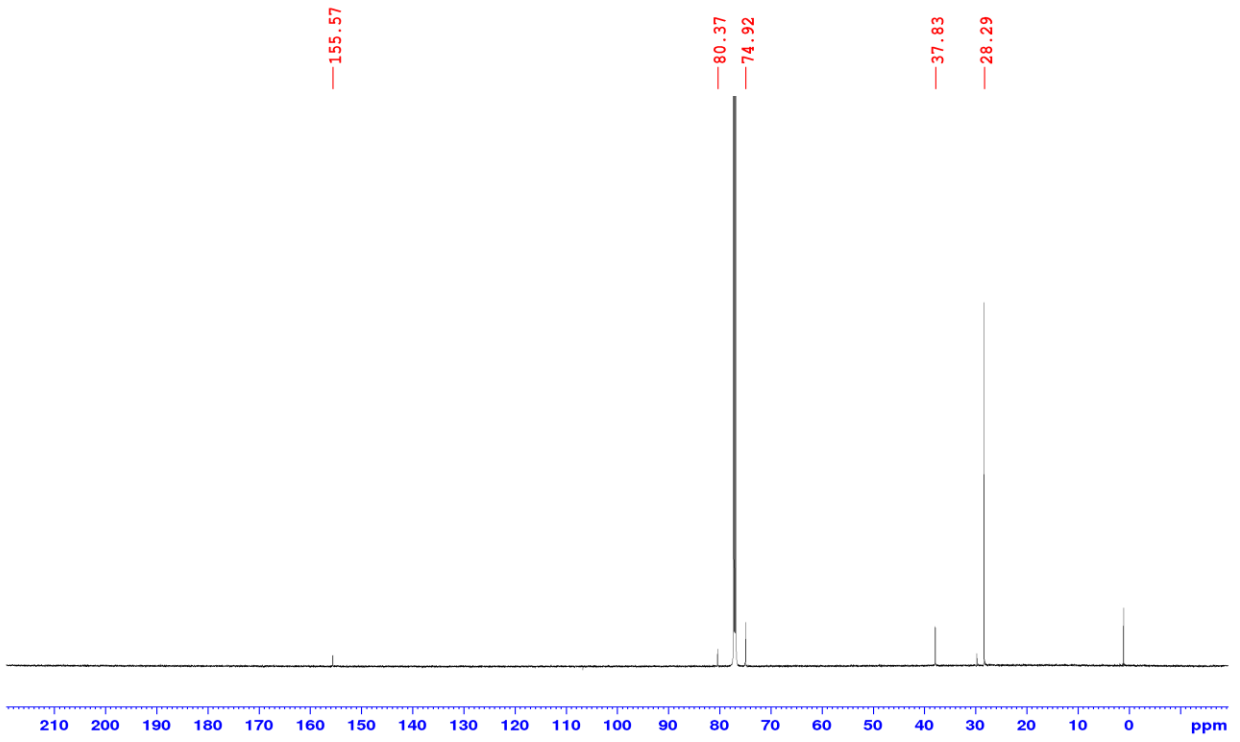

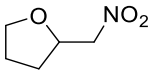

2m - 2-(Nitromethyl)tetrahydrofuran

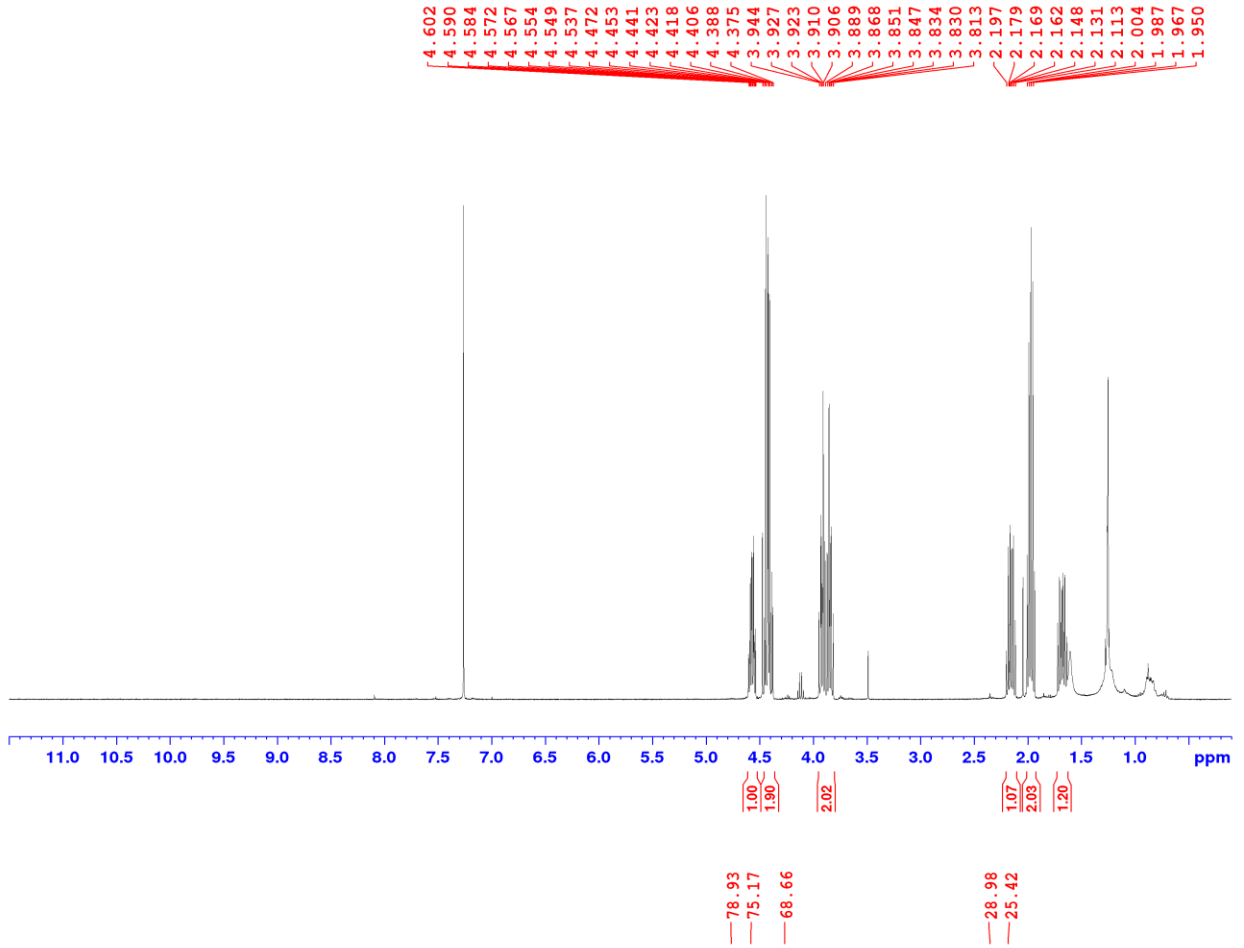

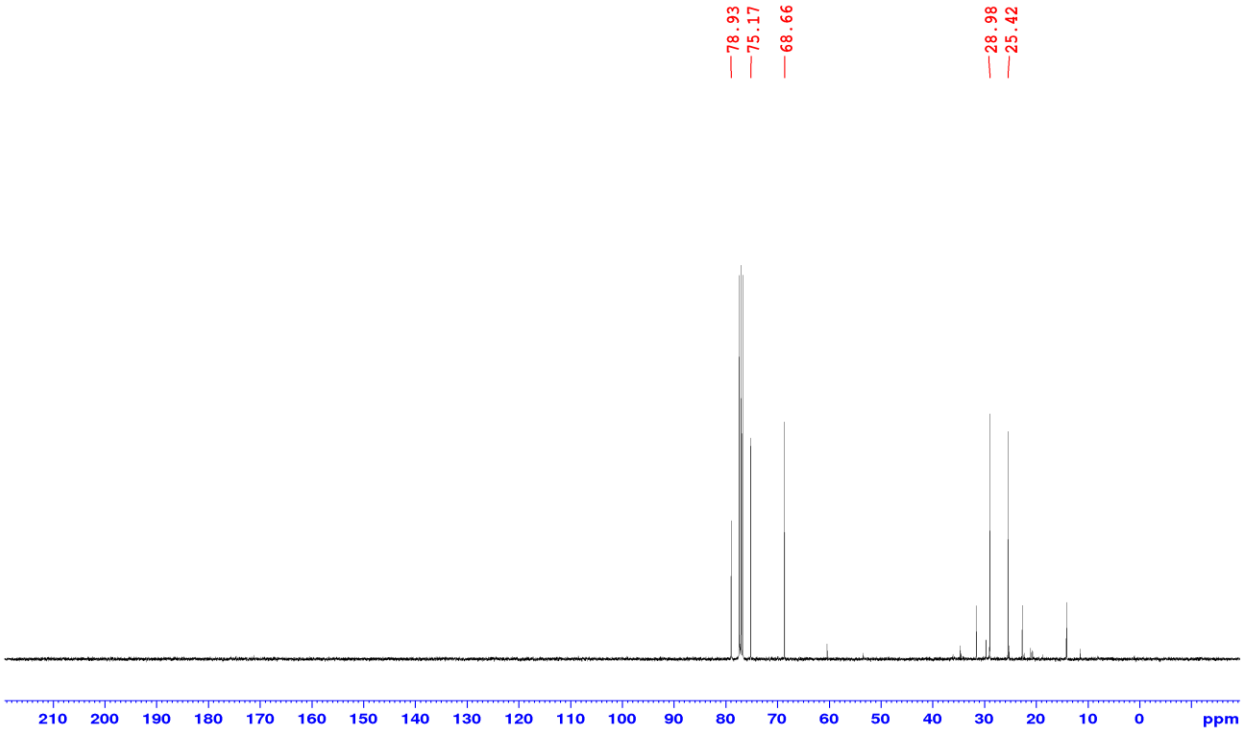

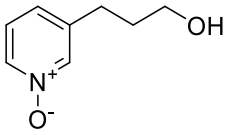

4a - 3-Pyridinylpropanol *N*-oxide

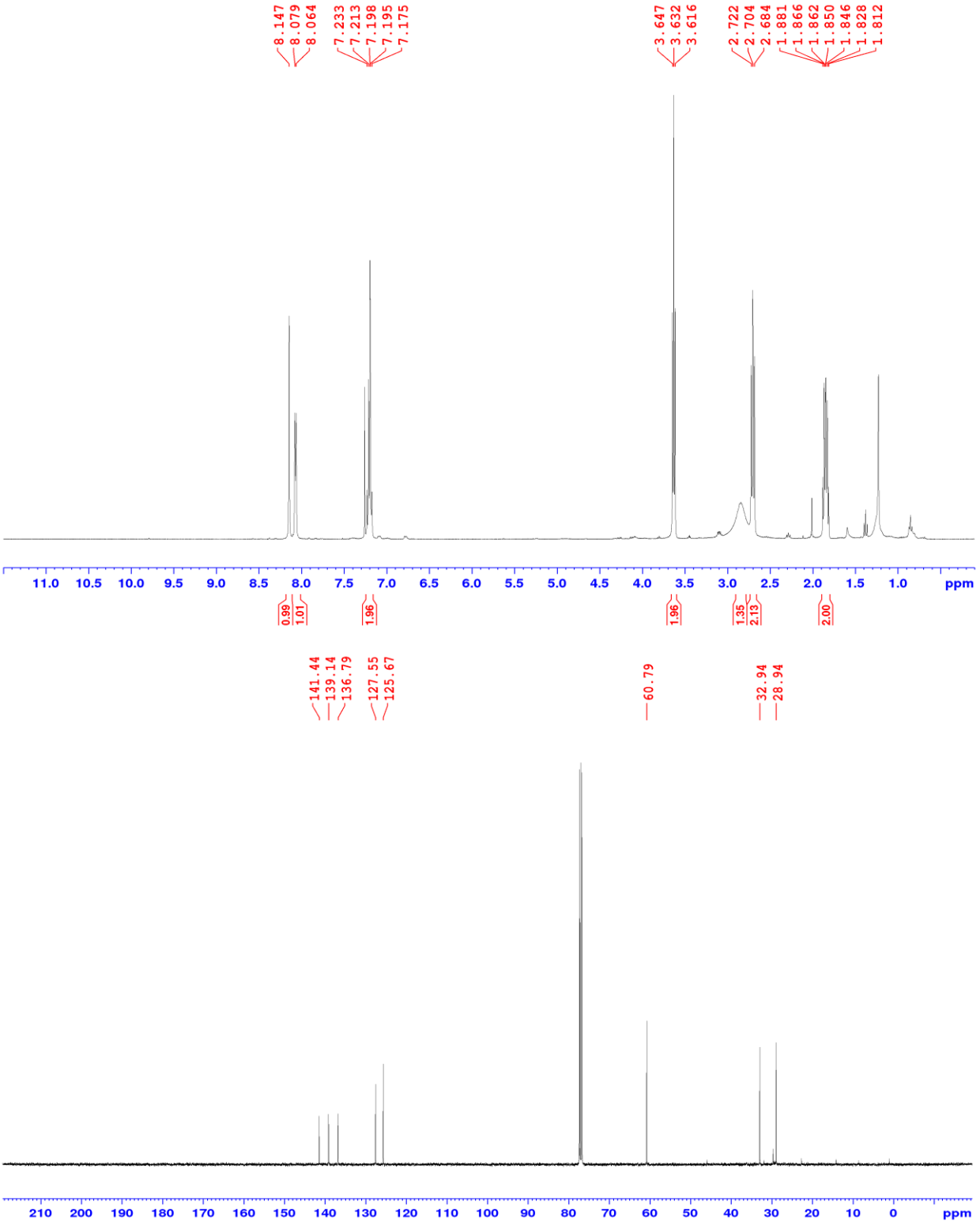

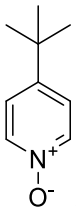

4b - 4-*Tert*-Butylpyridine *N*-oxide

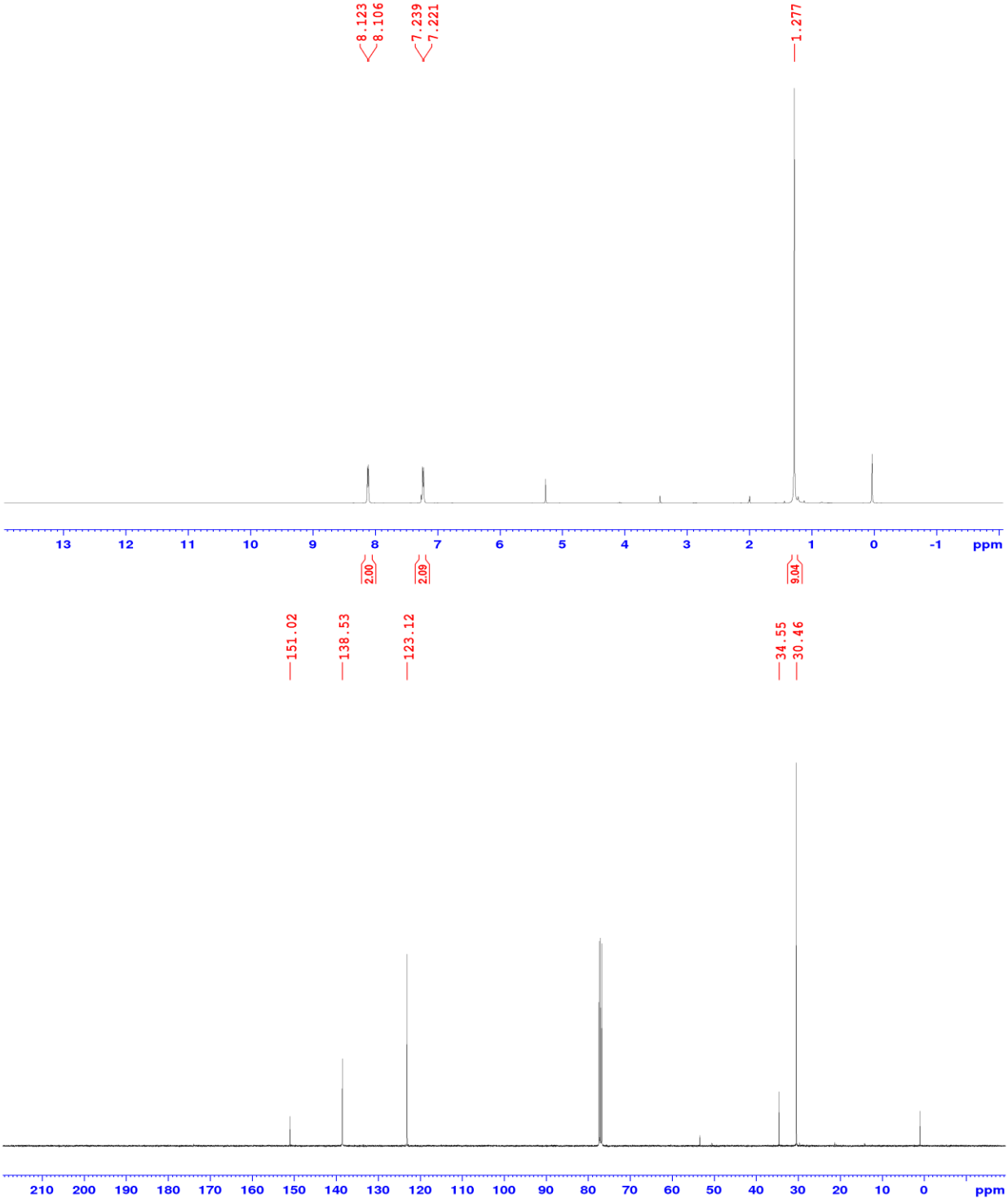

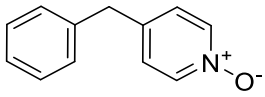

4c - 4-Benzylpyridine *N*-oxide

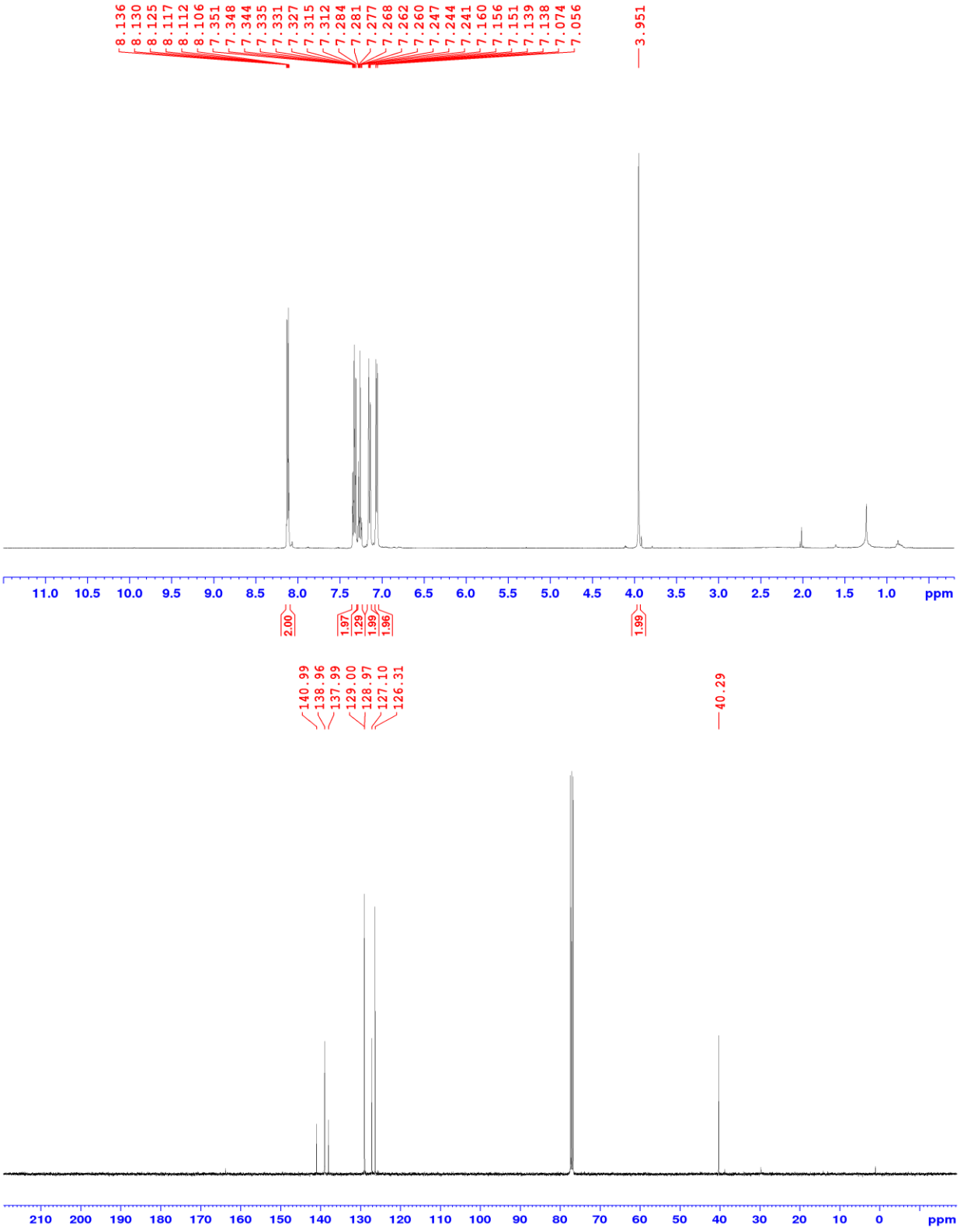

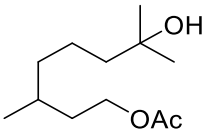

6a - 7-Hydroxy-3,7-Dimethyloctyl Acetate

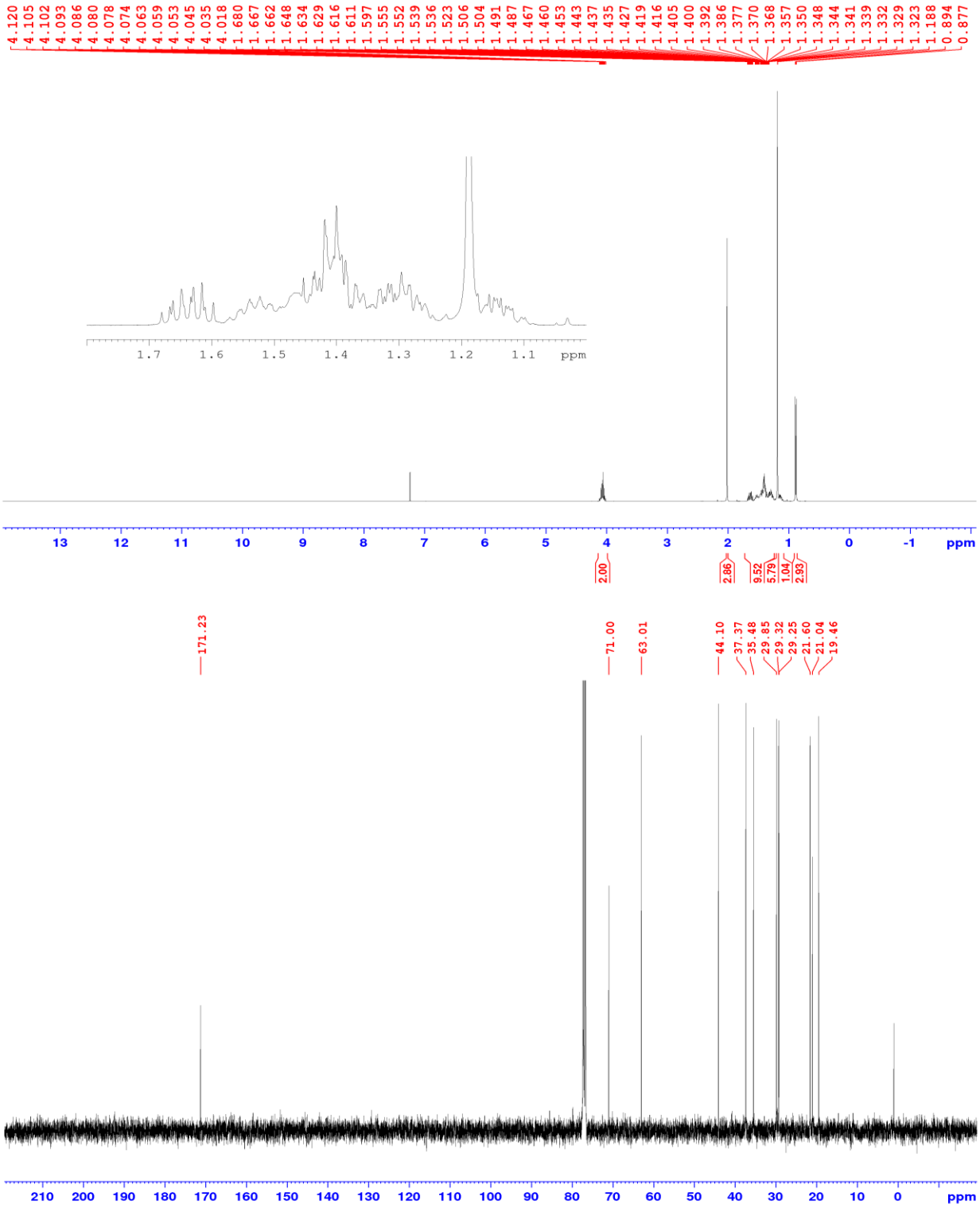

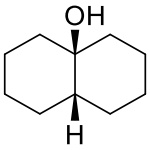

6b - Cis-9-Decalol

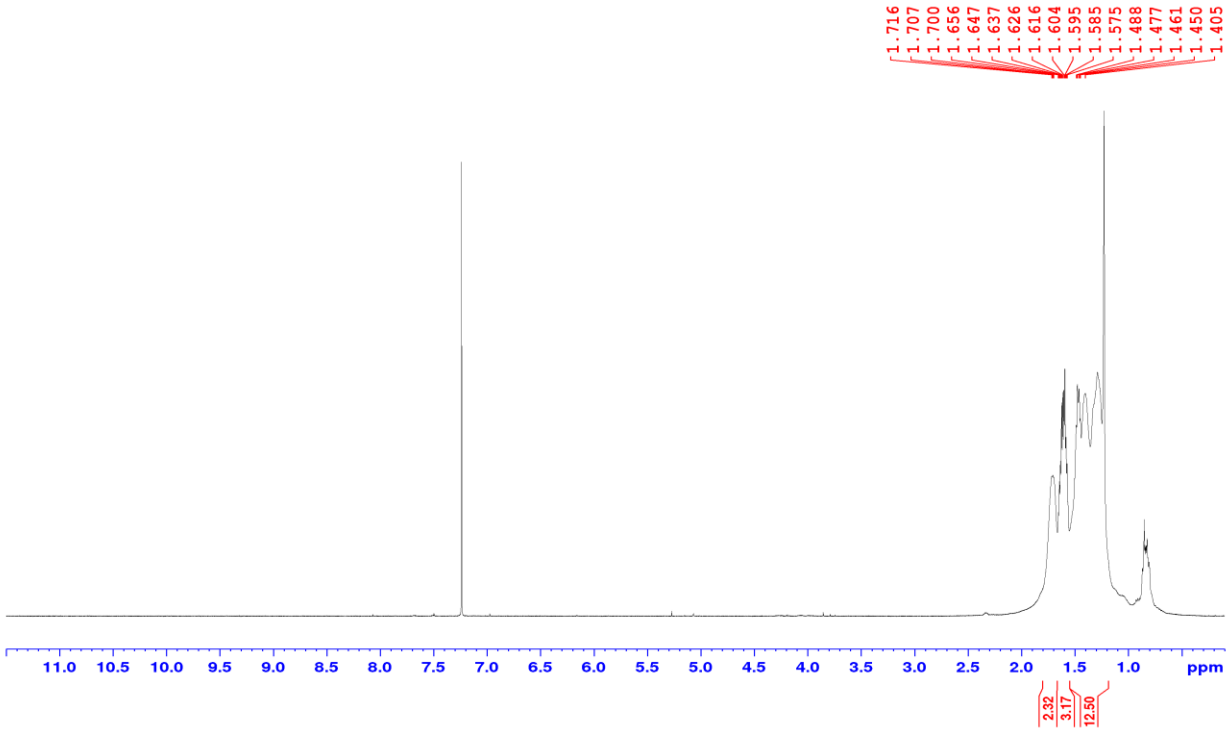

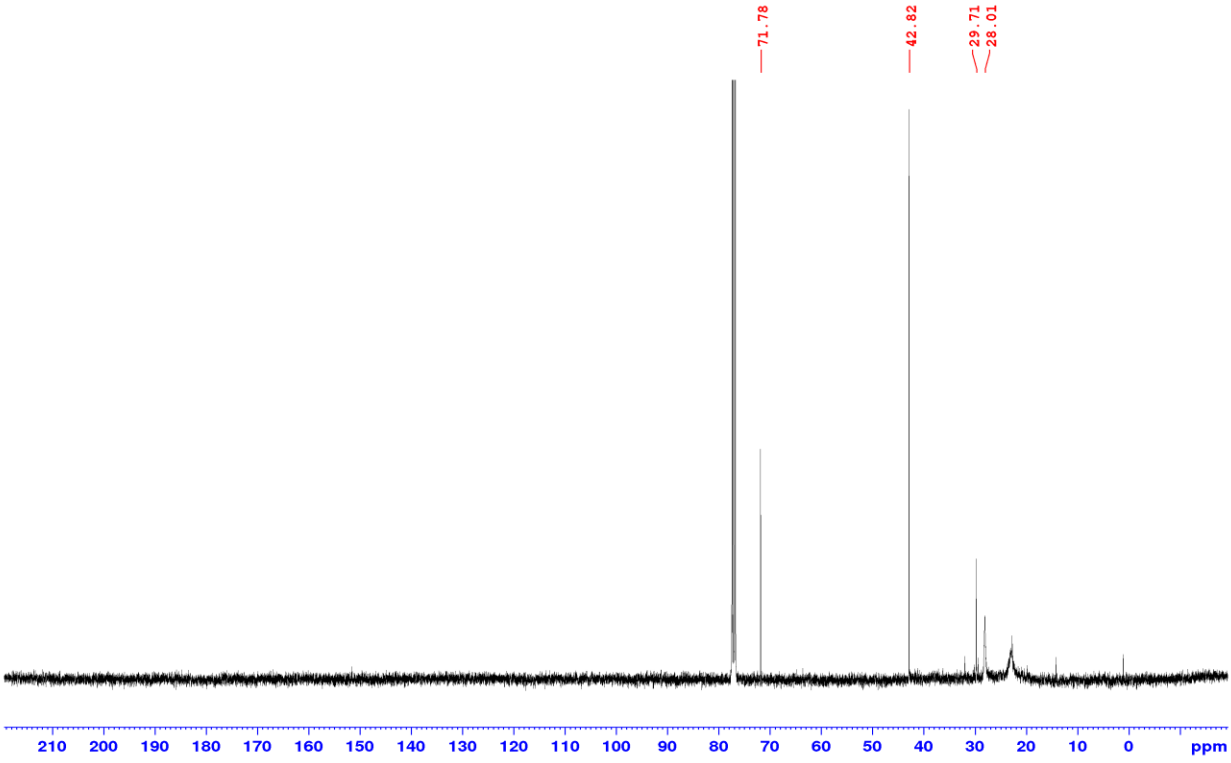

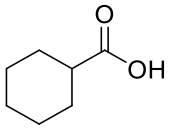

8a - Cyclohexane Carboxylic Acid

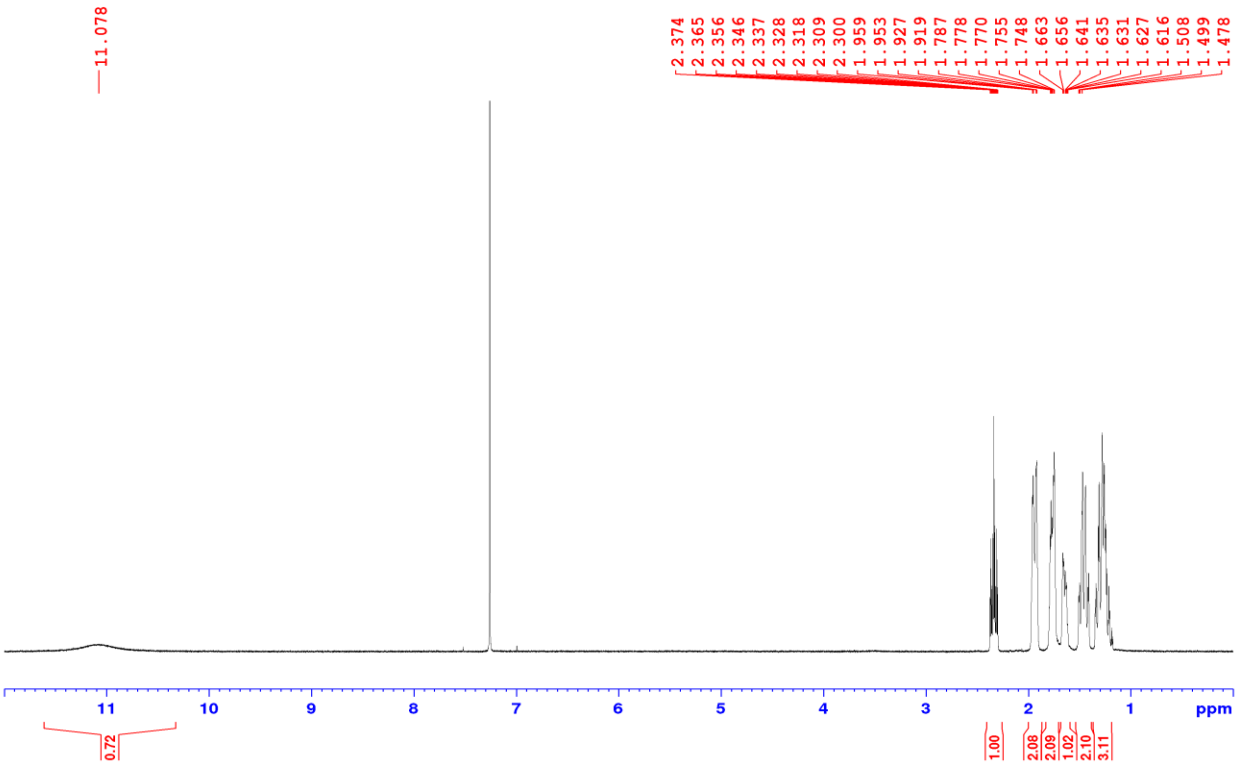

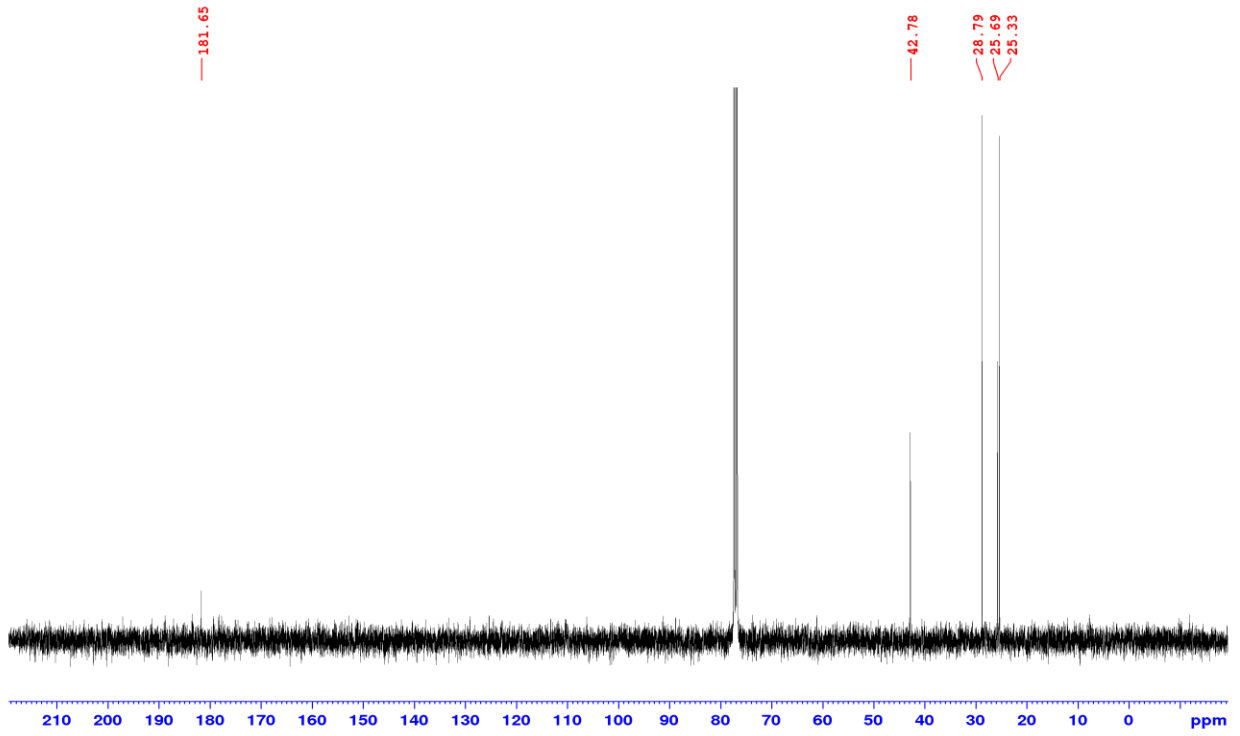

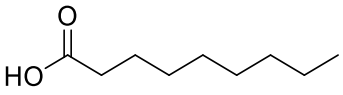

8b - Nonanoic Acid

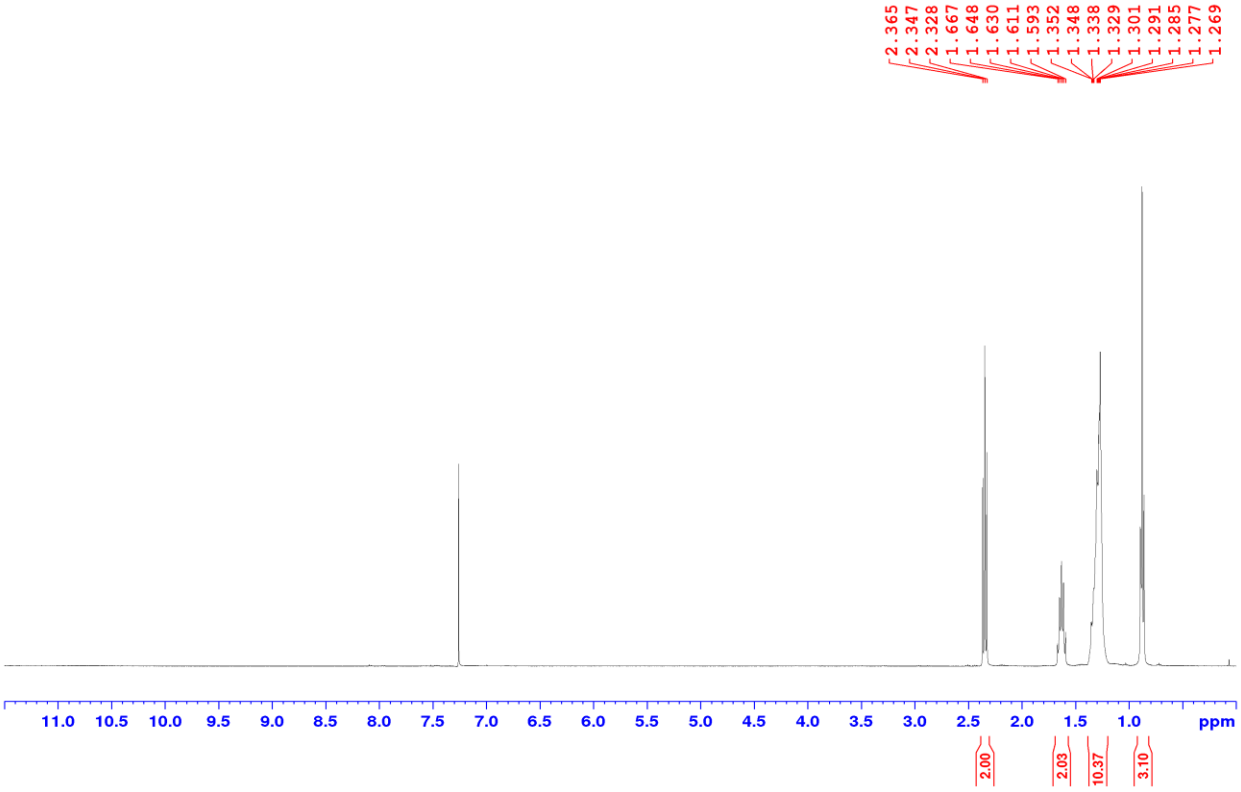

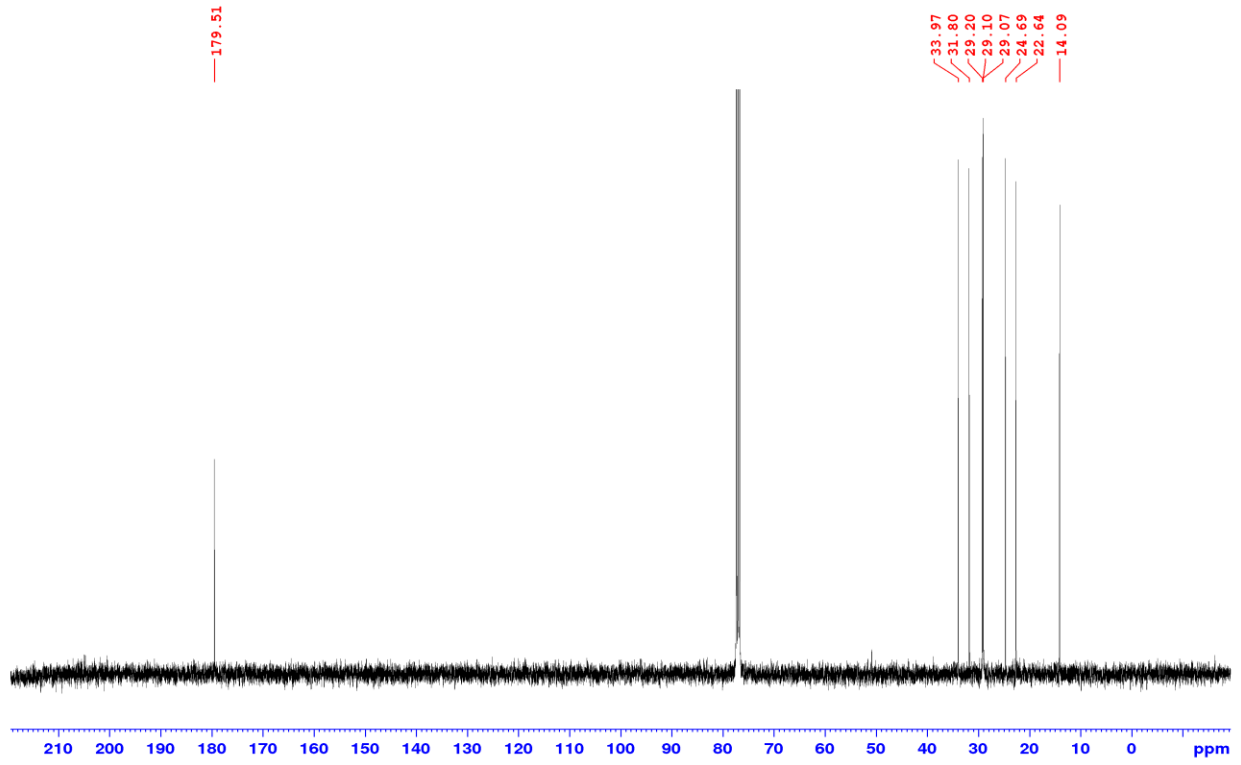

3.1.5: Supporting Information References

1. J. Wallgren, S. Vikingsson, A. Åstrand, M. Josefsson, H. Gréen, J. Dahlén, X. Wu and P. Konradsson, *Tetrahedron*, **2018**, *74*, 2905–2913.

2. US Pat., US20170209591A1, 2016.

3. Q. Zhang, L. Catti, J. Pleiss and K. Tiefenbacher, *J. Am. Chem. Soc.*, **2017**, *139*, 11482–11492.

4. K. Hock, J. Grimmer, D. Göbel, G. Gasaya, J. Roos, I. Maucher, B. Kühn, J. Fettel, T. Maier and G. Manolikakes, *Synthesis*, **2016**, *49*, 615–636.

5. C. B. McPake, C. B. Murray and G. Sandford, *Chem. Sus. Chem.*, **2012**, 5, 312–319.

6. M. Lesieur, C. Battilocchio, R. Labes, J. Jacq, C. Genicot, S. V. Ley and P. Pasau, *Chem. Eur. J.*, **2019**, *25*, 1203.

7. A. Palmieri, S. Gabrielli and R. Ballini, Beilstein *J. Org. Chem*., **2013**, *9*, 533–536.

8. J. A. Burkhard, B. H. Tchitchanov and E. M. Carreira, *Angew. Chem. Int. Ed*., **2011**, *50*, 5379–5382.

9. S. Chandrasekhar and A. Shrinidhi, *Synthetic Communications*, **2014**, *44*, 3008–3018.

10. K. Krohn and J. Kupke, *Chem. Eur. J*., **1998**, 679-682.

11. M. P. Crozet, P. Vanelle, O. Jentzer and M. Kaafarani, *Synthetic Communications*, **1990**, *20*, 7–14.

12. R. Bielmann, C. A. Grob and B. Schaub, *Helv. Chim. Acta*., **1982**, *65*, 1728–1733.

13. L. Huo, A. Ma, Y. Zhang and D. Ma, *Adv. Synth. Catal*., **2012**, *354*, 991–994.

14. T. Taniguchi, T. Fujii and H. Ishibashi, *Org. Biomol. Chem*., **2011**, *9*, 653–655.

15. J. Buonomo, D. Everson and D. Weix, *Synthesis*, **2013**, *45*, 3099–3102.

16. A. Palav, B. Misal, A. Ernolla, V. Parab, P. Waske, D. Khandekar, V. Chaudhary and G. Chaturbhuj, *Org. Process Res. Dev*., **2019**, *23*, 244–251.

17. C. J. Pierce and M. K. Hilinski, *Org. Lett.*, **2014**, *16*, 6504–6507.

18. L. Vanoye, A. Aloui, M. Pablos, R. Philippe, A. Percheron, A. Favre-Réguillon ,C. de Bellefon, *Org. Lett*., **2013**, *15,* 5978–5981.

19. C. Santilli, I. S. Makarov, P. Fristrup and R. Madsen, *J. Org. Chem*., **2016**, *81*, 9931–9938.

3.2: Organolithium Generation and Use via Challenging Deprotonations

3.2.1: General Experimental Details

Unless otherwise indicated, reagents were obtained from Sigma Aldrich, Acros, Alfa Aesar, Matrix Scientific, Oakwood, or Combi-Blocks, and used as received. Pd_2dba_3 was obtained from Johnson Matthey, XPhos (98%) from Combi-Blocks, and $ZnCl_2$ (anhydrous, >98%) and *n*-BuLi (1.6 M in hexanes) from Sigma Aldrich. Butyl lithium was used fresh and not titrated. ACS grade cyclohexane was purchased from Fisher Chemical, purged with UHP N_2, and dried under molecular sieves. Tetrahydrofuran and toluene were degassed with N_2 and passed through a PureSolv solvent purification system before use. Stock solution of $ZnCl_2$ in THF was prepared inside of a glovebox and stored under N_2. Unless otherwise indicated, all reactions were carried out in oven-dried glassware under an N_2 atmosphere. (±)-trans-*N,N,N′,N′*-tetramethylcyclohexane-1,2-diamine (TMCDA)[1], 4-(trimethylsilyl)toluene[2], 4-chloro-1-methyl-1H-indole[3], and 3-methoxypropylbenzene[4] were all prepared by literature procedures and their characterization data were all in agreement with that reported by the authors.

Silicycle F60 40-63 μm silica gel was used for column chromatography. Analytical thin layer chromatography (TLC) was conducted using aluminum-backed EMD Millipore Silica Gel 60. Visualization of developed plates was performed under UV light (254 nm) and/or using $KMnO_4$ stains. Yields for optimization were determined by NMR or GC analysis of the crude reaction mixture using 1,3,5-trimethoxybenzene as an internal standard.

NMR spectra were collected on a Bruker Avance 400 MHz spectrometer. Data for ^1H NMR are reported as follows: chemical shift (δ ppm), multiplicity (s = singlet, d = doublet, t = triplet, q = quartet, m = multiplet), coupling constant (Hz), integration. ^1H and ^{13}C were referenced to residual solvent signals. IR spectra of compounds were obtained using a Nicolet6700 FT-IR spectrometer with a diamond ATR crystal (ThermoScientific). Accurate mass data (EI) was obtained from an Agilent 5977A GC/MSD using MassWorks 4.0 from CERNO bioscience.

3.2.1.1: General Procedure A: Cross-Coupling of Primary Benzyl Lithiums with Aryl Chlorides

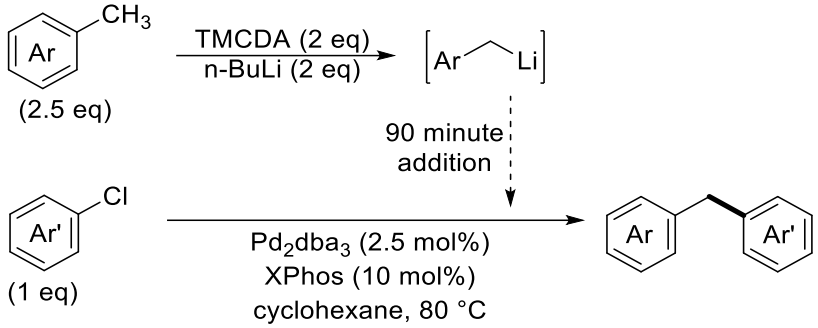

Pd_2dba_3 (4.6 mg, 2.5 mol%, 5 μmol), XPhos (9.5 mg, 10 mol%, 20 μmol) and aryl chloride (if solid; 1 eq, 0.2 mmol) were placed in an 8 mL screw top tube and flushed with N_2. Cyclohexane (2 mL) and aryl chloride (if liquid; 1 eq, 0.2 mmol) were added and the solution and stirred at 80 °C for 15 min. Separately, the toluene derivative (2.5 eq, 0.5 mmol) and TMCDA (74 μL, 2 eq, 0.4 mmol) were added to a 4 mL screw top vial under N_2. ^{n}BuLi 1.6 M in hexanes (250 μL, 2 eq, 0.4 mmol) was added dropwise over approximately 1 minute at room temperature before heating to 60 °C for 15 minutes, during which time the solution turns dark orange, with the colour varying slightly depending on the substrate. The deprotonated toluene derivative was then diluted with cyclohexane to a total volume of 2 mL, taken up into a 3 mL plastic HSW syringe, placed on a NewEra NE-300 syringe pump, and added to the aryl chloride solution at a rate of 1333.3 μL/h for 1.5 h (2 mL). The reaction was stirred an additional 15 min after the addition was complete, then quenched with methanol (2 mL), condensed under vacuo, dry-loaded onto silica gel, and purified by flash column chromatography.

3.2.1.2: General Procedure B: Cross-Coupling of Primary Benzyl Zincs with Aryl Halides

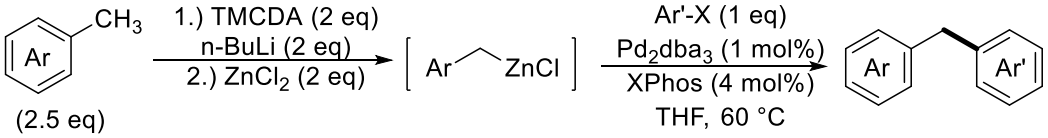

Pd_2dba_3 (1.8 mg, 1 mol%, 2 μmol), XPhos (3.8 mg, 4 mol%, 8 μmol) and aryl halide (if solid; 1 eq, 0.2 mmol) were placed in an 8 mL screw top tube and flushed with N_2. Tetrahydrofuran (2 mL) and aryl halide (if liquid; 1 eq, 0.2 mmol) were added to the solution and stirred at 60 °C for 15 minutes. Separately, toluene derivative (2.5 eq, 0.5 mmol) and TMCDA (74 μL, 2eq, 0.4 mmol) were added to a 4 mL screw top vial under N_2. ^{n}BuLi 1.6M in hexanes (250 μL, 2 eq, 0.4 mmol) was added dropwise over

approximately 1 minute at room temperature before heating to 60 °C for 15 minutes during which time the solution turns dark orange, with the colour varying slightly depending on the substrate. A solution of $ZnCl_2$ 0.5 M in THF (400 μL, 2 eq, 0.4 mmol) was then added to the benzyl lithium solution at room temperature to form a colourless solution, followed by dilution with THF to a total volume of 2 mL. The resultant benzyl zinc solution was then added to the mixture of catalyst and aryl halide and stirred at 60 °C. Once the reaction is complete (i.e. full consumption of aryl halide observed by GC-MS; usually less than 3 hours), the mixture is then quenched with methanol (2 mL), condensed under vacuo, dry loaded onto silica gel, and purified by flash column chromatography.

3.2.2: Characterization Data for Products

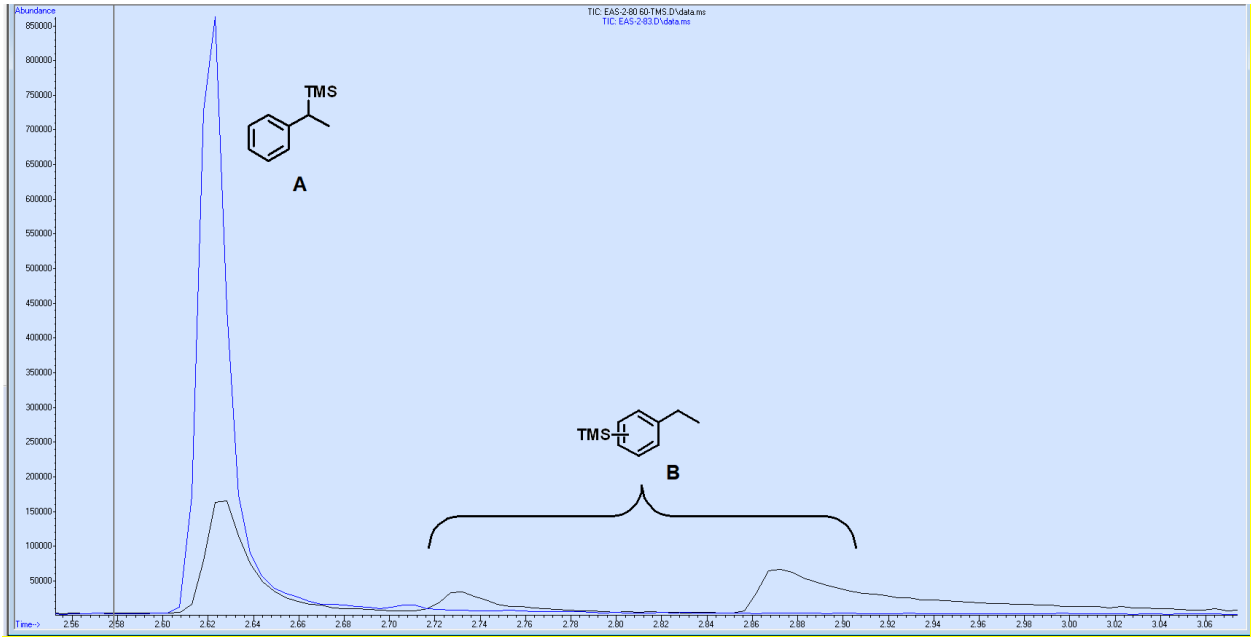

Figure S1: GC trace of TMS-Ethylbenzene product distribution overlayed with independently synthesized benzylic TMS (A) to verify elution time.

The coupling experiments and data collection were largely performed by Freure using the optimized deprotonation conditions. As such, only two representative examples are presented herein.

3.2.2.1:Organolithium Coupling

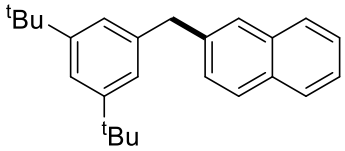

2-(3,5-di(tert-butyl)benzyl)naphthalene (8b) was prepared from 3,5-di(tert-butyl)toluene and 2-chloronapthalene by general procedure A and purified on silica eluting with 1% Et_2O in hexanes. Yield 50.2 mg (76%) white solid, melting point 113 °C. ^{1}H NMR (400 MHz, $CDCl_3$) δ 7.84-7.75 (m, 3H), 7.66 (s, 1H), 7.44 (m, 2H), 7.37 (dd, J= 1.7, 8.4 Hz, 1H), 7.30 (t, J= 1.8 Hz, 1H), 7.11 (d, J= 1.8 Hz, 2H), 4.16 (s, 2H), 1.31 (s, 18 H). ^{13}C{^{1}H} NMR (100 MHz, CDCl3) δ 150.8, 139.9, 139.0, 133.7, 132.1, 127.9, 127.8, 127.64, 127.63, 127.0, 125.9, 125.2, 123.3, 120.2, 42.6, 34.8, 31.5. **IR** ν(neat) 1508, 1593, 2865, 2895, 2960 cm^{-1}. **HRMS** calculated for $C_{25}H_{30}$ 330.2348, found 330.2342, spectral accuracy 98.6%.

3.2.2.2: Benzylzinc Coupling

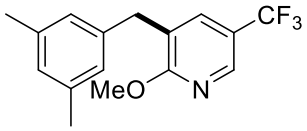

3-(3,5-dimethylbenzyl)-2-methoxy-5-(trifluoromethyl)pyridine (9a) was prepared from mesitylene and 3-chloro-2-methoxy-5-(trifluoromethyl)pyridine by general procedure B and purified on silica eluting with a gradient of 0-10% EtOAc in hexanes (R_f ~ 0.5 in 10%). Yield 53.1 mg (90%) colourless oil. ^{1}H NMR (400 MHz, $CDCl_3$) δ 8.33 (s, 1H), 7.45 (s, J= 2.2 Hz, 1H), 6.90 (s, 1H), 6.82 (s, 2H), 4.04 (s, 3H), 3.88 (s, 2H), 2.31 (s, 6H). ^{13}C{^{1}H} NMR (100 MHz, CDCl3) δ 164.06, 164.05, 143.4, 138.3, 138.2, 134.7, 128.3, 126.8, 124.8, 120.0, 54.1, 35.2, 21.3. **^{19}F NMR** (376 MHz): δ -61.3. **IR** ν(neat) 1116, 1482, 1624, 2867, 2926, 3018 cm^{-1}. **HRMS** calculated for $C_{16}H_{16}F_3NO$ 295.1184, found 295.1178, spectral accuracy 98.7%.

3.2.3: NMR Spectra

3.2.3.1: Organolithium Coupling

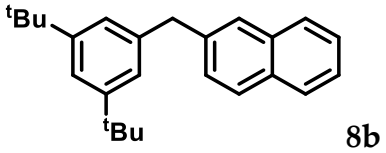

8b

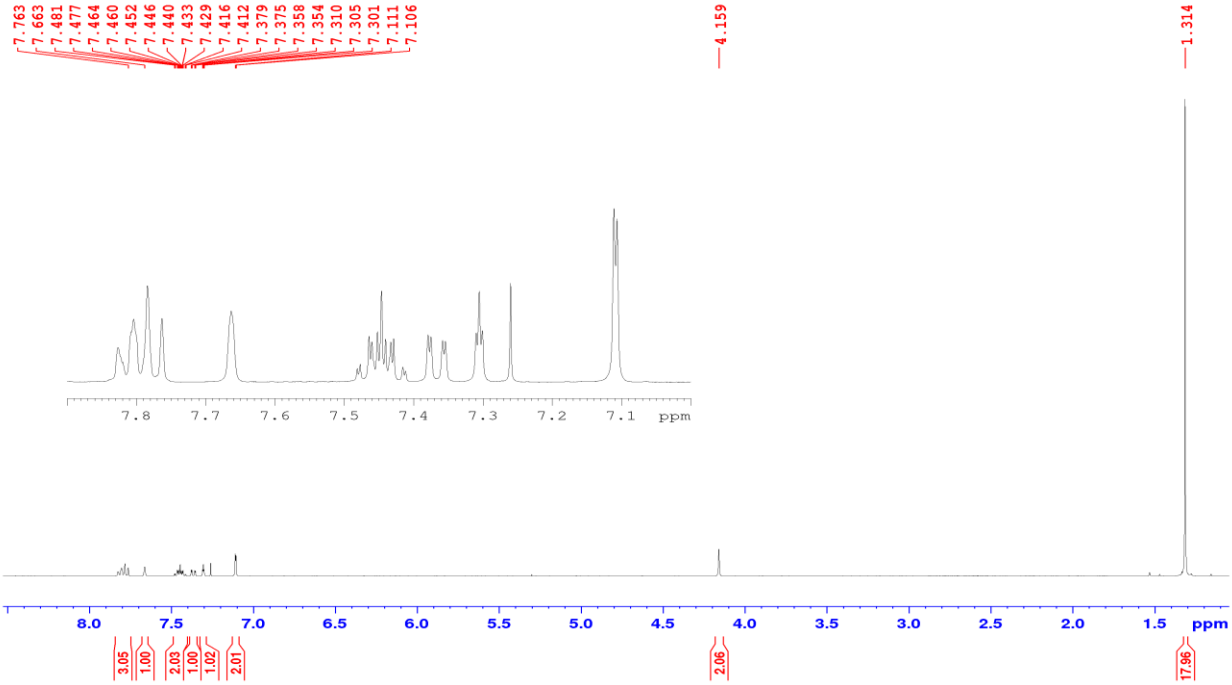

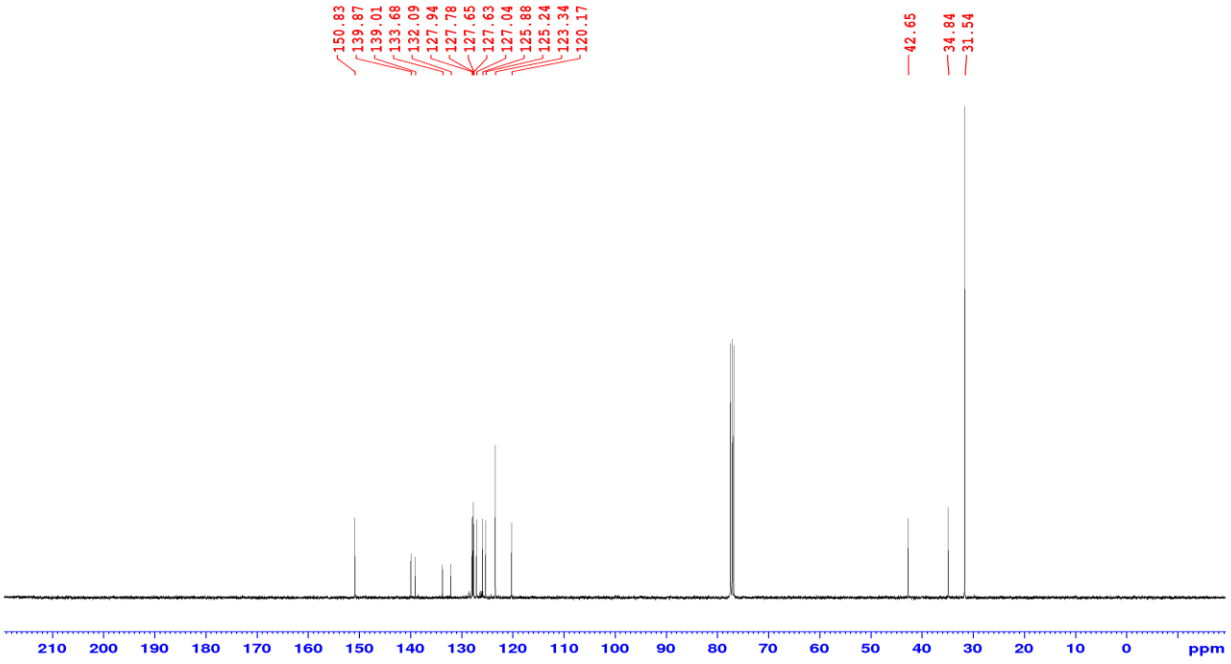

3.2.3.1:Benzylzinc Coupling

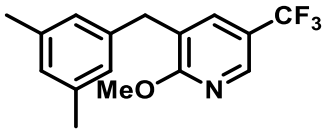

9a

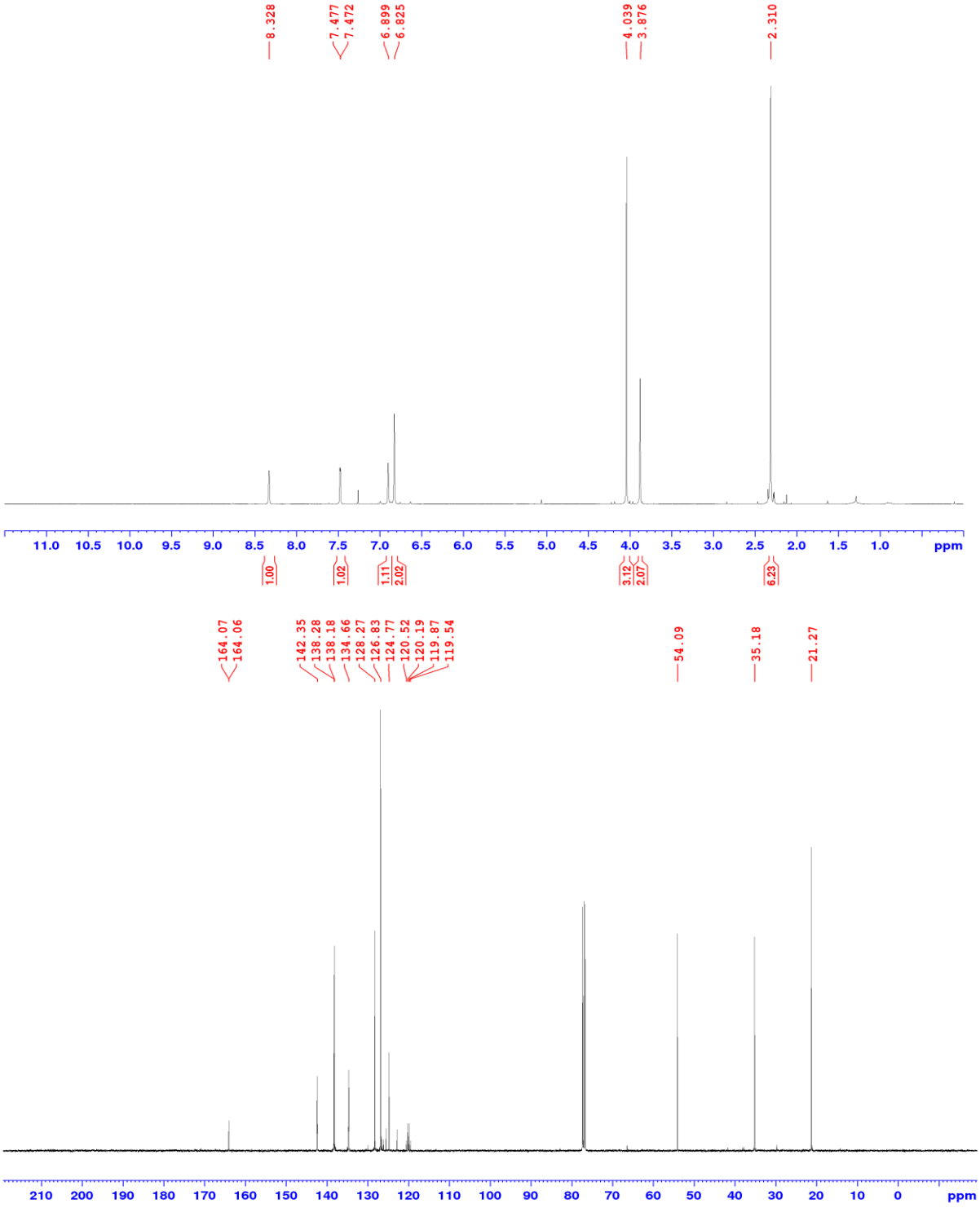

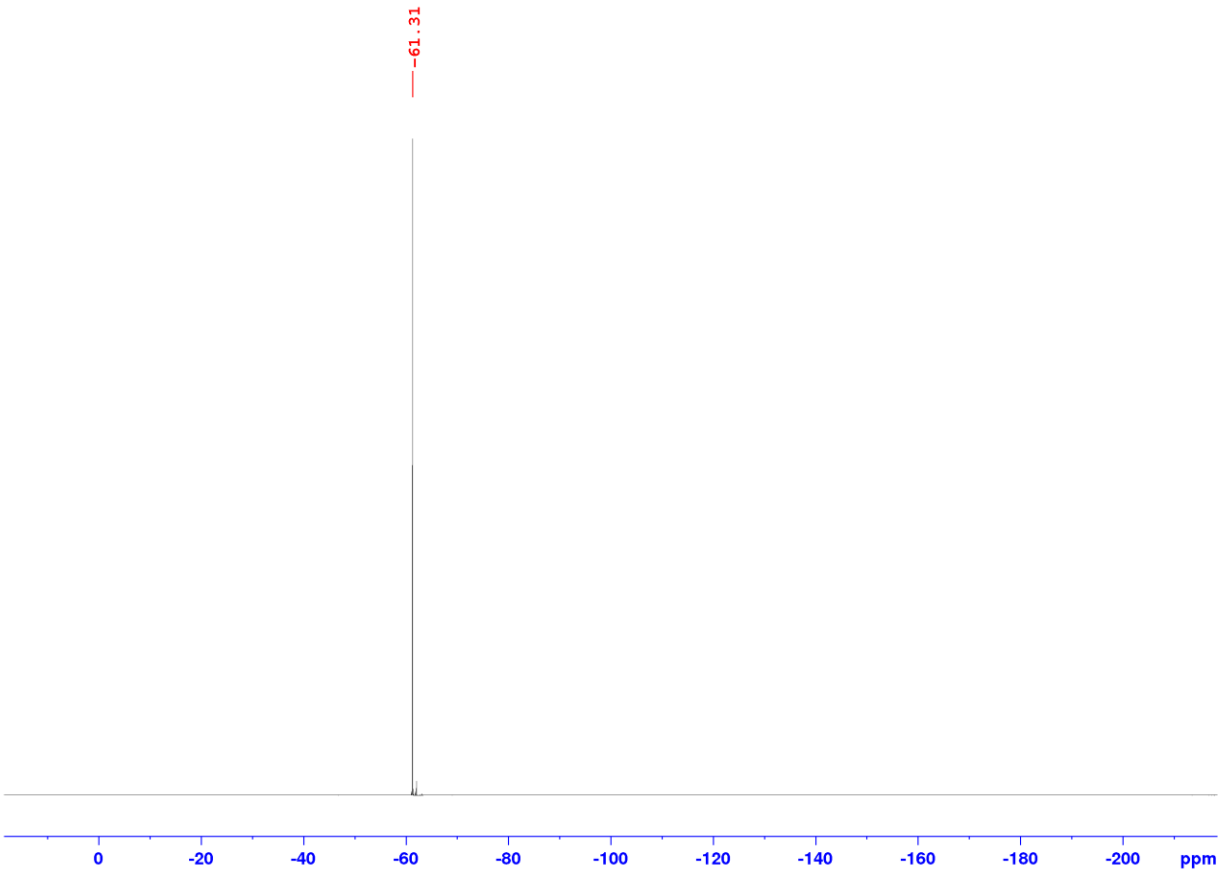

3.2.4: Supporting Information References

1. Remenar J. F., Lucht B. L., Collum D. B. *J. Am. Chem. Soc.* **1997,** *119*, 5567-5572.

2. Doszczak, L., Kraft, P., Weber, H. ‐ P., Bertermann, R., Triller, A., Hatt, H. and Tacke, R. *Angewandte Chemie International Edition*, **2007**, *46*, 3367-3371.

3. Jayaraman A, Misal Castro L. C., Fontaine F-G. *Org. Proc. Res. Dev.* **2018,** *22*, 1489-1499.

4. M. Iqbal, C. Li, J. H. Kim, S. M. Alshehri, T. Nakayama, Y. Yamauchi, *Chem. Eur. J*. **2017**, *23*, 51.

5. Zhao, C.; Zha, G.-F.; Fang, W.-Y.; Rakesh, K. P.; Qin, H.-L. *Eur. J. Org. Chem.* **2019**, *8*, 1801–1807.